Air Supported Structures and their response to Wind Loading

A parametric method for multiple geometries

Utkarsh Jaiswal

TU Delft

Air Supported Structures and their response to Wind Loading

A parametric method for multiple geometries

by

Utkarsh Jaiswal

to obtain the degree of Master of Science
at the Delft University of Technology,
to be defended publicly on Wednesday September 28, 2021 at 16:00.

Student number:	5066522	
Project duration:	December, 2020 – September, 2021	
Thesis committee:	Prof. dr. ir. L.J. Sluijs	TU Delft, supervisor
	Dr. A. Tsouvalas	TU Delft
	Dr. ir. P.C.J Hoogenboom	TU Delft
	Ir. S. Cox	Royal HaskoningDHV
	Dr. Ir. S. Meijers	Royal HaskoningDHV

This thesis is confidential and cannot be made public until December 31, 2021.

An electronic version of this thesis is available at http://repository.tudelft.nl/.

Picture on cover page taken from
https://www.pinterest.com/pin/812266482782783458/

Preface

Here I present to you my graduation thesis titled ”Air Supported structures and their response to Wind Loading - A parametric method for multiple geometries”. This thesis is written to obtain the Masters of Science degree from Delft University of Technology. The thesis project was conducted in collaboration with Royal HaskoningDHV, Rotterdam. I completed my research under the supervision of Prof. dr. ir. L.J. Sluijs (TU Delft), Dr. A. Tsouvalas (TU Delft), Dr. ir. P.C.J Hoogenboom (TU Delft), Ir. S. Cox (Royal HaskoningDHV), and Dr. Ir. S. Meijers (Royal HaskoningDHV), from December, 2022 until September, 2021.

It seems like yesterday when I first visited the TU Delft campus during the Introduction program 2019 and here I am writing this thesis to conclude the journey. At that time we were all excited to start a new phase of life, getting used to the never ending rain and wind of the Netherlands, attending lectures, giving exams. Life seemed very good and constant running but then Covid-19 hit us and the normal life came to a halt, but with TU Delft online support, everything became accessible quickly. Now, this phase of life is coming to an end and I am excited for the future challenges and endeavors. But before concluding this phase, I would like to acknowledge the people who helped me in the journey.

Firstly, I would like to thank Prof. dr. ir. L.J. Sluijs, Dr. A. Tsouvalas, Dr. ir. P.C.J Hoogenboom for the guidance and giving me the opportunity to conduct this challenging research work. I thank you, Ir. S. Cox, and Dr. Ir. S. Meijers for helping me to execute this research in such a way that it can be used in the practical world. Thank you to all the committee members for taking out all the time for the numerous meetings and brainstorming sessions. I would specially like to thank Simon for believing in me to successfully learn the three completely different areas of Structural Engineering to complete this thesis. I would also like to thank the Advance Technology and Research team at Royal HaskoningDHV, who with their specialized knowledge guided me to easily understand the practical aspects of this thesis and overcome the difficulties I faced.

Furthermore, I would like to thank my parents, my sisters and my friends who throughout the whole journey believed in me and supported me. I am grateful for their motivation and upliftment whenever it seemed impossible, especially during this uncertain Covid times.

Utkarsh Jaiswal
Delft, September 2021

Summary

In the presented work, we have developed a method to analyse the interaction between the wind and membrane structures. The complex behaviour of light weighted membrane structures can induce dynamic and wind effects, so this requires an appropriate method to analyse the structure. When the deformation of membrane structures is large, it becomes necessary to consider the interaction between wind flow and membrane. This interaction leads to aeroelastic problems.

The necessary properties to be considered for the aeroelastic coupled problem are considered and presented. The major focus of the thesis is to simulate the geometric non-linear behaviour of the membrane structures when subjected to wind loading. To derive the initial equilibrium shape, the method of form finding is applied. To properly simulate the wind flow around the structure, existing research regarding wind tunnel testing of a hemispherical air dome model is used. First, hemispherical model similar to existing research was made to verify the boundary conditions. The results are compared to the wind-tunnel testing results to get proper boundary conditions in Computational Fluid Dynamics models. In order to keep the simulation simple, the wind velocity is considered constant with height and constant wind flow with respect to time.

Partitioned analysis is used to simulate the physics behind the wind-membrane interaction simulation. By using this method, the multi-physics problem is separated into individual fields. Considering the wind-membrane interaction, the problem is separated into fluid domain and structural domain.

The structural and fluid domain mechanics are discussed in detail. For the single field solvers, methods are introduced based on the fundamentals. Finite Element method is used for the form-finding as well as numerical simulation of the structural field and SOFiSTiK software is used. For the fluid simulation, ANSYS CFX is used.

The strong physical coupling is done between the fluid and the structural domain. For this, the partitioned coupling simulation is used. The requirements and methods for the partitioned analysis are presented as well. For the coupling of separate solvers, a central coupling tool is made using Grasshopper. The transfer of coupling data such as displacement and wind pressure on the membrane structure is done using the developed coupling tool. In the development of this coupling method using Grasshopper, Python programming language is used. The developed method was used in iterations to analyse the effect of geometric non-linearity.

In order to make the developed method reusable for the air-supported membrane structures, the whole process is made parametric using grasshopper. This enables us to analyse the membrane structures with known base shape, internal air pressure. Ultimately this method can be used to analyse the effect of geometric non-linearity on membrane structures when subjected to wind loading. To show the use case of developed method, two different models are developed to analyse the fluid structure interaction. First model has been considered with a circular base shape and the second one has been considered with a square base shape. In order to analyse the effect of geometric non-linearity on these structures, the results such as maximum wind pressure on the membrane structure and maximum structural displacement are compared to the results without considering the geometric non-linearity.

Moreover, wind variation analysis is done to analyse the extent to which geometric non-linearity is dependent on the wind speed. Similarly, size variation analysis is also done to analyse the extent to which geometric non-linearity is dependent on the structure size, keeping the wind velocity constant.

Contents

List of Figures

1 Introduction

1.1. Incentive and Framework

The global rising demand of sustainable and eco-friendly buildings, along with advent of slender construction materials and modern techniques give rise to light weighted structures. A tremendous amount of effort goes into analysing the behaviour of these lighter structures so that they can meet the standard requirement of resistance to external loading. This analysis not only makes the structure safer but also makes it cost effective, which in-turn fulfils the requirement of being sustainable.

Much research is done on the subject wind loading but less research can be found on the pneumatic structures and their response to wind loading. In normal practice these days, the wind pressure on the membrane structures is calculated using the Eurocode [1] and then applied on the structure to see it's response. This approach ignores the effects membrane structure is going to have on the wind flow due to its deformation. As the force acting on the membrane structure depends on the incident angle it has with the wind flow, the force on the structure is going to change with deformation. This effect of deformation on the wind flow is known as the Geometric Non-Linear behaviour. In membrane structures, an interaction between the membrane and wind flow is there.

In the research such as [2], [3], [4], [5] different aspects to simulate fluid-structure behaviour can be found. With the theoretical aspects of this method described, they lack the practical application or development of the method. Moreover, most of the work focuses on membrane structures and the methods to simulate the fluid structure interaction. In this thesis, air-supported membrane structure will be covered, which are also known as Pneumatic Structures. In air-supported structures, due to the presence of pressurized air inside the membrane, the air gives the structural integrity to the structure. In this work, more focus will be on the development and application of the method to simulate the Geometric-nonlinear behaviour of the membrane. Though the detailed analysis of the membrane structures subjected to wind loading is very complicated due to the stochastic nature of the wind, but as Simiu and Scanlan stated in [6] that its the task of an engineer to ensure the adequate performance of structures when they are subjected to wind loading from safety and serviceability point of view.

The problem statement of the research is formulated as following:

The behaviour of the Pneumatic Structures is non-linear. How the deformation of the membrane structure is going to effect the wind flow around it and consequently its response to this wind loading ?

There are three sub questions which can be formulated from this problem statement:

1. How the maximum wind loading occurring on the membrane structure is going to be effected by the membrane geometric non-linear behaviour ?
2. How the maximum displacement of the membrane structure when subjected to wind loading is going to be effected by the membrane geometric non-linear behaviour ?

3. What is the dependence of this membrane's geometric non-linear behaviour on the wind speed and the size of the structure considered ?

The objective of this thesis can be divided into two parts:

1. Development of an iterative method using softwares to simulate the geometric non-linear behaviour of the membrane structure when subjected to wind loading. Moreover, making this developed method parametric to consider several pneumatic structures
2. Analyse several geometries using the developed method to estimate the effect of deformation on the structure's response and wind loading

The aim of this thesis is briefly explained in section 1.2.
In this chapter the existing research to understand this topic with be covered.

1.1.1. Membrane Structures

Membrane structures are spatial, light-weight and extremely optimized structures made out of tensioned membranes. The fabric strength is optimally used because of constant tensile stress over the thickness. Within the last years, the employment of membranes in structural engineering became a lot common. With the innovation of new material technologies, the choice of material available to construct membrane structures has increased. More and more membrane structures are being constructed such as the Amsterdam Air dome and the Shaded Dome in Netherlands.

Pertaining to the fact that membrane structures have little or no bending stiffness, it is a special type of construction. The load carrying capacity comes from the tension stresses tangential to the membrane surface. On losing this tensile stress, the membrane will lose its stiffness and will wrinkle. Relatively large deformation is caused due to non-tangential external loading. In order to avoid these large deformations, these structures are designed as doubly curved geometries and are stabilised by prestressing it. The initial form of the membrane is determined by the static equilibrium between membrane prestress and overpressure. Consequently, the initial form is usually unknown and must be derived by experimental approach or numerical form finding computations.

1.1.2. Analysis of Wind Effects on Membrane Structures

The delicacy and flexibility in membrane structures' material and construction makes it highly responsive to external loading. The external loading can be due to wind or snow. In contrast to other loads such as dead load and snow load, the wind load cannot be considered as static loading in general. Analysis of wind load on membrane structures become much more complicated when considering the aeroelastic effects. Aeroelastic effect comprises of the interaction between the wind loading and the deformation of the structure.

To simplify the analysis of membrane structures subjected to wind loading, necessary assumptions are made. The assumption may result in negligence of certain important effects such as interaction between the wind and the structure. To investigate the dynamic behaviour, experimental simulation in wind tunnels is a generic tool. A general requirement is to replicate the dynamic behaviour between experimental approach and reality. The aeroelastic effect is hard to acquire in small scale model. Moreover, the experimental approach is complicated and expensive as well.

With the steady development of the computational power, the Computational Fluid Dynamics (CFD) becomes a viable option for the analysis of wind effect on structures after the well established methods such as wind tunnel experiments.

1.1.3. Numerical Simulation of Wind-Membrane Structural Interaction

Not just being financially viable, the application of numerical methods also gives the opportunity to model the aeroelastic effects which is one of the limitations in experimental approach. The wind load on the structure can be calculated using Computational Fluid Dynamics Analysis and the response of the structure to these forces can be calculated from the Numerical Structural Analysis. Combining

these two methods we get a multi-physics approach. In this we couple the fluid domain analysis and the structural domain. In this thesis, application of numerical methods to analyse the surface coupled problem to model the wind and membrane structure interaction is done.

1.1.4. Pneumatic Structures

The usability of the developed method in this thesis is shown on an example of a Hemispherical Air-Dome Structure and a square base Dome Structure which are both examples of Pneumatic Structures. Pneumatic Structures are an example of light weighted tensile structures. This type of structures use minimum material and use pre-stress for the integrity. In Pneumatic Structures the internal pressure gives the tensile stress in the membrane. In general the external loading due to wind is assessed by the wind tunnel testing. The obtained wind pressure coefficient, in association with the wind loading code gives an estimation of wind loading acting on the structure. But still, the question about the extent to which the interaction between the membrane structure and the wind loading will effect the structure behaviour remains open.

1.2. Aim of This Thesis and Approach

The aim of this thesis is to develop a numerical tool using softwares to analyse the interaction between the air-supported structures and wind flow. This is a multi-physics problem. In order to simulate the behaviour of the structure, a strong coupling between the membrane structure and wind flow is done. For the wind flow modelling, Computational Fluid Dynamics (CFD) methods are used and to simulate the structural behaviour, Finite Element Method (FEM) is used.

In this thesis, the analysis is done for specific setups of wind speed and wind directions, and therefore necessary approximations are made. Because of this, the ultimate aim is not to show all the possible phenomena of wind induced effects. The outcomes of this thesis cannot be directly used for the design of structures. However, the developed method will help us to better understand certain aspects of the structural behaviour during the design phase such as geometric non-linear behaviour.

In order to simulate the Fluid Structure Interaction, partitioned analysis approach is chosen. In this approach, surface coupled problem is solved separately in single field solvers. The coupling in between the single field solvers is done by exchanging specific boundary conditions.

In this project, the form finding and structural analysis is done using the software SOFiSTiK, the fluid analysis is done using the Computational Fluid Dynamics Code (CFX), and for the coupling between the single field solvers Grasshopper is used. In Grasshopper, data pipelines are created in order to accurately transfer the data such as structural displacement and surface pressure due to wind loading. Moreover, using Grasshopper the whole developed procedure is made parametric. As a result, the user of the method has a choice of deciding the specification of the structure such as initial shape, material properties, internal air pressure, prestress and much more.

After the development of the method, aim is to moreover analyse the effects the membrane structure deformation on the wind flow around it. The geometric non-linear effect on the factors such as wind pressure coefficient, maximum wind pressure on the structure and maximum resulting deformation is considered. Further, the implication of the developed method such as calculation of design load using the method and the effects on the design code safety factors are discussed as well.

1.3. Organization of This Thesis

The Introductory Chapter 1 presents the inspiration for this work and a concise outline of the topic. A precise workflow is formulated to execute this thesis work.

To better address the multi-physics problem, it will be divided into partitioned approach which covers the structural and fluid domain. Within these two chapters (Chapter 2 and 3), the numerical modelling method and simulating the wind flow will be discussed.

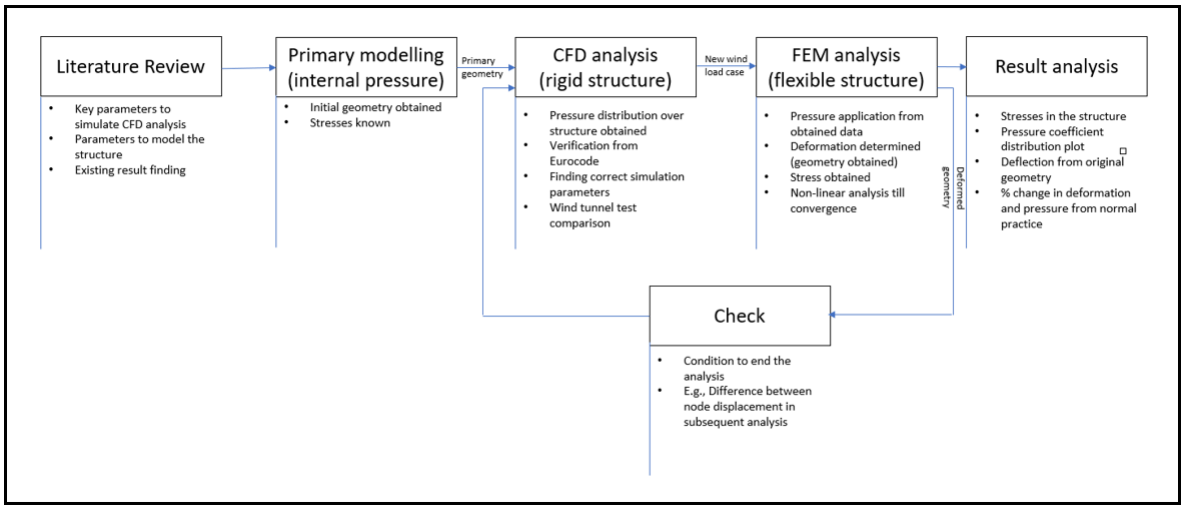

Figure 1.1: Workflow of the thesis

In chapter 2, the fundamental attributes of the membrane structure are examined. Further, appropriate Finite Element Method (FEM) is introduced to model the simulation based on the structure properties. Moreover, a method is developed to make the whole analysis procedure parametric. By this developed parametric method, any pneumatic structure with known boundary condition, internal pressure and prestress can be designed. This is used to setup the numerical model of the Hemispherical Air-Dome Structure and the Square Base Dome Structure.

In chapter 3, firstly the wind loading in general is described and the relation to the wind properties taken in this work are discussed. Ways to deal with the investigation of wind loading on membrane structures is presented. Fundamentals of fluid mechanics are discussed and further Finite Volume Method (FVM) determined. Firstly, wind simulation on the verification model is done to verify the boundary conditions for the CFD analysis. The results are verified from the existing wind tunnel research. Further, the wind loading is simulated on the developed rigid Pneumatic Structures.

In chapter 4, the different field simulations are combined together. Necessary computational setup concepts are discussed to simulate the fluid structural interaction problem. The development of the coupling method will be discussed in detail. Finally this coupled simulation method will be applied for the analysis of Pneumatic Structures subjected to Wind Loading.

In chapter 5, a thorough discussion is presented on the importance of this developed method. Further, possible use of this method in collaboration with the design codes is presented to calculate the design wind loading for the Pneumatic structures. The importance of considering the fluid-structure interaction for the design of membrane structure is discussed as well.

In chapter 6, conclusion from this research work is presented. The answers to the formulated research questions are answered in relation to the specific setup of analysis done in this thesis. Moreover, the limitations of the developed method are discussed. Furthermore, the recommendations to improve the developed method are presented as well.

2

Modeling of Light-Weight Structures

In this chapter, we are studying the membrane structure characteristics. For a detailed and correct simulation of structural behaviour subjected to wind loading, an appropriate model is necessary. In this thesis, to properly model and simulate the structural behaviour of membrane structures subjected to wind loading, the Finite Element Method is used.

In general, prestressed membrane structures are used in Civil engineering. In pneumatic structures, we get this tensile stress by internal air pressure. The initial geometry of the structure can be found using experimental or computational approach. This procedure is called Form-Finding process. In this chapter, this concept will be explained briefly.

The technique to model the Pneumatic Structures will be presented in this chapter and the obtained model will be used in the further chapter to analyse the effect of wind loading on it.

2.1. Characteristics of Membrane Structures

The structures built from membrane have very different load carrying phenomenon than the typical structure. This is due to the fact that the membranes have zero or negligible bending capacity. So, the load transfer in the membrane is done by the tangential stress acting on it, which is also known as membrane stress. This stress can only be tensile and when the membrane loses its tension, instability occurs in the structure, which leads to the formation of wrinkles. Because of this unique property, membrane structures are also known as tensile structures.

Owing to the fact that the structure gets it's integrity from the tensile stresses, the tensile forces are in equilibrium at every point on the membrane. If an external load is applied on the structure, this equilibrium gets disturbed. The structure then finds another equilibrium state in which the stresses are in static equilibrium with the external forces. Forces acting normal to the membrane can result in large deformation. The response of the structure mainly depends on the geometry and the stiffness of the membrane.

The shape of the membrane has to be curved in order to obtain the static equilibrium between the membrane prestress, internal pressure and the dead load. This initial geometry is usually unknown and has to be found by experiments or numerical computation, which is known as form-finding. The prestress in the structure can be mechanical or pneumatic.

- **Mechanically imposed prestress**
  The prestress in this kind of structure is caused by the tightened anchorage. Typically, the membrane forms an anticlastic shape in this case, which is a shape with negative Gaussian curvature. In Figure 2.1, four examples of anticlastic shapes are shown.

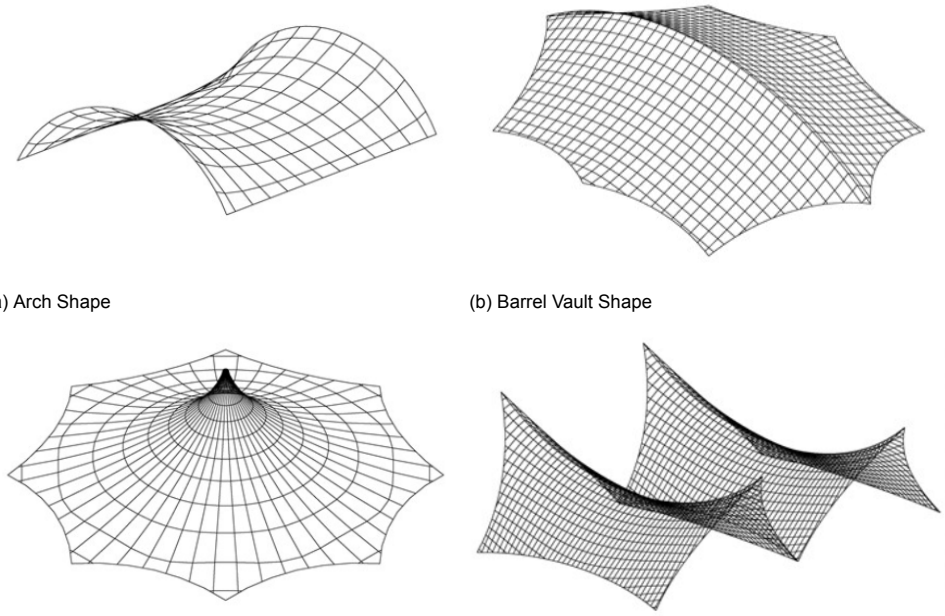

(a) Arch Shape

(b) Barrel Vault Shape

(c) Cone Shape

(d) Saddle Shape

Figure 2.1: General Anticlastic Shapes

- **Pneumatically imposed prestress**
  The prestress in this kind of structure is caused by the pressure difference between the inside and outside of the membrane. The internal pressure is caused by the confined air which is pumped in the structure. Fig. 2.2 show 2 examples of Pneumatic Structures.

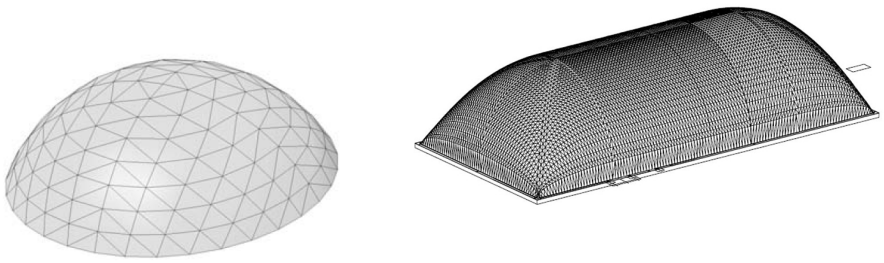

(a) Circular Shape

(b) Pneumatically Prestressed Shapes

Figure 2.2: Pneumatically Prestressed Shapes

In the following, only Pneumatically prestressed structures shall be considered.

2.2. Short History

The invention of pneumatic structures started from the ballooning and zeppelins design. Though it became very popular in the 19^{th} century, it's production was stopped due to an incident wherein a hydrogen filled zeppelin caught fire. By 1917, the concept of using the pneumatic structures as the roof was already developed by F.W. Lanchester. Inspite of the development, the structures were never made because the material required for construction was not available at that time. By 1948, the first Radome was built by Walter Bird, shown in Fig. 2.3. The Radome was used to protect the US - Air Force early warning systems [7]. Later in 1956, Walter Bird founded a company called Birdair Structures for pneumatic and other light weight structures[8].

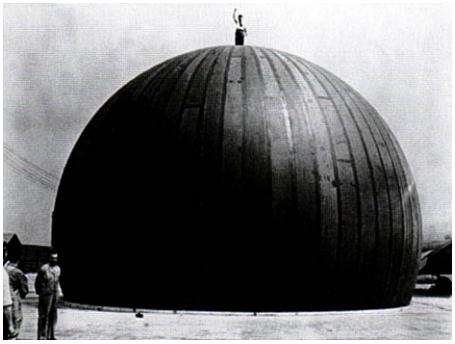

Figure 2.3: The first air-supported radome by Walter Bird

Encouraged by Walter Bird, in 1970 a German architect named Frei Otto experimented with the possibility of covering a whole city of diameter 2 km with membrane structure and steel cables. This design was called 'City in the Arctic' [9].

Now-a-days membranes are not only used for the purpose of covered structures which usually have lower air pressure, they are also used for the structures such as beams and arches which generally have higher air pressure. One such example are tensairity structures, where high internal pressure is used to prevent bucking in the compression members. [10]

2.3. Materials

In general the pneumatic structures are made up of membranes. The properties of the material play an important role in the behaviour of the structures. There are in general two types of membrane materials for pneumatic structures - fabrics and films.

2.3.1. Fabrics

This is made of threads which are interwoven together. The two directions of the weave are called the warp and fill directions. The property of the material can differ in these two directions, therefore the material is anisotropic. There are different materials available to make Fabric, the most commonly used are: Nylon, Polyester and Glass. The properties of these materials are in the table 2.1:

	Polyamide	Polyester	Fibre Glass
Density	$1.14g/cm^3$	$1.38 - 1.41g/cm^3$	$2.55g/cm^3$
Ultimate Stress	$1000N/mm^2$	$1000 - 1300N/mm^2$	$3500N/mm^2$
Ultimate Strain	$15 - 20\%$	$10 - 18\%$	$2 - 3.5\%$
Young's Modulus	$5000 - 6000N/mm^2$	$10,000 - 15,000N/mm^2$	$70,000 - 90,000N/mm^2$

Table 2.1: Properties of different fabric materials

To safeguard the fabric against water, coating is done. Most commonly used coatings are: PVC (Polyvinyl chloride) and PTFE (polytetrafluroethylene).

2.3.2. Films

They are extremely flexible and thin in nature and represent isotropic properties. Because of their low air permeability, they are more commonly used for the pneumatic structures. Commonly used films for membrane structures are ETFE (ethylene tetrafluoroethylene) and PVC (Polyvinyl chloride). PVC is usually used for structures which are temporary and have shorter span such as indoor structures. They are not suitable for outside structures. For outside, ETFE is more commonly used. ETFE was introduced in 1940 [11] and was first used in 1982 in plant houses at Burgers' Zoo in Arnhem. Due to it's properties such as self-cleaning, long-lasting, non-degradable by sunlight [7], it is now the most used material for the pneumatic structures.

In Pneumatic Structures, sometimes net made of steel cables are used on the membrane to reduce the membrane stresses with same internal air pressure. The mechanics behind this will be explained in the next section.

2.4. Structural Behaviour

The response of a pneumatic structure depends a lot on the tensile stress in the membrane. In Fig. 2.4, a 2-D section of a hemispherical pneumatic structure is presented. The structure has a internal pressure P which is the difference between the external and internal pressure of the structure.

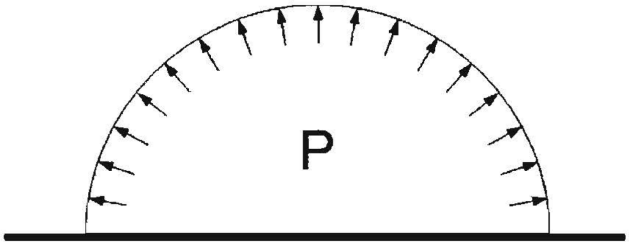

Figure 2.4: Internal Air Pressure on Pneumatic Structure

As the membrane has no bending capacity, the stresses can only be tensile. In the undeformed regular shape, a relation between the internal pressure, Radius of curvature and the stress can be derived. In Fig. 2.5 a small part of the membrane is considered. The forces generated by the stress and the internal pressure must be in static equilibrium.

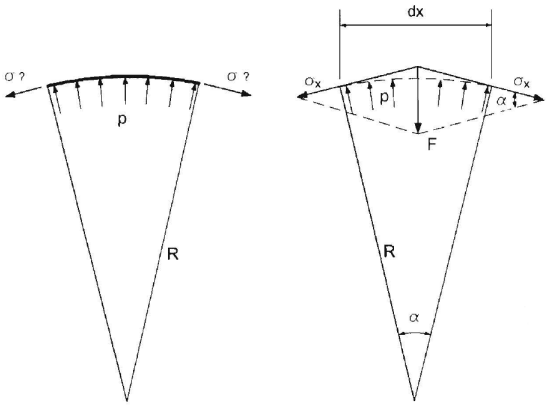

Figure 2.5: Detailed consideration of a small section from Figure 2.4

The equation to evaluate the internal air pressure can be obtained by vertical force equilibrium:

$$\Sigma F_z = 0 \tag{2.1}$$

$$p.dx - F = 0 \tag{2.2}$$

$$\sigma_x * t * \theta = F(\textit{vertical component of membrane stress}) \tag{2.3}$$

$$p = \frac{\sigma_x * t}{R}(\textit{Here t is the thickness of the membrane}) \tag{2.4}$$

For a three dimensional case, the expression for the internal pressure can be obtained similarly:

$$p = \frac{\sigma_x * t}{R_x} + \frac{\sigma_y * t}{R_y} \tag{2.5}$$

It can be concluded from the equation 2.4 and 2.5 that with the constant internal pressure, stress in the membrane is directly proportional to the Radius of curvature of the structure. This is the reason why sometimes steel cables are used in pneumatic structures, as they reduce the radius of curvature and consequently the stresses in the membrane. These equations are only applicable when there is no external loading. When the external loading will be acting, there will be deformations in the structure which will also change the stresses in the membrane. With change in the stresses, the stiffness of the whole structure will change as well. This concept can be explained through a very simple example of a string with prestress and a vertical force F acting in the middle of the string Fig. 2.6. In the first picture 2.6a, the string has zero stiffness when the horizontal force is 0, and the stiffness will increase with increase in the force. Thus equilibrium with the vertical force can be found. In the second picture 2.6b, the stresses will increase with deformation and with this the stiffness will increase as well. This phenomenon is called stress stiffening. [12]

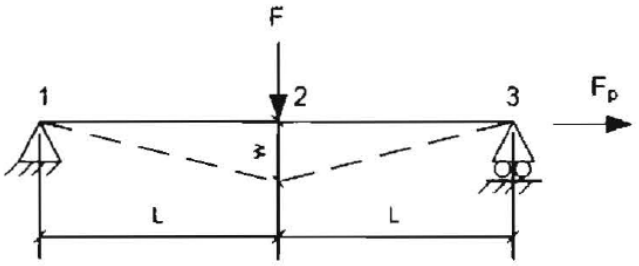

(a) 1 hinged 1 pinned

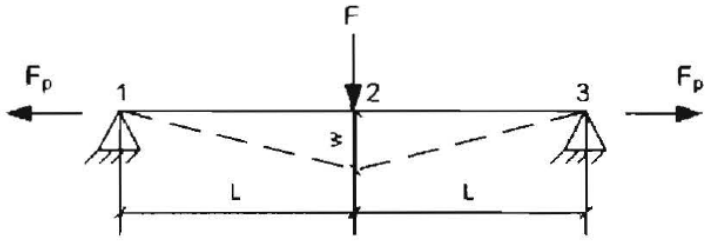

(b) 2 hinged

Figure 2.6: String with different boundary condition

As the behaviour of the pneumatic structure is complicated, a non-linear analysis is needed. This analysis takes into account the deformed shape and the change in stresses. Moreover, the structure is non-linear in many other ways, such as the material is non-linear in itself and the loading on the structure can also change with change in the geometry. [13]

2.5. Modeling of Membrane Structures

2.5.1. Form Finding

The initial undeformed form of the pneumatic structure is subjected to dead load, prestress and internal air pressure. As discussed earlier, the initial state of the structures needs to have static equilibrium between all these forces. This initial equilibrium geometry cannot be obtained easily, therefore experimental or numerical methods are required. The obtained geometry is a free form surface. This process of finding the initial geometry is called form-finding. As form-finding is an essential and challenging process, the fundamental equations and solution methods will be discussed in the following sections.

One way to get the initial geometry is by the experimental approach [14]. In this, a small scale model of the pneumatic structure is constructed with desired prestress and internal pressure. If the model satisfies all required conditions, it is used as basis for the up-scaled model and moreover for further structural analysis.

Typically, the deformation and stress in a structure is a result of the material characteristics, geometry of the structure and loading. In form-finding, it is different as the initial geometry is obtained depending on the equilibrium between the stress state, internal pressure and moreover has to satisfy the geometric boundary conditions. So basically, form finding is the inverse of typical structural analysis.

Numerical Form Finding

The Pneumatic structure's geometry differs from that of a conventional structure. The structure has to find it's initial shape under prestress. The resulting shape must be in static equilibrium and there should be a uniform stress distribution in the membrane.

Before 1970, the form finding was done using experimental approach which is explained earlier. In 1972, with the design of Munich Olympic complex, the method of design really changed, going from experimental to computational form finding. In current time, the computational softwares most commonly use three methods:

- transient stiffness
- force density
- dynamic relaxation

In all three methods, the iterative computation is done to find static equilibrium. Moreover, discretization of the membrane is done to implement the listed form finding methods. In the following section, each method will be discussed briefly.

- **Transient stiffness method**

  This method is based on small displacement theory which presumes that the deflection linearly varies with the force applied on the structure. For discretization line elements are used in both directions which meet each other at nodes Fig. 2.7.

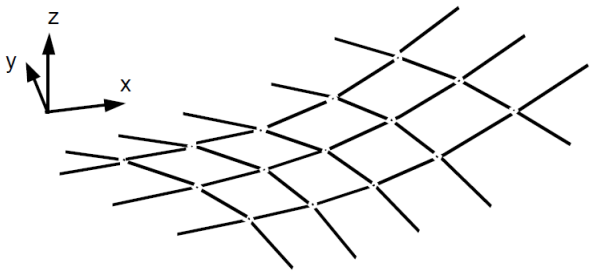

Figure 2.7: Surface Discretization

The process of form finding is initiated by assuming a geometry configuration X with known boundary conditions and prestress T. At each node the resulting internal force vector P in global directions can be calculated resulting from neighbouring elements. To achieve the static equilibrium, the resultant force P also known as residual force R needs to be zero. With stiffness of the structure as K and the displacement δ, the relation can be written as:

$$[K]\{\delta\} = \{R\} \tag{2.6}$$

and the resultant displacement to the force can be found as:

$$\delta = [K]^{-}1\{R\} \tag{2.7}$$

But, with this approach there is one problem that if the first taken geometry is not very close to the final obtained geometry, the residual forces are going to be big. And consequently the displacement will also be large. This invalidates the assumption of small displacement used while calculating the stiffness matrix. This can only be valid if the process is done in iterations with increasing residual force. This process is explained below.

With n denoting the nth iteration, the corresponding geometry will be $\{X\}_n$ and the calculated stiffness matrix corresponding to this geometry will be $[K]_n$. The total residual force at the starting can be calculated from the prestress and the external forces at each node. Then in order to satisfy the small displacement assumption, a small residual force of $\{\Delta R\}_n$ is applied which will result in small displacement $\{\Delta\delta\}_n$. Thus the displacement can be found as :

$$\{\Delta\delta\}_{n+1} = [K]_n^{-1}\{\Delta R\}_n \tag{2.8}$$

and the next geometry can be found as:

$$\{X\}_{n+1} = \{X\}_n + \{\Delta\delta\}_{n+1} \tag{2.9}$$

The new stiffness matrix $[K]_{n+1}$ is calculated based on the updated geometry. With this the residual force $\{R\}_{n+1}$ is found and iterated again by adding $\{\Delta R\}_{n+1}$ to find the increased displacement and subsequently the updated geometry. This iterative procedure is ended with the residual forces reaching zero. It should be kept in mind while deciding the incremental force that the small displacement assumption is satisfied.

- **Force Density Method**

Along with Transient stiffness method, this method was developed for the design of Munich Olympic roofs. Physical models were built for the assessment and the computational method to optimize the geometry of the model. The relation for equilibrium between the inner forces and the geometry is non-linear and can be solved by iterations [15]. The relation can be made linear by replacing the force by force densities [16]. But by the additional constraints, the problem becomes non-linear again and can be solved using gradient based method (Gauss-Newton Method). Moreover, Grundig et al. gave detailed calculation for Multihalle Mannheim geometry in Germany. From the physical model the coordinates of the nodes were used in the computational approach to find the equilibrium state. This method can be used to find the equilibrium state with the input as support conditions, load vectors at each node and the force density per element. Henceforth, a new geometry will be obtained with different value of force density. In 1970s, this method was more often used to optimize the geometry but not for the process of form finding.

- **Dynamic Relaxation Method**

In this method, the non-linear problem of form finding is equated to a dynamic problem which is solved by known methods in dynamic analysis. This requires to assume a fictitious mass at each node and also the damping. The resulting force at each node is treated as the residual force which will give acceleration to the fictitious mass. As the motion of the nodes will reduce, the structure will find an equilibrium shape with prestress. The difference between sum of membrane forces and the applied force which in case of pneumatic structure is internal air pressure is treated as the residual force.

$$R_n = \Sigma F_n - P_n \tag{2.10}$$

where:
R_n = Residual force at the considered node n
ΣF_n = Sum of internal forces at the considered node from neighbouring members
P_n = Applied Load at the considered node

The equation of motion can be written as:

$$M_n \ddot{y} + K_n y + C_n \dot{y} = F(t)_n \tag{2.11}$$

where:
M_n = Mass at the node
K_n = Stiffness
C_n = Viscous damping coefficient
$F(t)_n$ = Applied force
y = displacement

As the membrane lacks stiffness, the equation of motion along with residual forces can be written as:

$$R_i = M_n\ddot{y} + C_n\dot{y} \tag{2.12}$$

The system will reach equilibrium when the residual force will be less than the tolerance. The solution can be approximated using finite difference:

$$R_{(t+1/2)} = \frac{M}{\Delta t}(V_{t+1} - V_t) + \frac{C}{2}(V_{t+1} - V_t) \tag{2.13}$$

Where:
t = time step considered

Δt = time step

V_t = velocity of the node before the time increment

The velocity after time increment can be found by:

$$V_{t+1} = V_t \frac{\frac{M}{\Delta t} - \frac{C}{2}}{\frac{M}{\Delta t} + \frac{C}{2}} + \frac{R_{(t+1/2)}}{\frac{M}{\Delta t} + \frac{C}{2}} \tag{2.14}$$

The velocity at time t can be written as:

$$V_{(t)} = \frac{u_{(t+1/2)} - u_{(t-1/2)}}{\Delta t} \tag{2.15}$$

u = position of the node considered

In form finding, the membrane forces are known and the resultant equilibrium configuration is unknown. The stiffness in membrane comes from the membrane force and the resultant configuration. While choosing the value of mass, we must ensure that it can capture the vibration cycle while analysing. The viscous damping ensures the convergence of the solution. Though the mass, damping and time are fictitious, they are used for analytic convenience.

2.6. Example: Hemispherical Air Dome, Square base Air Dome

In this section, structural model of the Hemispherical Air Dome and the Square Base Air Dome, introduced in chapter 1 will be generated. This part concerns the FEM modelling of the Pneumatic Structures which will be further used in the Wind loading analysis. The membrane in the structure is prestress and internal air pressure is applied, which gives the tensile stress in the membrane. For this, the introduced form finding method will be used and non-linear analysis will be done.

2.6.1. Initial considerations

The hemispherical Air Dome as well as the Square base Air Dome gain their stiffness from tensile stresses in the membrane. This stress is induced in the membrane from the prestress and the internal air pressure. The membrane structure is usually mounted on a wall like structure where the connection is made air tight. This is important in a Pneumatic Structure as internal air pressure gives the tensile stresses in the membrane and excessive leakage of air will result in collapse of the structure.

As we know that the membrane material is very flexible, large deformations can happen in the structure and therefore the numerical model must take into account the geometric non-linear analysis.

For geometrically non-linear analysis, multiple loading cannot be applied just by super positioning of the forces. The structure deformation and stress state is the result of the order in which the forces are applied. The first step of applying the internal air-pressure and the prestress in the membrane can be considered as ”initial load case”. This will give the initial geometry with prestress in the structure, on which the wind loading analysis can be done. This is obtained by form finding computation.

In this thesis, a total of 3 geometries will be created. First geometry closely resembles the Hemispherical Air Dome for which the Wind Tunnel Testing literature is available. Proper setup of the Computational Fluid Dynamics will be done based on existing literature and the results will be verified. Then, based on the obtained CFD setup, a second more practical and space efficient Hemispherical Air Dome will be created and will be analysed under wind loading. To show the usability and capability of the developed parametric method to generate any pneumatic structure with geometric specifications, a Square base Pneumatic Structure will be modelled and further tested to see the interaction between the membrane and wind.

To setup the first model which is the Hemispherical Air Dome Structure, detailed geometry information and stress state of the structure is required. From the literature [17], the shape and dimension such as base diameter and height of the structure are known. The internal air pressure of the structure is known from the literature as well. The initial stress state of the membrane is not available. Moreover the membrane properties such as Shear Modulus and Poisson’s coefficient are also not available. Using trial and error, the prestress in the membrane is adjusted to get the geometrical dimensions similar to the existing literature. As the shape closely resembles the one with existing wind tunnel testing, we can compare the obtained Computational Fluid Dynamics results for this specific shape. We create this model to be the verification model to setup the Wind Tunnel Testing in Computational Fluid Dynamics environment.

2.6.2. Form Finding Computation

In the Finite element modelling of the membrane structures, the membrane surface is discretized using 3-noded triangular elements for the circular geometries and 4-noded quadrilateral elements for square geometries. For both element type, membrane action is chosen in SOFiSTiK. The element thickness is taken as 0.6 mm.

For the form finding of the membrane, the internal air pressure on the membrane is applied by defining a volume element on membrane elements. This will keep the internal pressure acting on the membrane perpendicular with each iteration during the form finding. In practical, with the deformation of the pneumatic structure due to external loading, the internal air shifts and consequently the pressure on the membrane due to internal air changes. This results in internal air pressure which is not homogeneous anymore. To take care of this phenomenon, an air element with volume equal to the structure is defined inside the structure. This air element will change the pressure on the membrane with deformation due to wind loading. To keep the model simple, the air is assumed to be incompressible.

For all models, the membrane properties were taken from the existing research [17]. The Polyester Fabric is considered with properties mentioned in table 2.2. For the form finding computation, SOFiSTiK software is used which uses the transient stiffness method 2.5.1. The initial geometry and properties such as prestress and internal air pressure is changed to get 3 different models.

E_w, MPa	E_f, MPa	v_{wf}	v_{fw}	G_{wf}, MPa	t, mm
200	200	v 0.1	0.09	0.1	0.6

Table 2.2: Reference Material Properties

- **Parametric methodology**

As mentioned before, SOFiSTiK is used in this work to perform the form finding of the membrane structure and the structural analysis. In the SOFiSTik, .dat files are used for user input such as membrane properties, nodal information of the geometry and moreover the forces as well. In this work, to make the process parametric, these .dat files are generated using the python programming in Grasshopper. The python code is written in such a way that a pneumatic structure with a base geometry of any shape can be generated. This will enable the re-usability of developed method.

Hemispherical Air Dome : Verification model (Model-1)

To get the first verification geometry, the prestress of 0.845 kN/mm^2 is assumed. The internal air pressure is taken as 1 kN/mm^2. The side length of each element is taken as 0.1 m. Figure 2.8 shows the initial flat mesh which is used for form finding. The finally obtained structure similar to the existing research was obtained and shown in figure 2.9.
As the whole developed method is parametric, any desired pneumatic structure can be modelled easily. To test this capability, 2 more models are created as mentioned before. Not just the shape, the internal pressure, prestress and the membrane properties can be adjusted easily. The whole method is developed in such a way that with just certain desired changes, the initial pneumatic geometry can be obtained.

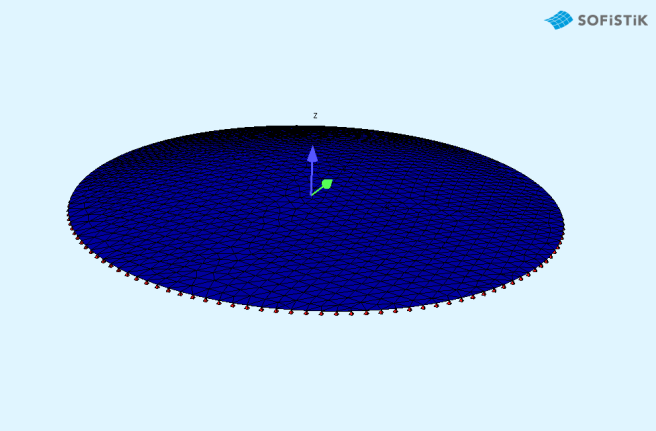

Figure 2.8: Verification model (Model-1) Flat Membrane

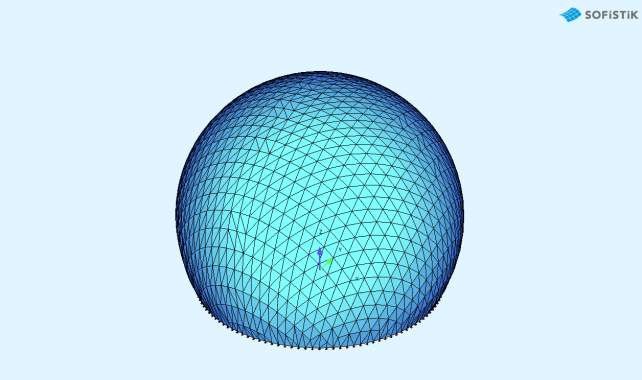

Figure 2.9: Model-1 Initial Geometry after form-finding

Hemispherical Air Dome : Model-2

Second model, which is Hemispherical in shape is generated by same internal air pressure of 1 kN/mm^2 and altered prestress of 1.1 kN/mm^2 . The base diameter is taken same as the verification model (Model-1) which is 2.1 m radius. For this model as well the side length of 0.1 m is used for each element. The flat membrane surface before the form finding is shown in Fig. 2.10. The generated shape after form finding is shown in figure 2.11. The reason to create this specific geometry is that in comparison to the verification model, this is more space efficient. Moreover, because of the less volume of the dome, less volume of air is required to be pumped in to withstand the structure, which also makes it energy efficient.

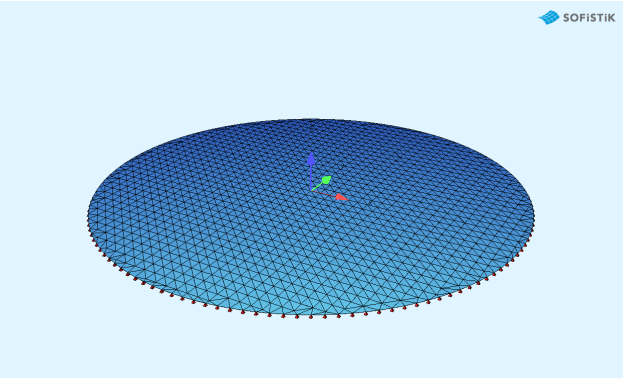

Figure 2.10: Model-2 Flat Membrane

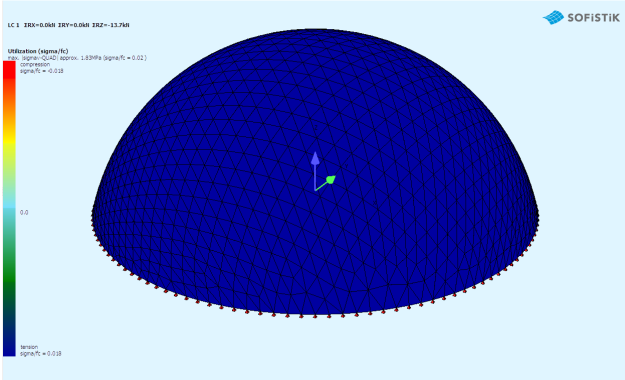

Figure 2.11: Model-2 Initial Geometry after form-finding

Square Base Air Dome : Model-3

A third model is generated which is a square base pneumatic structure. The reason to choose this specific geometry is to show the usability of the developed parametric method with not just circular geometry but with other shapes as well. As long as we know the geometry and boundary conditions, this developed method can be used. The square base model will also show the differences between the interaction of the wind with different geometries and the difference in responses. For this model, to have comparison with the second developed model, the membrane properties are taken same as other models. The side length of the structure is taken is 15 m and the side length of each element is taken as 1 m. The internal air pressure of 0.5 kN/mm^2 and prestress of 2.3 kN/mm^2 is taken. The flat square membrane before the form finding is shown in Fig. 2.12 and the geometry after form finding with prestress in the membrane is shown in Fig. 2.13.

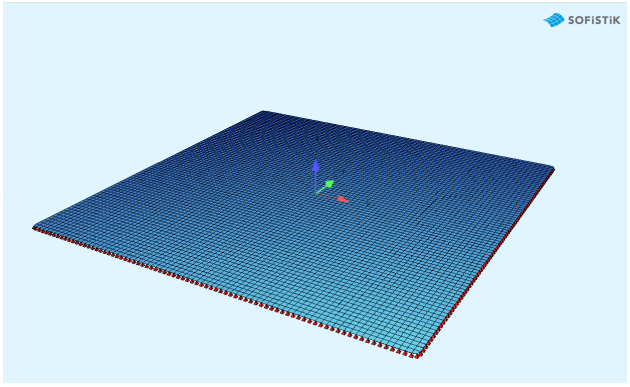

Figure 2.12: Model-3 Flat Membrane

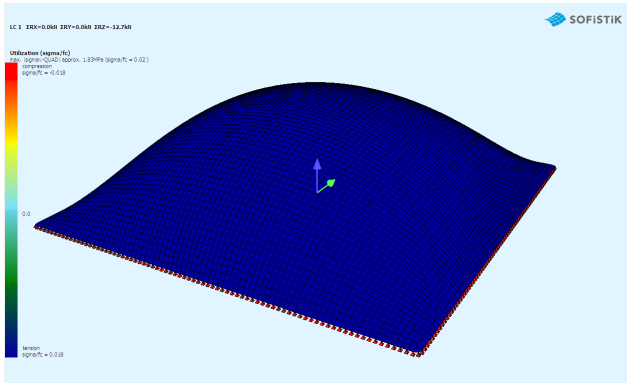

Figure 2.13: Model-3 Initial Geometry after form-finding

Prestressed model with internal air pressure are created using computational form finding. These models will be used for further analysis of Computational Fluid Dynamics.

2.7. Summary

Due to the lack of bending stiffness in membrane material, large deformations can happen in the structure. To use these structures in typical civil engineering, certain additional considerations need to be addressed such as geometrically non-linear effects. To withstand the external forces, tensile stresses in the membrane are used. In case of pneumatic structures, we get this tensile stress from internal air pressure and also from mechanical prestress. To obtain the initial geometry, prestress and internal air pressure are treated as initial load case. This is done by computational form finding. As a result of this computation, we obtain the initial shape and tensile stress state of the structure, which are used as initial configuration for further wind loading analysis.

This chapter comprises of the the form-finding methods which are used in general. Further, a parametric method is developed with is capable of generating pneumatic structures with known properties such as, membrane properties, internal air pressure, prestress and the boundary conditions. An example is taken from the existing research to verify the developed method. Further, two more structures are generated using the developed method to show the usability of the method with different shapes. These generated initial configurations will be used as the basis for further structural analysis of the structure when subjected to Wind Loading.

3

Modeling of Wind Loads on Membrane Structures

It's really difficult to predict the effects of wind loading on the membrane structure. This is because the membrane structures have complex load carrying behaviour and geometry. In this chapter, firstly the wind in general will be discussed and further we will discuss the ways to analyse the wind loading on membrane structures.

In this thesis, to analyse wind flow around the membrane structures and to calculate the resulting wind loading, numerical fluid simulation is used. For this, the fundamentals of fluid mechanics are important to discuss. As this work focuses on the interaction between wind flow and membrane, the deformation and consequently changing wind loading due to deformation needs to be considered. Therefore, modeling of moving boundary conditions is necessary.

The developed computational fluid dynamics method in the end is applied to three models developed in section 2.6. One thing to note here is that the structures considered in CFD numerical models are rigid.

3.1. Wind

For the wind flow and the wind loading on the structure, the local wind climate, shape of the structure plays an important role. The mean wind speed ($\bar{v}$) is the main parameter of the wind which is calculated for certain period of time. For example if we take the time period as 1 hour, the mean wind speed ($\bar{v}$) is going to be different hourly which is called as *long-term distribution* (3.1.1). Around the mean, there is *short term description* (3.1.2) as well, which is the fluctuation ($\tilde{v}$) around the mean. This can be visualized in figure 3.1.

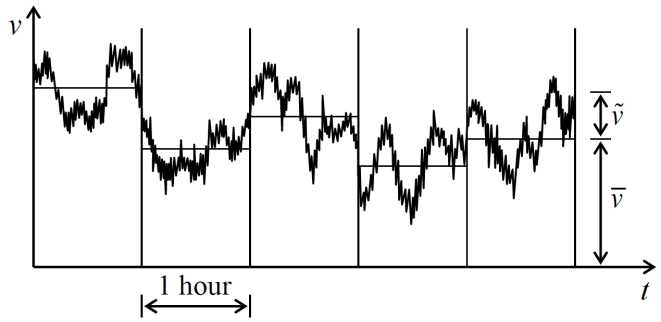

Figure 3.1: Variation in wind speed

The wind speed vector can be decomposed as:

$$v(t) = \begin{bmatrix} v_x(t) \\ v_y(t) \\ v_z(t) \end{bmatrix} = \begin{bmatrix} \bar{v}_x + \tilde{v}_x(t) \\ \bar{v}_y + \tilde{v}_y(t) \\ \bar{v}_z + \tilde{v}_z(t) \end{bmatrix} \tag{3.1}$$

Usually the coordinate system is adjusted such a way that the y and z components are negligible and the x direction is chosen as the mean wind speed direction then.

3.1.1. Hourly-averaged wind speed

Hourly averaged wind speed variation with height

The atmospheric air flow is influenced by the ground friction, pressure difference and Coriolis forces. The lowest atmospheric layer is important here to consider for structures, which is mostly effected by the ground friction. This ground friction gives rise to the wind profile development which is the variation of wind speed with height (z). The wind profile can be theoretically described by the logarithmic function 3.2 [18]. A wind profile can be visualized in figure 3.2

$$\bar{v}(z) = \frac{u_*}{\kappa} ln \frac{z-d}{z_o} \tag{3.2}$$

where:

$\bar{v}$ (z) = mean wind speed at height z
κ = Von Karman constant = 0.4
d = average height of the building
u_* = shear velocity
z = height above earth
z_o = roughness length of terrain

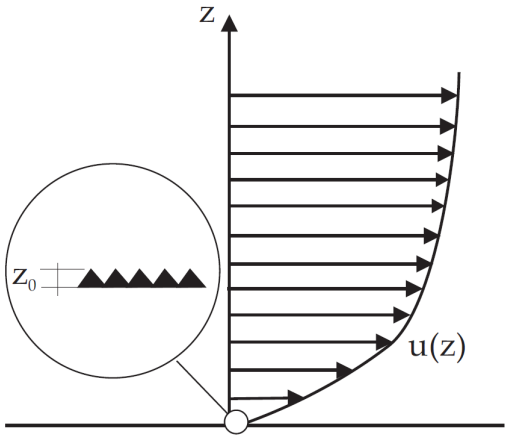

Figure 3.2: Velocity distribution in boundary layer [19]

Instantaneous value of the mean wind speed

The instantaneous value concerns the hourly mean wind speed. A distribution of the instantaneous hourly wind speed can be given by Weibull distribution function. The function fairly described the distribution for 10 m height with wind speed in the range 4 to 16 m/sec. [20]

$$F_{\bar{v}}(v) = 1 - exp(-(v/v_0)^k) \tag{3.3}$$

where:
$F_{\bar{v}}(v)$ is the probability of $\bar{v}$ smaller than v
k is the shape parameter

3.1.2. Wind fluctuation within one hour

Turbulence intensity and profile

Wind speed fluctuation $\tilde{v}$ magnitude is expressed in terms of standard deviation σ_v (3.3). With the height from the earth, the standard deviation varies as well (3.4). Power profile law [18] can properly describe the standard deviation variation (3.4). More turbulence is generated by the rough earth surface. Often quantity turbulence intensity (I) is used to define the turbulence with height which is obtained by dividing the standard deviation with mean wind speed. The plot of turbulence intensity with respect to height is shown in figure 3.4.

$$\sigma_v(z) = \sigma_v(h_0)\left(\frac{z-d}{h_0}\right)^{\delta} \tag{3.4}$$

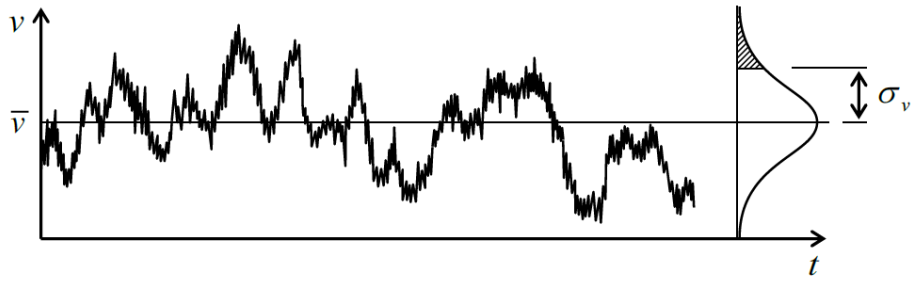

Figure 3.3: Turbulence

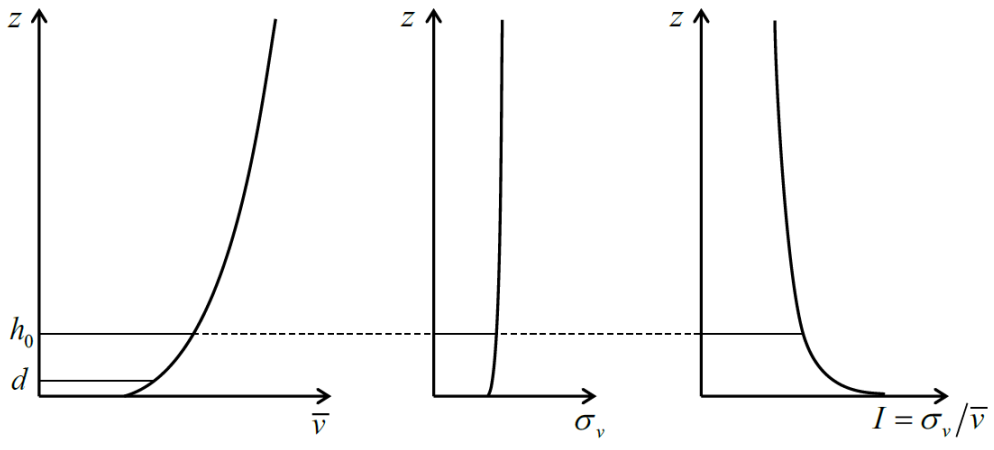

Figure 3.4: Variation of wind speed ($\bar{v}$), standard deviation (σ_v) and Intensity (I) with respect to height

The auto spectrum

The spectra for fluctuations parallel to the mean wind direction is derived by several researchers. As the spectra changes with time and place, mostly the reduced spectrum F_D is used.

$$F_D(f) = \frac{f.S_{vv}(f)}{\sigma_v^2} \tag{3.5}$$

where

σ_v = standard deviation of wind speed
S_{vv} = variance spectrum
$x = fL/\bar{v}(10)$ = dimensionless frequency
f = frequency
$\bar{v}(10)$ = mean wind speed at 10 m height
L = characteristic length

The most commonly used reduced spectra are by Davenport [20], Harris [21] and Simiu [22]. The shape of spectra is a function of x which is independent of the height. The spectra can be seen in figure 3.5

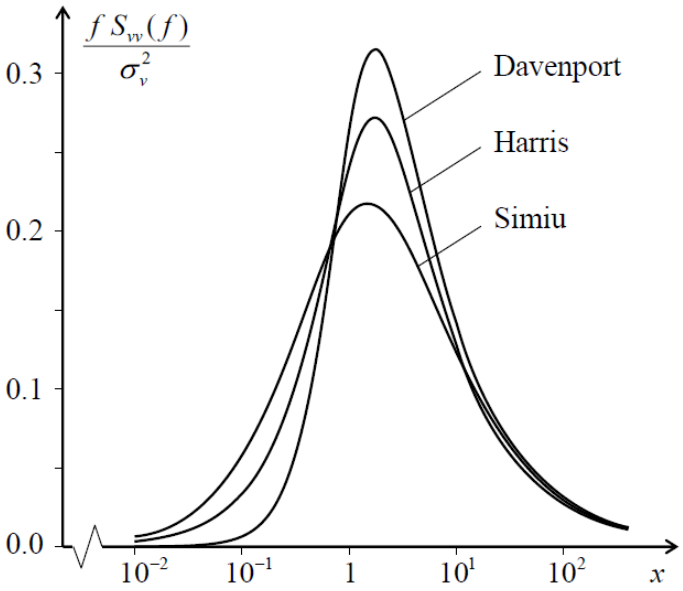

Figure 3.5: Spectra by Davenport [20], Harris [21] and Simiu [22]

In the Eurocode, the spectra by Solari is used:

$$F_D = \frac{6.8x}{(1+10.2x)^{5/3}} \tag{3.6}$$

3.1.3. Wind consideration in this work

In this thesis work, the ground surface is considered as smooth and therefore the variation of wind speed with the height not be presented. Consequently, the wind speed with respect to height is taken constant in this work. Moreover, as the presented work concentrates more on the simulation of fluid-structure interaction, the averaged wind speed with respect to time is taken constant and moreover the wind fluctuation (wind gust) with respect to time is neglected as well. An example of wind considered in this thesis work with respect to the wind plot shown in figure 3.1 is shown in figure 3.6.

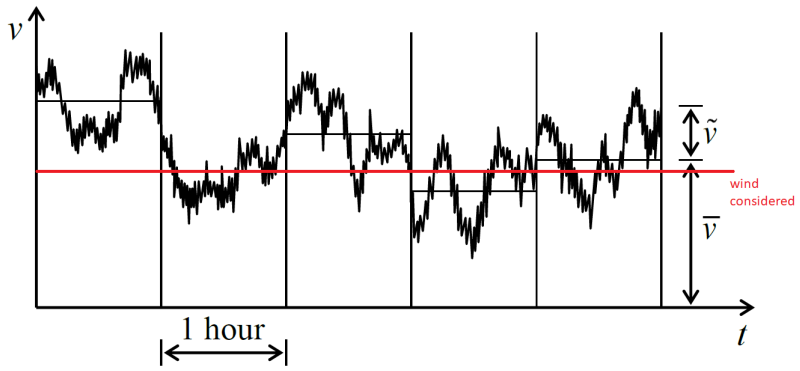

Figure 3.6: Example of wind consideration in this work

3.2. Wind Loading on Membrane Structures

The loading nature and cable stress in light weighted membrane structures is most commonly attributed to wind load.[23].

Quasi-static approach

If we assume no dynamic effects for membrane structures and negligible deformation, we can consider wind loading as a static load case. With these assumptions, the wind loading on the structure can be calculated using building codes such as EN1991-1-4 [24].

Using EN1991-1-4, the average wind load on the structure at certain point can be calculated as the product of dynamic pressure, the pressure coefficient c_p and certain coefficients. The value of the pressure coefficient depends on the building geometry and the incident angle of the wind. These coefficients include the effect of topology, exposure, wind turbulence, etc. c_p at the point of interest can be calculated as the ratio of characteristic pressure value and dynamic pressure q_{ref} at the reference height z_{ref}. Where $\overline{u}_{ref}$ is the mean velocity at z_{ref} height and ρ is the air density. In general the value of c_p is calculated from the wind tunnel testing of a scaled down similar model of structure [25].

$$p = c_p * q_{ref} w_{ref} = \frac{1}{2} * \rho * \overline{u}_{ref}^2 \tag{3.7}$$

The distribution of c_p on simple structures are usually available in building codes and existing literature such as [26] and [27]. Geometries for which the data of pressure coefficient distribution is not available, wind tunnel testing has to be done. With membrane structures it's even more common because of the fact that the structure's geometry requires static equilibrium between forces and can have free form shapes.

Dynamic Effects

Membrane Structures are generally recognized as lightly damped structures. As the weight of membrane is often less than the weight of air surrounding it, the air has a damping effect due to its inertia. In general it is considered that membrane structures are insusceptible to aerodynamic instability [23]. Though a local flutter can happen in the membrane structures at the places where a change in wind direction can significantly change the surface pressure. This can usually happen at the windward side of the structure near the ground support, as the incident angle of the wind is maximum there.

Membrane structures can have fatigue effects as they can have large deformations. This will reduce the lifespan of the structure and can even have acoustic and visual effects problems. As the membrane structures are very thin, they can be punctured or can tear from flying debris in extreme wind conditions. An idea of this effect can be found in [28].

Experimental Approach

As mentioned before, wind tunnel testing is important for the membrane structures due to their varying geometries. Wind tunnel testing is usually performed on the rigid models of the structures, and therefore cannot consider the change in wind flow around the structure due to deformations. It is true that the wind pressure on the structure can be calculated from wind tunnel testing and consequently the deformation can be found using FEM analysis. Although this approach is ignoring the effect of deformation in the membrane on the wind flow, this is the only option. Example results of the wind tunnel testing on membrane structure rigid models can be found in the literature such as [23].

Sometimes for advanced purposes, aeroelastic small scale model of the structure is used. This model's accuracy to predict the behaviour is very limited because of the similarity requirement between the actual model and the small scale testing model. Similarity between these models is required for the flow condition and dynamic structural properties [29]. Some examples of wind tunnel testing of aeroelastic models can be found in [30] and [31].

Numerical Approach

There are a few occurrences where for analysis of the membrane structure, researchers have applied numerical methods to the Computational Fluid Dynamics. Some examples are [32], [33].

In this thesis, numerical approach is used to analyse the wind loading on the structure. In chapter 4 4, the coupling of structural modelling with wind flow modelling is done to predict the Fluid Structure Interaction (FSI). In the following, some basic fundamentals of fluid mechanics will be discussed.

3.3. Fundamentals of Fluid Mechanics

3.3.1. Basic Equations

Three building fundamentals of the Fluid Dynamics are as follows: [34]:

- Conservation of mass
- Newton's second law
- Conservation of energy

To derive basic equations, chemically and isothermally inert flow is assumed. Therefore, conservation of energy principle is not relevant. Based on a point in material, the derivation of Conservation law can be done. The Eulerian description is frequently utilized in fluid mechanics. The spacial region in which the conservation laws are defined is called control volume, which has fixed dimension in fluid domain Ω_F.
Newtonian fluid is assumed in the analysis. The stress tensor σ for the fluid can be written as:

$$\sigma = -(p + \frac{2}{3}\mu\nabla u)I + 2\mu D \tag{3.8}$$

According to Reynolds transport theorem, the rate of change of any property N within a controlled volume is equal to the rate of it's change with respect to time and the flux of N through the controlled surface equation 3.9. Here u is the velocity vector and n is the normal unit vector to the surface S.

$$\frac{d}{dt}\int_V NdV = \int_V \frac{d}{dt}NdV + \int_S N(n.u)dS \tag{3.9}$$

Conservation of mass

This law states that the mass (m) of fluid inside a control volume shall remain constant with time.

$$\frac{dm}{dt} = \frac{d}{dt}\int_V \rho(x,t)dV = 0 \tag{3.10}$$

Using Reynolds transport theorem for density field:

$$\frac{d}{dt}\int_V \rho dV + \int_S \rho(n.u)dS = 0 \tag{3.11}$$

Now applying Gauss divergence theorem on equation 3.11.

$$\int_V \frac{d\rho}{dt}dV + \int_V \nabla.(\rho u)dV = 0 \tag{3.12}$$

Finally writing the differential form of the equation:

$$\frac{d\rho}{dt} + \nabla.(\rho u) = 0 \tag{3.13}$$

Conservation of momentum

Newton's second law states that the momentum is influenced by the force f:

$$\frac{d(mu)}{dt} = f \tag{3.14}$$

Using the Reynolds transport theorem 3.9, the rate of change of momentum per unit mass ρu can be written as 3.15:

$$\frac{d}{dt}\int_V \rho u(x,t)dV = \frac{d}{dt}\int_V \rho u dV + \int_S \rho u(n.u)dS = \int_S \sigma.ndS + \int_V \rho b dV \tag{3.15}$$

Using Gauss divergence theorem in equation 3.15, we get:

$$\frac{d}{dt}\int_V \rho u dV + \int_V \nabla.((\rho u) \otimes u)dV = \int_V \nabla.\sigma dV + \int_V \rho b dV \tag{3.16}$$

Equation 3.16 can be written in differential form as:

$$\frac{d(\rho u)}{dt} + \nabla.((\rho u) \otimes u) = \nabla.\sigma + \rho b \tag{3.17}$$

This equation describes the conservation of momentum and is historically known as Navier-Stokes equation. These equations form the partial differential equations which are non-linear in nature. To solve these equations, initial and boundary conditions are required, which will be introduced in the following section.

Initial and boundary conditions

At time t=t_0, the velocity vector is defined in fluid domain Ω_F. The conservation of mass principle has to be satisfied here.

$$At\ t = t_0, \qquad u = u_0 \ \ in \ \ \Omega_F \qquad with \quad \nabla.u_0 = 0 \tag{3.18}$$

The boundary conditions are divided into Dirichlet Γ_D and Neumann Γ_N, same as in Solid Mechanics. A prescribed velocity is defined for Dirichlet boundary condition 3.19:

$$u = \hat{u} \quad for \quad t \in [t_0, T] \tag{3.19}$$

The Neumann boundary condition can be defined as prescribed normal stress 3.20:

$$t = n.\sigma = \hat{t} \quad for \quad t \in [t_0, T] \tag{3.20}$$

The incompressible flow condition with conservation of mass implies that the volume entering the fluid domain should be equation to the flow coming out 3.21:

$$\int_{\Gamma_D} n.\hat{u} d\Gamma_D = 0 \quad for \quad t \in [t_0, T] \tag{3.21}$$

The boundary conditions which are used in this work are:

1. **free slip boundary condition**

   Only the normal component of the velocity is prescribed at the boundary surface in free slip boundary condition 3.22:

   $$n.u = n.u_w \tag{3.22}$$

2. **no slip boundary condition**

   With no slip boundary condition at the walls, the velocity at the wall is 0 and it develops with the distance. This velocity development is called the law of wall.

   $$u = u_w \tag{3.23}$$

3. **inflow boundary condition**

   This is a Dirichlet type boundary condition. At the boundary surface, velocity of the flow as well as the distribution is prescribed.

4. **outflow boundary condition**

   To simulate the actual wind flow, the decision of outflow condition is difficult. To simplify, zero gradient condition or average pressure boundary condition is chosen.

Incompressibility condition

In this thesis, the fluid flow is considered to be incompressible, which means that the fluid density will remain constant. The incompressible condition applied with conservation of mass condition, the equation 3.13 becomes:

$$\nabla.u = 0 \tag{3.24}$$

Conservation of momentum equation (3.17) can be modified as:

$$\frac{du}{dt} + \nabla.(u \otimes u) = \frac{1}{\rho}\nabla.\sigma + b \tag{3.25}$$

Equation 3.8 can be simplified using 3.24 to:

$$\sigma = -pI + 2\mathrm{M}D \tag{3.26}$$

3.4. Wind Loading analysis on Membrane Structures using Computational Fluid Dynamics

Here the fundamentals of fluid mechanics and numerical methods will be applied to analyse the wind loading on membrane structures. The simulation will be done in such a way that it resembles the results from wind tunnel testing of similar geometry. When CFD analysis is applied to simulate the wind flow around a structure, it is called Computational Wind Engineering (CWE).

3.4.1. Computational Wind Engineering

The numerical simulation of wind in Computational Wind Engineering is primarily based on the Navier-Stroke equations. Till now, engineers are hesitant in using the results from CWE. But with the increasing computational power and technology, this could change. The quality of result obtained from CWE depends a lot on the experience and knowledge of the engineer who is performing the analysis. Still, the CFD analysis is not very accurate in predicting the fluctuating wind pressure due to turbulence. Because of this, the turbulence has to be kept simplified in order to manage the computational efforts. Use of CFD to predict the wind flow around structure can still be very helpful as a supplement to experiments, but will not replace wind tunnel testing in near future.

Guidelines for Computational Wind Engineering

As mentioned before, the accuracy of wind flow simulation around the structure using CFD is dependent on the experience and knowledge of the engineer. The recommendations for the simulation can be found in Best Practice Guidelines. They contain summarized information, knowledge and discussion to accurately simulate wind flow from different publications and books. In this thesis, Best Practice Guidelines are used to model the CFD simulation [35]. Decisions such as resolution of computational grid, approximations, convergence criteria are taken from this guideline.

3.4.2. Definition of the Computational Domain

Brief knowledge and literature regarding the computational domain definitions can be found in [36], [37], [38]. CFD analysis has certain limitations, which includes the modelling of limited distance in horizontal and vertical direction in the computational domain. The fluid domain should be large enough to contain the area of interest, which in this case is the structure. The wind flow around the structure has to be approximated by defining appropriate boundary conditions.

Size of the Computational Domain

The simulation of the wind around the structure has to resemble with the wind in wind tunnel testing of the model and therefore, the requirement has to be similar. The floor plan of the computational domain is assumed to be rectangular. The dimension of the domain should be large enough, so that it doesn't effect the wind flow on the structure. The vertical height of the domain is recommended to be 5-6 H_{max} according to [37], where H_{max} is the maximum height of the structure. In lateral direction, it is recommended to have $5H_{max}$ distance. A maximum of 3% blockage ratio is recommended. While simulating the wind tunnel testing if the inflow conditions are unknown, larger fluid domain dimensions can be chosen. The outflow of fluid domain should be at a distance of 10-15 H_{max} from the building. These recommendations can be visualized in Figure 3.7.

Boundary Conditions

To simulate the results similar to that of wind tunnel testing, the choice of boundary conditions is crucial. The boundary conditions should resemble the boundary conditions of Wind tunnel testing.

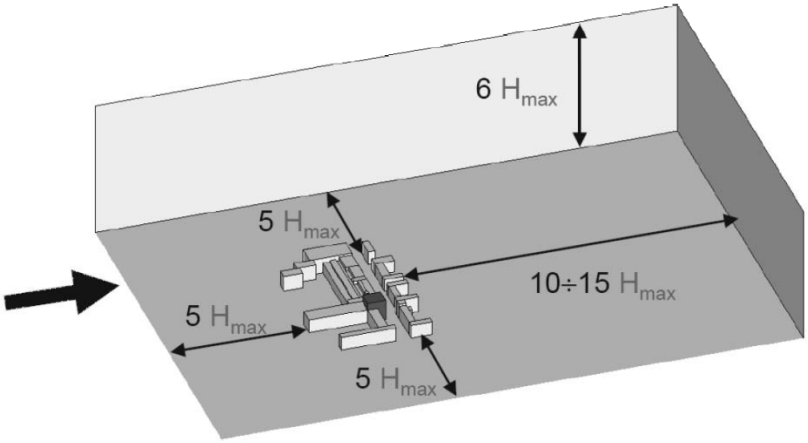

Figure 3.7: Recommended Computational Fluid domain dimensions [37]

1. **inflow boundary condition**

   The wind speed at the inflow is taken as 40 m/sec from the existing research [39]. As the initial goal is to setup a computational fluid model which resembles the wind tunnel testing in existing research, its important to take similar boundary conditions. In reality, the velocity of the wind is zero at the ground level and it increases gradually with height. But, as in wind tunnel the boundary walls are smooth, the wind velocity is constant throughout the height of inlet. To simulate the similar effect, the wind velocity is taken constant with respect to height in computational fluid model.

2. **Walls boundary conditions**

   The boundary condition for side walls is taken as slip condition from the existing research [39]. This condition is similar to the condition we have in wind tunnel testing. This condition implies that the wind velocity near the side walls will be equal to the wind velocity prescribed at the inlet. The surface of structure is taken as no-slip boundary condition. This would imply that the wind velocity will be zero near the membrane of the structure.

3. **Outflow boundary condition**

   The outflow boundary condition has to be kept in such a way that it does not influence the flow at the structure in the fluid domain. The pressure at the outlet is kept as 0.

3.4.3. Validation of developed model

Though we are using a certified software, the verification of the numerical simulation is important. We will need to verify the wind simulation around the structure. The results obtained on the basis of developed numerical simulation needs to be verified. There are two ways to validate these results :

1. **Wind Tunnel Experiments Comparison**

   For this comparison, small scale models are simulated in CFD. To accurately compare the obtained results, there are certain criteria which need to be fulfilled.

2. **Full scale experiments comparison**

   With respect to Wind tunnel testing, full scale experiment comparison is difficult to achieve because there are large uncertainties in the boundary conditions. Simulating such a large structure in CFD modelling also brings certain challenges such as high computational effort.

   After the initial validation with respect to existing research, slight modifications can be made in the setup. This will enable us to predict the wind loading on the deformed structure.

3.5. Static Wind Load Analysis on developed Pneumatic Structures

The simulation of wind flow around the structure is done using Ansys CFX 11. The modeling of wind flow is done using the conditions described in the earlier sections.

3.5.1. Ansys CFX Software

CFX is a commercial Computational Fluid Dynamics program. It is used to simulate fluid flow around various kinds of applications in a virtual environment. There are various fields such as, aircraft, fans, pumps, turbine engines where this software can be used. In the eighties and early nineties, CFX was known as FLOW3D, which was later renamed as CFX-4 in mid-nineties. The computational fluid dynamics setup of developed models in section 2.6 will be shown in the following sections.

3.5.2. Setup

Ansys CFX shall be used here to setup three computational models to analyse the wind flow around the structures. Here, the previously mentioned Best Practice Guidelines is used to appropriately setup the models.

Wind Direction : In order to simulate similar effect as in wind tunnel experiment, the wind is considered to be parallel to the axis of symmetry which is the positive y-direction. It is assumed that there is no large object near the structure which could effect the wind flow. As mentioned before (3.4.2), to verify the results with existing research the wind velocity is taken as 40 m/sec.

1. **The computational Domain**

   To reduce the computational effort required to simulate the wind flow around the structure, the CFD simulation is divided into two domains named as inner domain and outer domain. We need the mesh near the structure to be fine in order to correctly simulate the wind flow near the structure. The mesh away from the structure can be coarser. So, it is a better idea to divide the domain in two sections to create structured mesh.

   Outer Domain

   In the outer domain of the simulation, coarser discretization is used. This will help us to reduce the computational effort, as we will have less finite volume elements. For the discretization, tetrahedral elements are used. Inflation is used to further reduce the computational effort. Inflation means that the size of the element will increase gradually as we go further from the point of interest. The dimension of the fluid domain is decided using the recommendations mentioned in section 3.4.2.This will ensure that the boundary conditions have least influence on the flow around the structure.

   Inner Domain

   In the inner domain of the simulation, fine discretization is used. For this domain as well tetrahedral elements are used. To accurately model the flow near the structure surface and the flow separation phenomena, prism elements are used.

   CFD Model - 1 (Verification model)
   Visualization of the first developed verification model is shown in the figures below. The division of fluid domain into inner and outer domain can be seen in figure 3.8. The structured mesh developed with the divided domain can be seen in figure 3.9. Here we can see that the mesh is coarser in the outer domain and fine in the inner domain. As mentioned before, tetrahedral elements are used for the discretization of the fluid domain with a maximum size of 3 m, maximum internal domain size is taken as 0.15 m, this can be visualized in figure 3.10. And the prism layers created near the structure surface with first layer thickness of 0.005 m can be closely seen in figure 3.11.

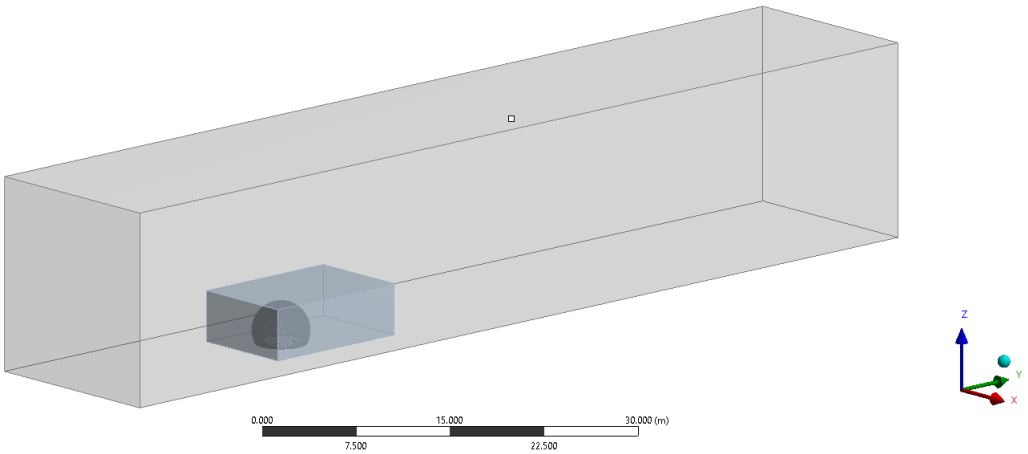

Figure 3.8: Inner and Outer Fluid Domain in Model-1

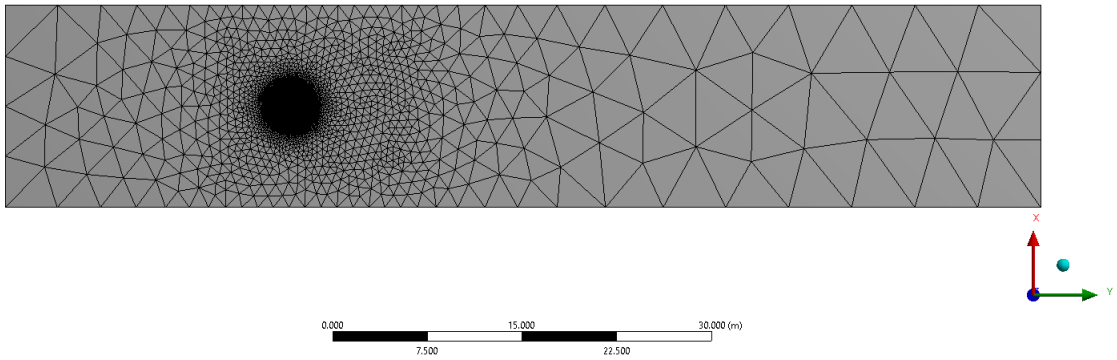

Figure 3.9: Inner and Outer domain discretization in Model-1

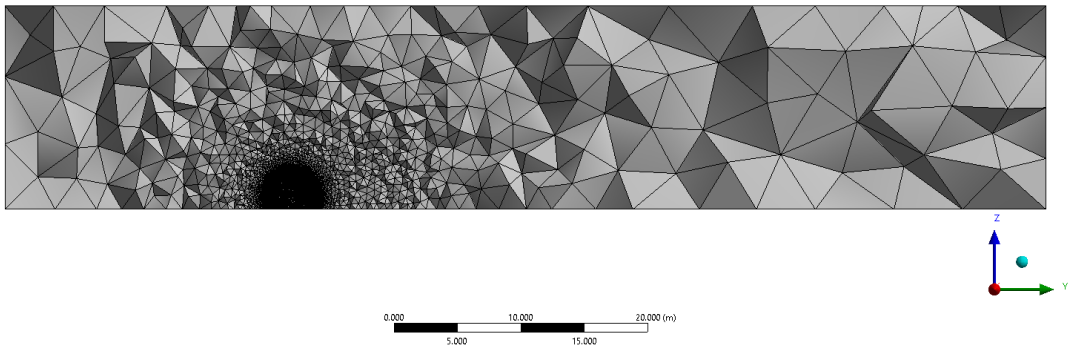

Figure 3.10: Mid-cross section of model 1 showing tetrahedral discretization

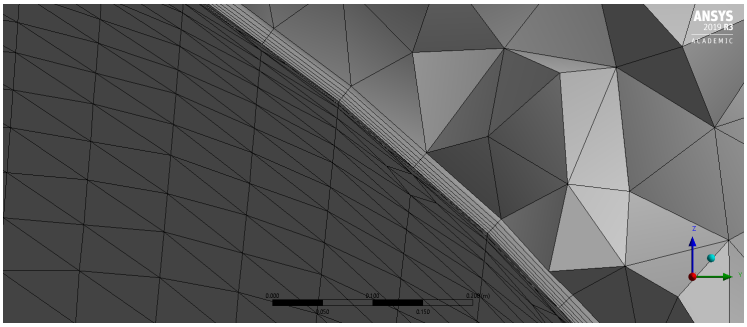

Figure 3.11: Inner Domain: boundary layer prism elements in model 1

CFD Model - 2

Visualization of the second developed model is shown in the figures below. Similarly as before, the fluid domain is divided into inner and outer domain (figure 3.12). The structured mesh developed with the divided domain can be seen in figure 3.13. Tetrahedral elements are used for the discretization of the fluid domain with a maximum size of 3 m, maximum internal domain size is taken as 0.15 m, this can be visualized in figure 3.14. Figure 3.15 shows the prismatic layers with thickness of 0.005 m.

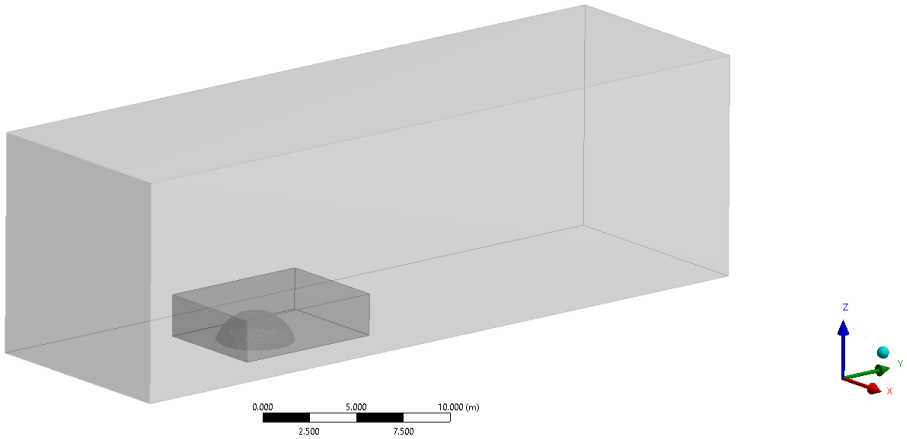

Figure 3.12: Inner and Outer Fluid Domain in Model-2

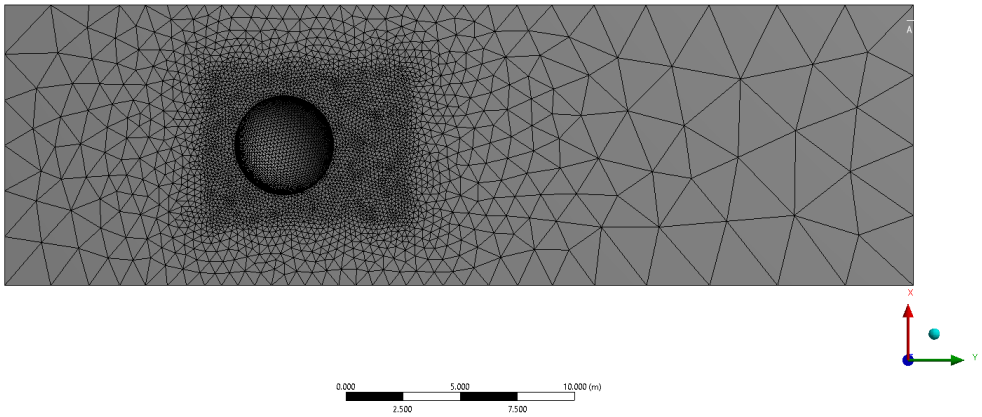

Figure 3.13: Inner and Outer domain discretization in Model-2

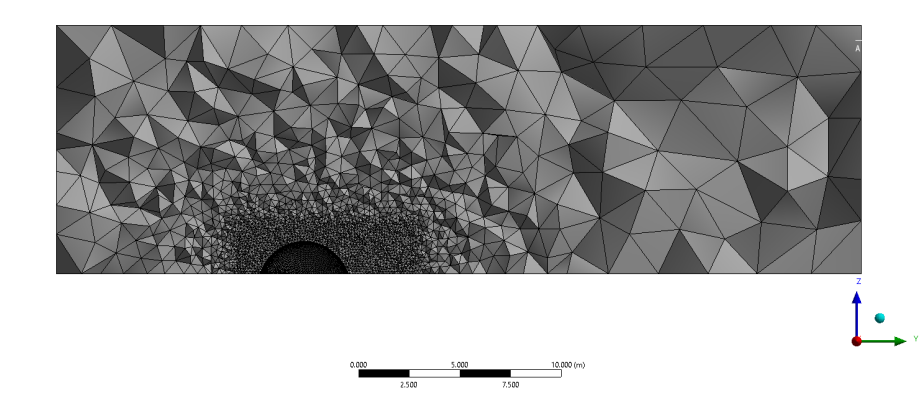

Figure 3.14: Mid-cross section of model 2 showing tetrahedral discretization

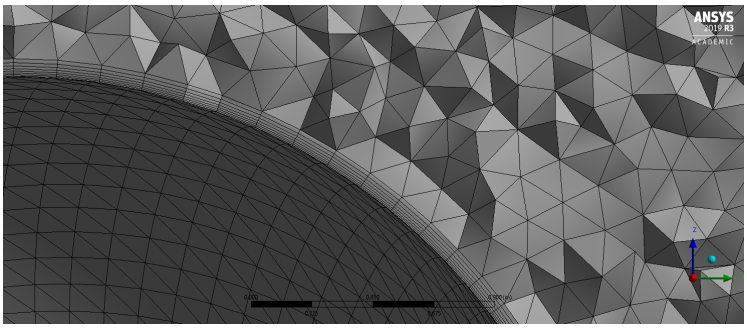

Figure 3.15: Inner Domain: boundary layer prism elements in model 2

CFD Model - 3

Visualization of the third developed model is shown in the figure below. The inner and outer fluid domain can be seen in figure 3.16. The structured mesh developed with the divided domain can be seen in figure 3.17. Similar to before, tetrahedral elements are used for the discretization of the fluid domain with a maximum size of 10 m, maximum internal domain element size is taken as 1.5 m and this can be visualized in figure 3.18. And the prism layers created near the structure surface with first layer thickness of 0.05 m can be closely seen in figure 3.19.

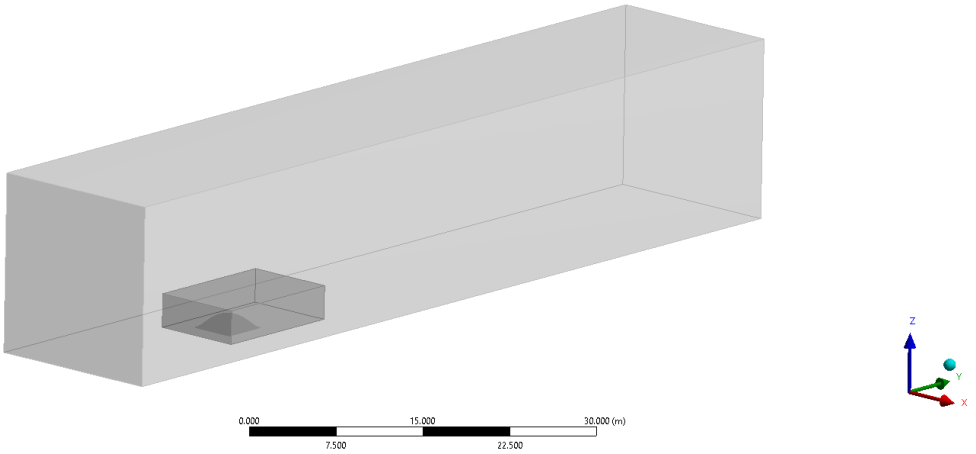

Figure 3.16: Inner and Outer Fluid Domain in Model-3

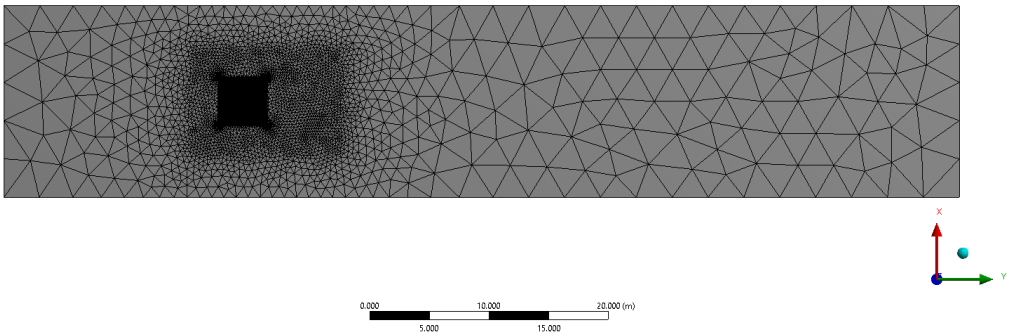

Figure 3.17: Inner and Outer domain discretization in Model-3

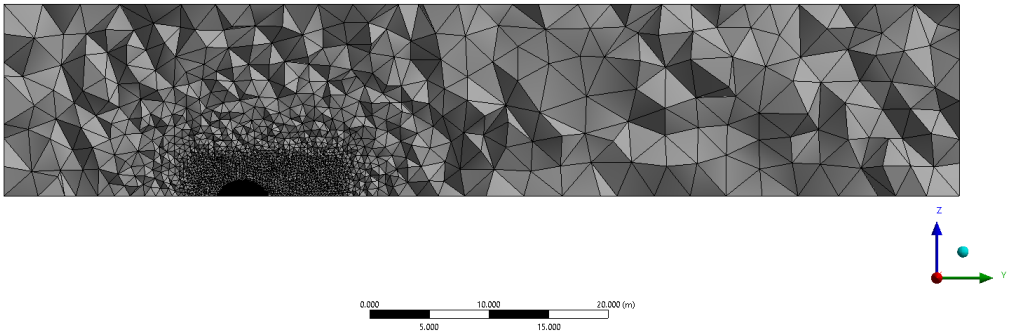

Figure 3.18: Mid-cross section of model 3 showing tetrahedral discretization

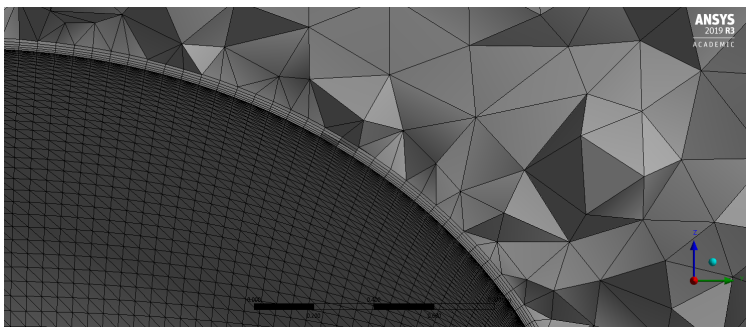

Figure 3.19: Inner Domain: boundary layer prism elements in model 3

2. **Applied Models**

As in wind tunnel testing, the turbulence in the wind is usually very low. So, a turbulence of 1% is adopted for the modelling of wind flow. The value of wind density is taken as the recommended value of 1.25 kg/m^3 from the Eurocode 1 [1]. As the fluid is assumed to be incompressible, the density will remain constant. The computational modelling is for steady state. For the convergence of simulation, a limit of 10^{-5} is chosen for RMS of transport quantities.

3.5.3. Results and Discussion

For the analysis of Pneumatic Structures when subjected to wind loading, the surface pressure on the membrane is of prime concern. To verify the modelling of wind flow around the Model-1, the dimensionless pressure coefficient c_p will be compared to the existing data from wind tunnel testing.

Visualization of the Wind Flow around the developed structures

The wind flow is simulated around the structure with visualization of the wind movement around the structure. Moreover, the pressure distribution on the structure due to wind will be shown as well. For the verification model-1, the pressure distribution contour will also help to verify the model.

1. **Wind Flow around the developed model-1**

   From the simulation of wind on the Model-1, the velocity vector in the symmetrical plane parallel to the wind velocity is shown in figure 3.20a. The distribution of wind pressure on the structure can be seen in figure 3.20b. The air flow gets deflected when the wind hits the membrane surface. We can also observe that the velocity of wind increases at the top of the structure, this can be explained by Bernoulli's theorem. Because of the structure, the cross-section of the domain decreases and consequently the wind velocity increases. We can also observe that at the top of the structure separation of wind from the structure is occurring. Because of this negative wind pressure (suction) occurs. Because of complex circulation at the bacl of structure, an error can be there. But, this error can be ignored as the maximum wind pressure at the top and front of the structure will dominate the behaviour of the structure.

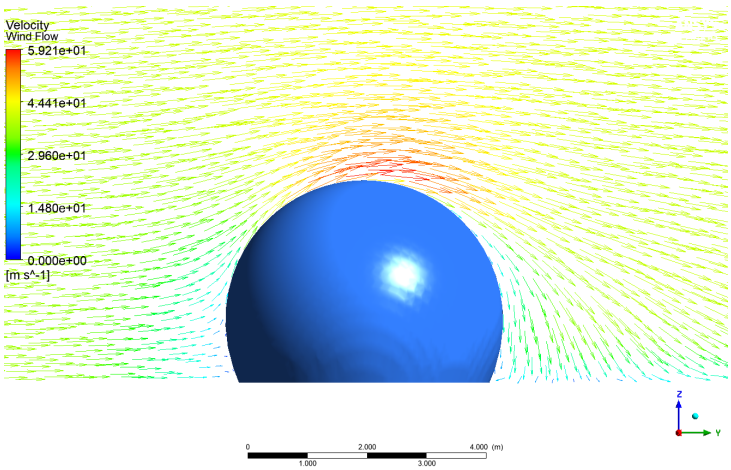

(a) Wind flow around the Model-1

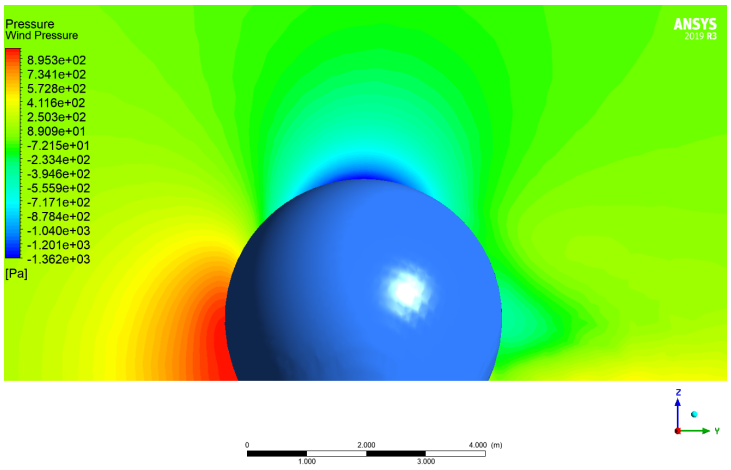

(b) Wind Pressure around the Model-1

Figure 3.20: Simulation of Wind around Model-1

2. **Wind Flow around the developed model-2**

   In a similar way as the verification model-1, the computational fluid model of the model-2 geometry can be created as well. The wind velocity vector in the positive y direction is shown in figure 3.21a. The distribution of pressure on the structure due to wind is shown in figure 3.21b.

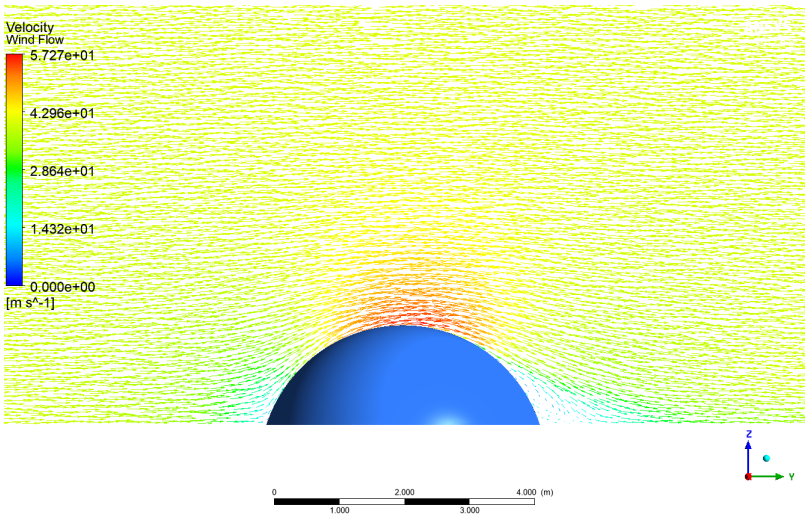

(a) Wind flow around the Model-2

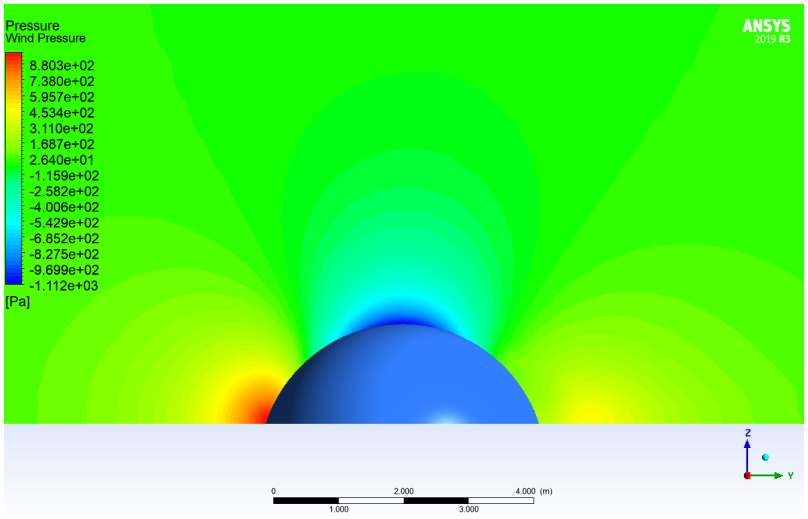

(b) Wind Pressure around the Model-2

Figure 3.21: Simulation of Wind around Model-2

3. **Wind flow around the developed model-3**

   Though the geometry of Model-3 is different that the other 2 developed models, the computational fluid modelling can be done in a similar way. Figure 3.22a shows the wind velocity vectors around the structure and the wind pressure on the structure due to the wind is shown in figure 3.22b. To further verify that the modelling is appropriate, we can observe that though with the same wind velocity inflow, the pressure occurring on the square geometry membrane is less than the other developed models. This is due to the fact that the angle of incidence of wind on membrane is less than the other geometries.

   To verify the first developed model from the existing data of wind tunnel testing, the dimensionless pressure coefficient will be compared in the following section 3.5.3.

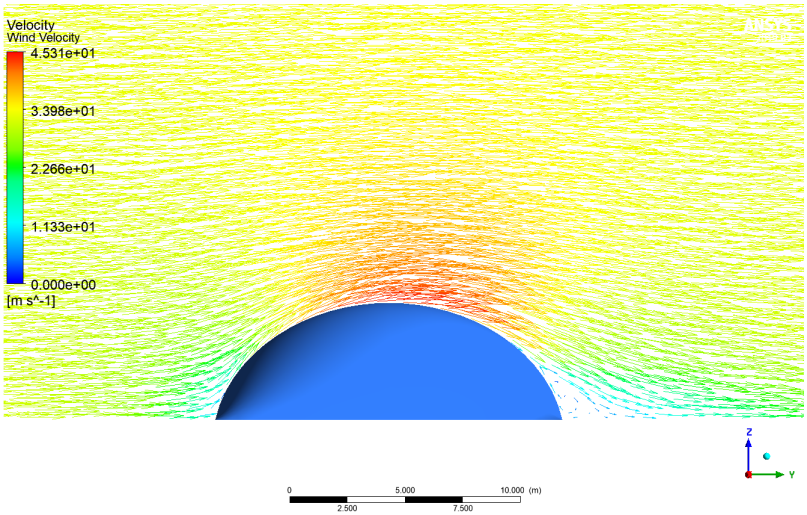

(a) Wind flow around the Model-3

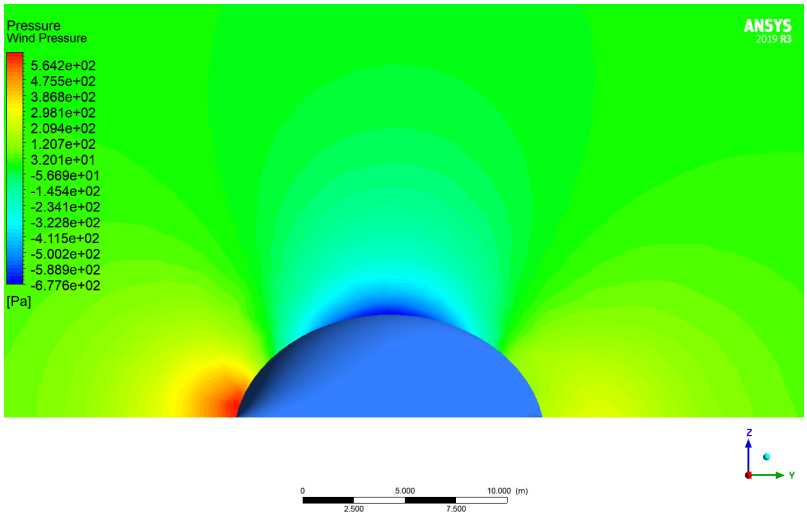

(b) Wind Pressure around the Model-3

Figure 3.22: Simulation of Wind around Model-3

$\mathbf{c}_p - values$

In civil engineering practice, the wind loading on the structure due to wind is calculated using the value of pressure coefficient c_p as introduced in section 3.2. To calculate the pressure coefficient, the z_{ref} is taken as the maximum height of the structure. The c_p value is calculated on the polyline which is the intersection of membrane surface with the mid-section of the fluid domain in the wind direction. For 3 developed models, this can be visualized in figure 3.23 The reason to choose this specific section is that the pressure coefficient data in the existing wind tunnel experiment research is also available for this section. So, it will be possible to directly verify the developed verification model-1.

Wind tunnel results are taken from the existing tunnel testing results published in [17]. The small scale model of hemispherical air dome used in the wind tunnel testing is shown in figure 3.24 . The distribution of wind pressure coefficient is shown in figure 3.25 [17]. From the performed CFD analysis on the developed model-1, the obtained wind pressure coefficient distribution is shown in figure 3.26

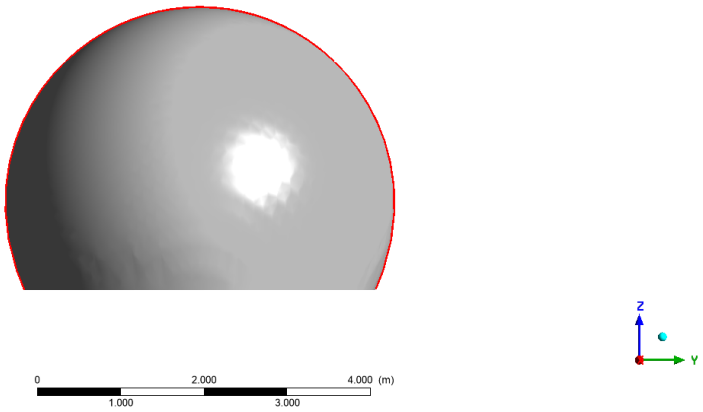

(a) Model 1: Intersection line of membrane with domain mid-section

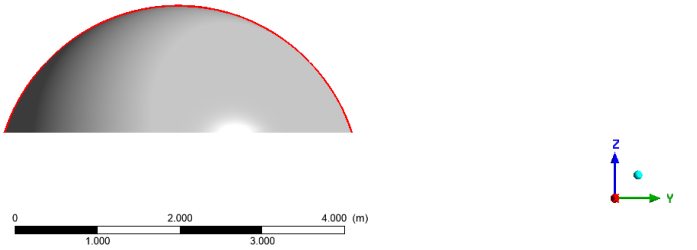

(b) Model 2: Intersection line of membrane with domain mid-section

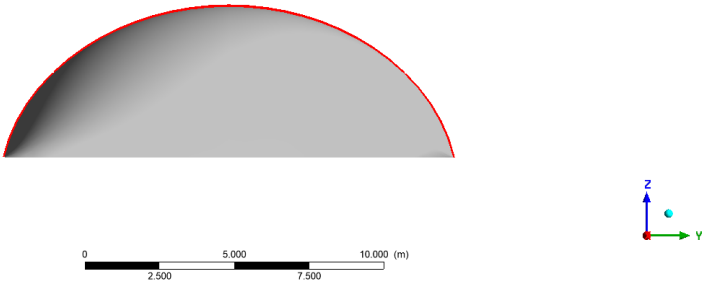

(c) Model 3: Intersection line of membrane with domain mid-section

Figure 3.23: c_p plot polylines of all 3 developed models

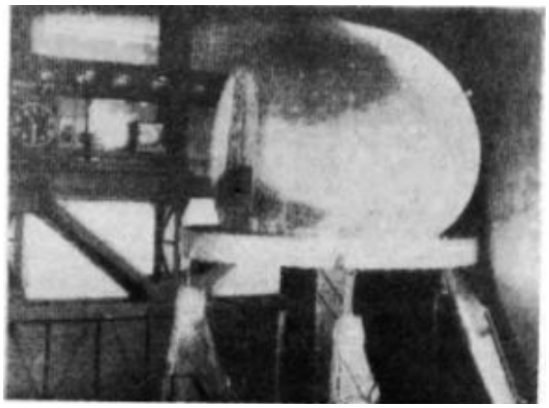

Figure 3.24: Wind Tunnel model Experiment setup [17]

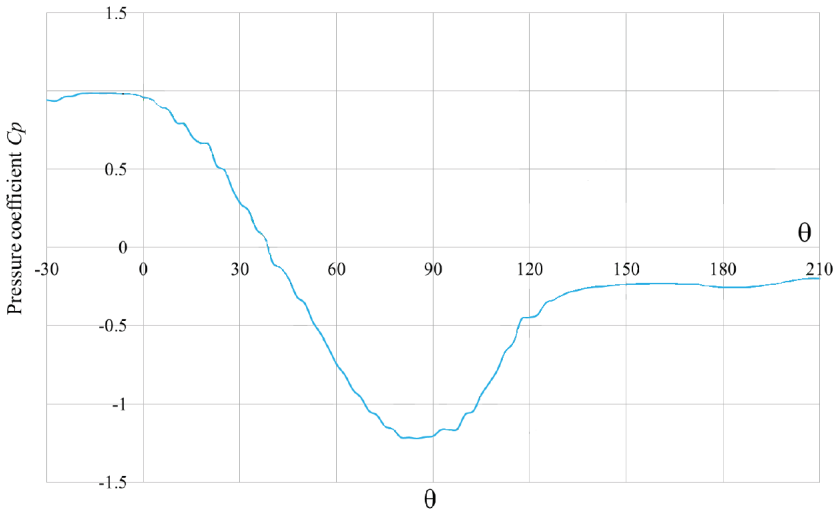

Figure 3.25: Pressure coefficient distribution along wind direction (+y) from existing research [17]

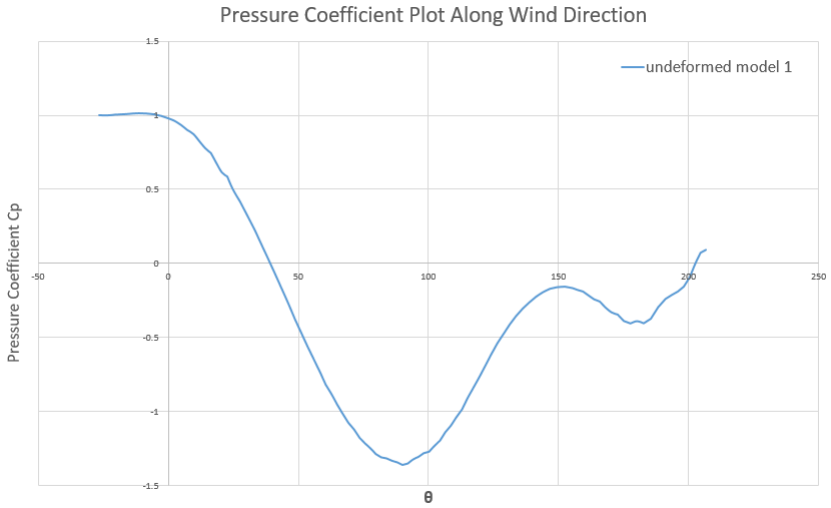

Figure 3.26: Pressure coefficient distribution along wind direction (+y) for verification Model-1

Several observations can be made on comparing the results obtained from the CFD analysis and the wind tunnel experiment:

1. Pressure coefficient on the windward side of the structure is positive and similar to the one obtained in wind tunnel testing.

2. On the top of the structure, suction force is observed and the maximum value of negative pressure coefficient is similar to the wind tunnel testing. The fluctuation in the pressure coefficient in wind tunnel testing cannot be precisely modelled in the CFD analysis. This is due to the face that wind separation is happening there and the flow becomes complex.

3. On the leeward side of the model, the pressure coefficient is comparable to the one obtained in wind tunnel testing. This is due to the limitations of k-ϵ turbulence model. But as mentioned before, this slight discrepancy in the pressure coefficient can be ignored as the magnitude of pressure is very less in comparison to the maximum pressure on the structure.

Some differences in the modelling is because of unavailability of complete data about the setup of wind tunnel experiment.

Concluding from the above, we can say that the developed Computational Fluid Dynamics model is in comparison to the wind tunnel experiment. After achieving the appropriate setup of CFD model, the geometry of the structure can be slightly changed and an educational idea of wind pressure coefficient distribution around the Pneumatic Structure of similar kind can be taken.

3.6. Summary

In this chapter, the fluid mechanics fundamentals were presented. An introduction of computational fluid dynamics method to analyse the wind loading was done.

The use of CFD in wind Engineering is relatively a new discipline of Computational Wind Engineering (CWE). In CWE, the used methods as well as the experience and knowledge of the engineer performing the analysis plays an important role. The importance of boundary conditions to simulate the wind flow similar to the wind tunnel testing was briefly explained.

The suitable techniques along with the necessary boundary requirements were utilized to setup a numerical model for the analysis of wind flow around the Hemispherical Air Dome (Model 1). As a result, the dimensionless pressure coefficient (c_p) and the pressure contour around the structure was compared to the existing wind tunnel data. After verifying the setup of computational fluid dynamics model, the other 2 developed model (section 2.6, Model-2, Model-3) were analysed. The wind flow and the pressure contour around Model-2 and Model-3 were also presented.

In the following chapter, to incorporate the effects of structural deformation on wind flow, strong coupling between the two separate solvers is done. This will help us to analyse the interaction between the membrane and wind flow.

4

Coupling Fluid and Structural Analysis

In the previous sections, the fundamentals, numerical simulation and the application of structural and fluid problem to study the influence of wind on membrane structures is introduced. Till now, the fluid and structural domain are being considered as separate domains. For a proper prediction of membrane structure behaviour, the coupling of these two separate fields is done. This multi-physics problem is commonly known as coupled analysis.

4.1. Fluid - Structure Interaction in Coupled Problem Analysis

As mentioned before, the membrane lacks bending stiffness. Because of this, the membrane structure can have large deformation due to the perpendicular loads acting on it. These deformations can be large, which can effect the wind flow around the structure.

The fluid-structure interaction is highly dependent on the type of structure. For example, in case of rigid structures such as small houses, or buildings with low height, the geometry of the structure does not change so much that it will effect the wind flow. So, in these type of structures the problem can be solved by considering separate analysis for the wind and the structure. In case of slender structures such as high towers or even bridges, the deformations can be large and can effect the wind flow. For these structures, the interaction between the structure and wind flow is questionable.

For membrane structures, due to large deformation and non-linearity, there are limitations in applying the simplified method. Here, a better prediction of the wind flow around the structure can be done considering the multi-physics problem. In this work, a workflow is created in which the fluid simulation is done to analyse the wind flow around the structure and consequently to compute the resulting surface load on the membrane. This surface pressure loading is considered as the input loading to compute the structural response. To take into consideration the deformation effects on wind flow, the structural deformation is considered in the wind simulation.

For the fluid-structure interaction in membrane structures, the membrane is the surface separating the structural and fluid domain. This is known as surface coupled problem. To simulate the interaction, the deformation of membrane structure is used to update the boundary conditions in the computational fluid domain. The displacement field (${d_\Gamma}^{\Omega_S}$) is used here to update the fluid system, this can be identified as Dirichlet-Neumann coupling. The surface loading from the fluid domain can be identified as Neumann boundary conditions. The non-linearity can be caused due to large membrane deformations, moving boundary conditions in fluid domain.

4.2. Strategies to Solve Multi-Physics Problems

There are two general approaches which can be used to address the multi-physics problem:

Simultaneous Analysis

In this approach, the problem is summarized in one set of equations, which is discretized and solved as one. The fluid and the structural domain are simulated together. Analysis considering the Simultaneous analysis can be found in literature such as: [3], [2], [40], [4].

Partitioned Analysis

In this approach, the fluid and the structural domain are considered separately. The coupling of these two domains is done by exchanging the boundary conditions such as displacement and surface pressure. Analysis considering the partitioned analysis can be found in literature such as: [41], [42], [43], [5], [44].

Certain differences and aspects of the two mentioned general approaches are discussed below:

1. With respect to convergence of solution, the Simultaneous analysis shows superior performance.
2. With respect to spatial discretization, in Simultaneous analysis the discretization is same for both fluid and structural domain. Where as, in Partitioned analysis different discretization can be used in separate solvers. This way, suitable discretization can be used which can reduce the computational efforts.
3. In Simultaneous approach, the equations can be ill-conditioned due to the varying boundaries. This can result to inaccurate results. In Partitioned analysis, separate equations exist and different specialized methods can be used to solve specific problem.
4. In Partitioned analysis, as single field solvers are combined together it becomes a modular setup. It enables the reuse of the developed methods for different structures.

Due to the mentioned advantages of Partitioned analysis, in this work the Partitioned technique is used to simulate the Fluid-Structure interaction. Moreover, for the fluid domain much finer mesh is required with respect to structural domain to correctly simulate the wind flow. For this different discretization is required for different fields and can be done best using Partitioned analysis.

4.3. Partitioned Analysis of Multi-Physics Problems

To simulate the fluid-structure interaction using Partitioned Analysis, there are certain requirements which need to be fulfilled. Based on these requirements, two coupling approaches named as Strong coupling and weak coupling are introduced.

4.3.1. Requirements for Partitioned Analysis

In partitioned analysis, the coupling between the two separate solvers is done by exchanging the boundary conditions. The instance and method of exchanging this boundary is determined by the coupling algorithm. For the correct simulation, there are certain conditions that needs to be fulfilled:

1. **Conservation of volume**

   This law states that there cannot be any generation or discreation of volume at the fluid-structure interface. With respect to coupled simulation, this means that at the interface, fluid-structure domain have to stick together. Any deformation in the structure at any time has to be identified by the domains:

$$d_{\Gamma}^{\Omega_F}(t) = d_{\Gamma}^{\Omega_S}(t) \tag{4.1}$$

2. **Conservation of momentum**

No additional momentum δm_Γ can be created or lost at the interface [43].There can only be the transfer of momentum from one field solver to another. Therefore, the sum of momentum transfer from fluid domain to the interface and from interface to structural domain and vice versa has to be zero.

$$\Delta m_\Gamma^{\Omega_{n\to n+1}} = \Delta m_\Gamma^{\Omega_{F,n\to n+1}} + \Delta m_\Gamma^{\Omega_{S,n\to n+1}} \tag{4.2}$$

Equation 4.2 can be rewritten in terms of Cauchy stress tensors as:

$$\int_{t^n}^{t^{n+1}} (\int_\Gamma \sigma_{cauchy,\Gamma}^{\Omega_F}(t) {n_\Gamma}^{\Omega_F}(t) dA) dt + \int_{t^n}^{t^{n+1}} (\int_\Gamma \sigma_{cauchy,\Gamma}^{\Omega_S}(t) {n_\Gamma}^{\Omega_S}(t) dA) dt = 0 \tag{4.3}$$

where $n_{\Gamma,F} and n_{\Gamma,S}$ are surface normal at the interface

Equation 4.3 can be satisfied when the Cauchy stress tensor are equal to each other at interface in fluid and structural domain:

$$\sigma_{cauchy,\Gamma}^{\Omega_F}(t) {n_\Gamma}^{\Omega_F} = \sigma_{cauchy,\Gamma}^{\Omega_S}(t) {n_\Gamma}^{\Omega_S} \tag{4.4}$$

To simplify, the stress integration over the interface can be assumed as forces acting on the nodes of the interface. Therefore the requirement can be modified as:

$$f_{\Gamma_d}^{\Omega_F}(t) = f_{\Gamma_d}^{\Omega_S}(t) \tag{4.5}$$

3. **Conservation of energy**

Similar to conservation of momentum, this law states that the energy can neither be created not be dissipated at the boundary interface. The transfer of energy from fluid domain to interface and from interface to structural domain and vice versa has to be zero.

$$\Delta E_\Gamma^{\Omega_{n\to n+1}} = \Delta E_\Gamma^{\Omega_{F,n\to n+1}} + \Delta E_\Gamma^{\Omega_{S,n\to n+1}} \tag{4.6}$$

Equation 4.6 can be rewritten in terms of Cauchy tensor as:

$$\int_{t^n}^{t^{n+1}} (\int_\Gamma \sigma_{cauchy,\Gamma}^{\Omega_F}(t) {n_\Gamma}^{\Omega_F}(t) {d_\Gamma}^{\Omega_F}(t) dA) dt + \int_{t^n}^{t^{n+1}} (\int_\Gamma \sigma_{cauchy,\Gamma}^{\Omega_S}(t) {n_\Gamma}^{\Omega_S}(t) {d_\Gamma}^{\Omega_S}(t) dA) dt = 0 \tag{4.7}$$

where $n_{\Gamma,F} and n_{\Gamma,S}$ are surface normal at the interface.

4. **Coupling conditions**

Resulting from the requirement of conservation of volume, momentum and energy, two coupling conditions which have to be satisfied for correct simulation of wind-structure interaction can be identified:

•Kinematic continuity condition

$$d_{\Gamma_d}^{\Omega_F}(t) = d_{\Gamma_d}^{\Omega_S}(t) \tag{4.8}$$

•Dynamic continuity condition

$$f_{\Gamma_d}^{\Omega_F}(t) = f_{\Gamma_d}^{\Omega_S}(t) \tag{4.9}$$

4.3.2. Weak Partitioned Coupling

A visualization of this coupling method is shown in figure 4.1. In this method the fluid domain is solved to find the resulting wind pressure on the undeformed geometry of the structure. These obtained forces are then transferred from Fluid domain to Structural domain. The structural domain then solves the response of the structure to the forces applied till the convergence criterion is reached. In case of considering the wind flow varying with time, the next time step is started till the maximum time step is reached.

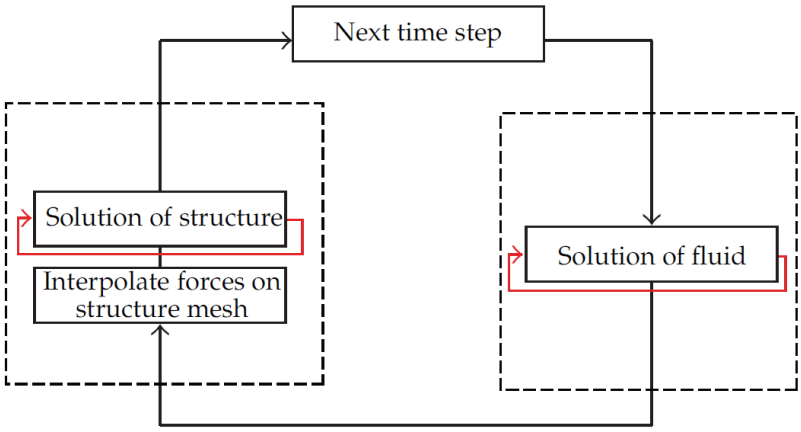

Figure 4.1: One-way coupling

4.3.3. Strong Partitioned Coupling

A visualization of Strong coupling method is shown in figure 4.2. In this method, within one time step iterative procedure is followed. Firstly, a CFD analysis is done on the undeformed structure to obtain the wind pressure. Then these forces are transferred from the fluid domain to the structural domain and consequently FEM analysis is done to find the response of the structure to the applied force. But this while procedure is repeated with exporting the deformed structure to the fluid domain and then considering the wind flow change due to the structure's deformation. If considering the wind flow to be varying with time, before starting the next time step the force and displacement change needs to be below a prescribed amount.

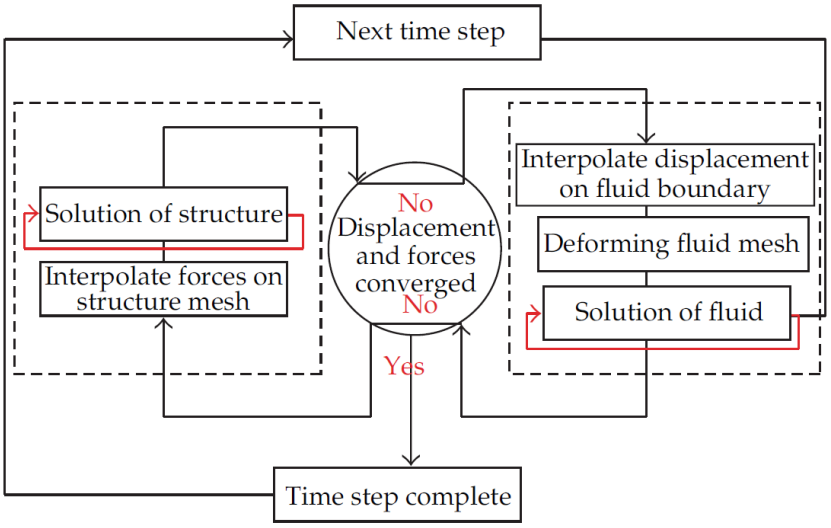

Figure 4.2: Two-way coupling

4.4. Computational Concept

After discussing the necessary elements required to perform Fluid-Structure interaction (FSI) simulation, this section will be about implementing those concepts in the software environment. In this work, the partitioned anaysis with strong coupling is used to perform the FSI simulation. As described in the section 3.1, wind speed is taken constant with time so the outer loop of time variation is ignored in the strong coupling method. For the coupling of the Structural and the Fluid Domain, Grasshopper is used to develop a method containing the pipelines to transfer the data such as Wind Surface pressure and the deformation of structure. For the structural computation SOFiSTiK software is used and ANSYS CFX is used for the fluid computation. The individual single field solver setup has already been introduced in the previous chapters.

Setup of Three softwares

To minimize the computational effort, the developed structural and fluid setup can be reused for each iteration with minimum modifications. In the SOFiSTiK software, .dat file is used to input the data such as membrane material properties, structural nodal positions, surface pressure on the elements. This .dat file is created using the python programming in Grasshopper. The coupling method generated using Grasshopper is used just to transfer the boundary condition between single field solvers. For the single field solvers it is sufficient to consider the data on their side of the interface. The surface pressure is exported from the Fluid solver to the coupling tool and from there it is transferred to the Structural solver and similarly the resulting displacement is exported from the FEM solver to the coupling tool and the model with updated geometry is created for the CFD analysis. The flow chart showing the developed method with the analysis loop followed to do the analysis can be seen in figure

4.4.1. Structural Solver: SOFiSTiK

As mentioned before, static analysis of the structure subjected to wind loading is done. The method has been developed to take into consideration the geometric non-linearity of the structure. For this a looped analysis is done in which the change in wind force on the structure due to the deformation of the structure. To do the form-finding of the membrane structure and moreover for the structural analysis, a FEM software SOFiSTiK is used. One of the main reason to use this software is that it uses the .dat files to input data for the analysis. In this work, the .dat file is created using programming feature in Grasshopper. This feature enabled to develop a general method which can be used for the Fluid Structure Interaction analysis of membrane structures. After form finding the initial geometry with the obtained stress state is saved in the memory of the FEM software itself. The nodal coordinates of the initial geometry are exported to the coupling tool (Grasshopper) using excel. After doing the CFD analysis on the exported geometry, the force is imported to the FEM software using excel. The force applied is converted to surface pressure to simulate the actual behaviour. This surface pressure is applied to the previously saved geometry with stress state and consequently a deformed geometry with new stress state is obtained. The obtained deformed geometry with new stress state is saved in the FEM software memory. After this the described loop can be repeated till the desired convergence is obtained.

4.4.2. Fluid Solver: ANSYS CFX

As discussed before, the simulation of wind flow around the structure is done using CFD package Ansys CFX. The loop considered to do the analysis is mentioned in the previous section. Using CFD analysis wind pressure on the structure with changing geometry is obtained. The CFD model of the structure in each loop is exported from the coupling tool - Grasshopper. In each loop, the coupling tool is updated with the deformation of the structure from FEM software. Initially, the undeformed structure is considered in the wind simulation and consequently the wind pressure is obtained. The wind pressure data is exported from the CFD software using excel. The data is exported in form of nodal forces on the membrane structure. After getting the deformed geometry, the coordinates of the nodes are updated in the coupling tool and we again export the CFD model with updated boundary condition. As strong coupling is important to simulate the realistic behaviour, it is used in this analysis.

4.4.3. Coupling and Data Transfer Tool: Grasshopper

A third separate program is used in this work to handle the data transfer between the Structural solver and Fluid solver. Pipelines are created in grasshopper to transfer the data, python programming feature is used to properly handle the data. This is important as the proper application of force to each element is important. In the first loop, which is the process of doing form finding in the FEM software. The membrane material properties, form finding properties as well as the base geometry is decided in the grasshopper. A visualization of this can be seen in figure 4.3.

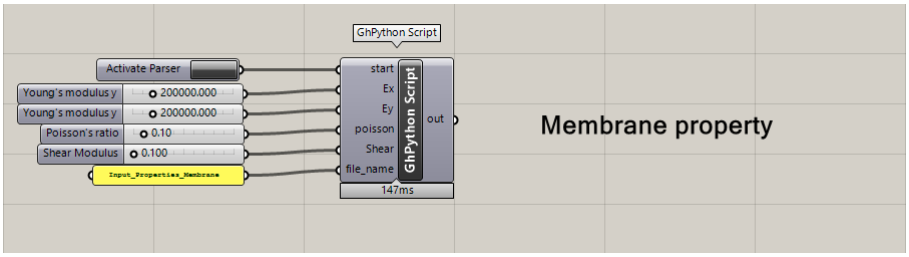

(a) Membrane properties

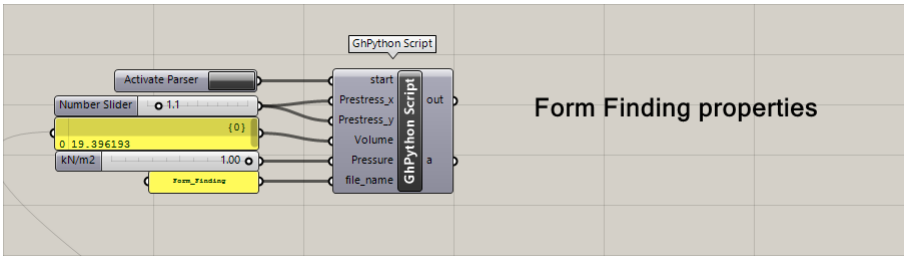

(b) Form-finding properties

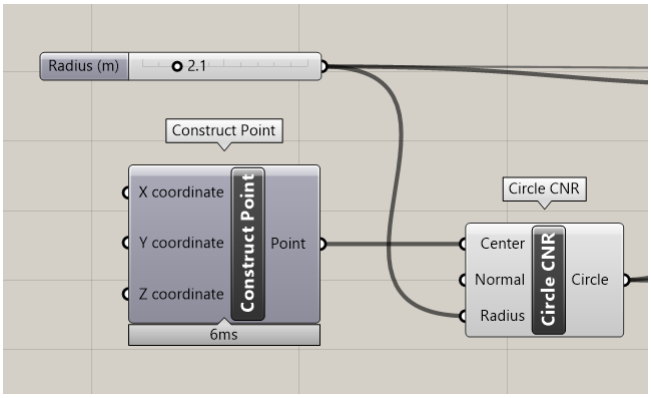

(c) Base geometry

Figure 4.3: Development of initial geometry

The .dat file of membrane properties, form finding properties and the base geometry with nodal coordinates is exported from grasshopper to SOFiSTiK. After performing the form finding, the base geometry coordinates are exported from SOFiSTiK to grasshopper. With the dimensions of geometry, the model following the recommendation of Best Practice Guidelines for the CFD analysis is created and exported. After performing the CFD analysis, the force on the interface nodes is exported to coupling tool and consequently the surface pressure on the membrane is exported to the FEM software. After which the structural deformations are received from the Structural analysis and the boundaries of the CFD analysis is updated.

There are some of the key features in the concept of Grasshopper as coupling tool:

1. **Different field solver support :** Though in this thesis, SOFiSTiK and ANSYS is used for the Structural analysis and CFD analysis respectively, a very common feature - 'excel' is used for the data import and export between the 2 solvers. This way, other FEM and CFD softwares can be easily used with this data coupling tool.
2. **Non-matching grid data transfer :** In the fluid domain, finer mesh size is required to properly simulate the wind flow around the structure. Because of this, the mesh on fluid side of the interface is finer than the structural side. To solve this, an algorithm is used in the coupling tool to properly transfer the wind pressure data from fluid domain to structural domain. The wind force on the structure is known as nodal forces on the fluid side of the interface. Using the nearest point algorithm in Grasshopper, the force is approximated on the nodes of the structural side of the interface. This way, the force is interpolated.
3. **Surface pressure data transfer :** To keep the analysis realistic, the wind force should be applied as surface pressure on the membrane. As the wind force from the CFD analysis is known as the nodal forces on the fluid side of the interface, the force has to be calculated in such a way that we get surface pressure on each element of the membrane structure. The nodal force on each of the element is averaged and then divided by the updated surface area of each element, this way we get the correct surface pressure on each element of the membrane surface. It is important to consider the change in element area due to deformations.

4.4.4. Convergence Criteria in Partitioned Analysis

The developed method here to simulate the interaction between membrane structure and the wind reaches a state of equilibrium with iterations. The method converges to this state of equilibrium between the wind force and stress in the membrane. A proper convergence criteria needs to be formulated to assess the convergence of the solution.

While executing the iterations using the developed method, the interface displacement and interface load are the two quantities which are exchanged between the separate solvers. The difference between the consecutive iteration displacement and load should diminish while approaching the convergence. The residual for force and displacement can be written as:

$$\frac{||d_{\Gamma,k+1} - d_{\Gamma,k}||}{d_{\Gamma,k}} < \epsilon_{Tot} \tag{4.10}$$

$$\frac{||f_{\Gamma,k+1} - f_{\Gamma,k}||}{f_{\Gamma,k}} < \epsilon_{Tot} \tag{4.11}$$

where $f_{\Gamma,k}$ and $d_{\Gamma,k}$ are the force and displacement in the previous iteration step. There are some benefits using this convergence approach such as the convergence criteria will not be dependent on the type of structure considered and moreover the variables are with same accuracy. In this work, a relative large convergence of 10^{-2} is used.

In the partitioned analysis, the overall convergence is going to be dependent on the individual field convergence criteria as well. To proceed with the iterations, single field solvers need to converge as well. In order to reach overall convergence, the individual convergence limit should be smaller than the overall. Deparis [45], in his work on fluid-structure interaction arising in blood flow has suggested to use the tolerance limit of $\epsilon_{Tot}/10$ for the individual solvers, which is used in this work as well.

4.5. Wind Effects on Air-supported Membrane Structures in Coupled Computation

The described fluid-structure interaction methods and the software implementation is now applied to analyse the interaction between the membrane structure and wind flow.

4.5.1. Setup of Coupled Computational Model

The coupled analysis in this work consists of structural analysis and numerical fluid modelling described in the previous chapters. Both separate solvers are combined together to do the coupled analysis. The models which are generated in the section 2.6 are used as the base numerical model. The structural part is done using the finite element program SOFiSTiK. The fluid models which are generated in the section 3.5 for the 3 developed models will be used as the basis for the CFD analysis. The properties of the developed CFD model are discussed in the section 3.5. To consider the deformation with each loop in the membrane structure, the boundary conditions are updated. As the membrane structure is within the inner domain of the fluid model, the boundary changes are just made in the inner domain.

The membrane acts as the interface between the structural and fluid domain. In the coupling tool, the two sides of of the membrane are considered as two sides of the partition. The coupling between the two separate solvers is done in the form of displacement and surface pressure. The surface pressure is interpolated from the nodal forces obtained by the CFD analysis. Due to the difference in the mesh size between the structural and the fluid domain, the nodal force from the fluid domain is interpolated to the nearest structural node for the best approximation. The convergence criteria for the structural and fluid domain is decided separately. For each domain solver, the Room Means Square (RMS) is used as the tolerance limit metric. For structural domain a limit of 10^{-6} and for the fluid domain a limit of 10^{-5} is used.

4.5.2. Simulation of Steady-State Solution

Steady state response of the Pneumatic membrane structure is analysed with the flow in the positive y direction. As the wind flow is constant, a static state deformation behaviour of the structure is expected. In this analysis, the structural inertia effect is neglected as there will be no displacement over time and therefore no resulting acceleration.

Steady state solution using coupled simulation

In this section, the proposed method is applied to find the steady state response of the developed models with the wind in positive y direction. The basic wind velocity is taken from the existing research which is equal to 40 m/sec. To understand the behaviour of membrane structures subjected to wind loading, variation in the wind velocity is also considered. The dependence of fluid structure interaction on wind velocity is also investigated with this analysis. To have an even deeper idea, eigen frequency analysis of the structure after each loop is also done. As we know that the frequency increases with the increase in the stiffness, we expect to see the same behaviour from the structure.

In normal practice when a membrane structure is constructed, it is analysed when subjected to wind loading. The recommendation for the wind loading on curved structure is given in section 7.2.8 of Eurocode 1 [1]. This recommendation in Eurocode doesn't take into consideration the change in wind force due to the deformation of the structure. In the following sections each developed model will be discussed and the results from the FSI analysis will be shown. The deviation from normal practice analysis will be pointed out as well.

Hemispherical Pneumatic Structure - 2nd Model

When the structure is subjected to wind loading, it deforms. To understand the extent to which the fluid structure interaction plays a role in the behaviour of the structure, the point on the structure with maximum deformation after 1st loop loading is investigated. Moreover to see the maximum change in the surface pressure due to deformation of the structure, the element will maximum pressure is investigated. This will help us to estimate the amount of error we are making in estimating the maximum deformation and maximum wind pressure on the structure.

In figure 4.4 the point (A) with the maximum deformation after the first iteration (normal practice) is shown and in figure 4.5 the element (B) with the maximum wind pressure is shown. The reason to choose these is that it has the extremities of pressure and deformation when we use the general

practice according to Eurocode. This will help us to see how much of change we should expect due to geometric non-linearity.

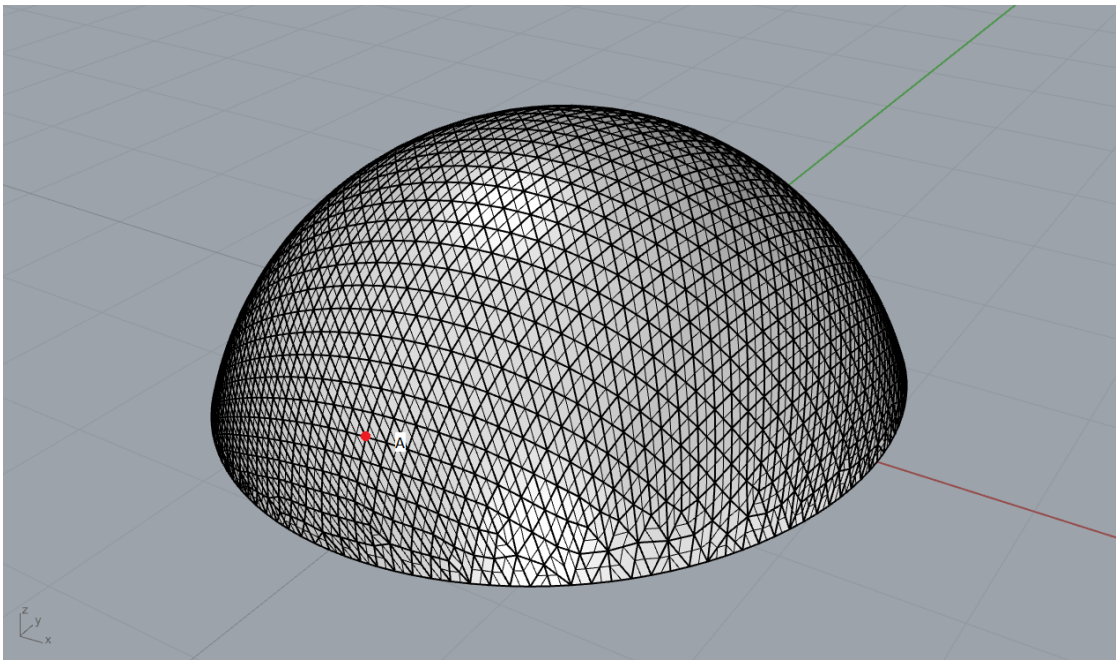

Figure 4.4: Model-2 maximum deformation point when subjected to undeformed loading case

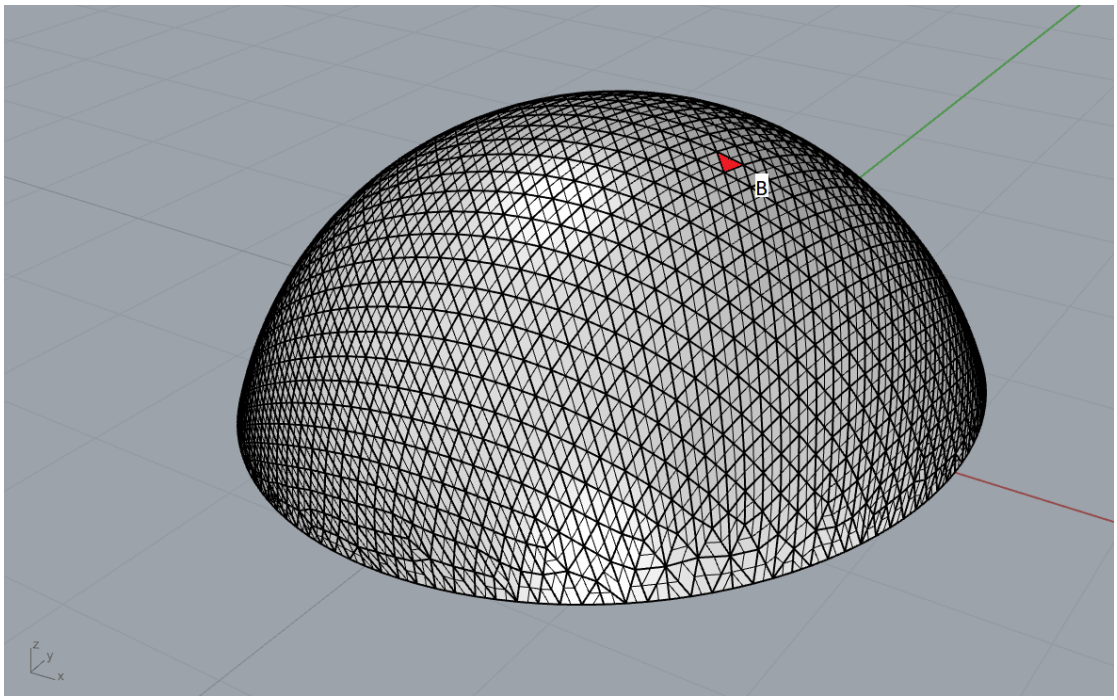

Figure 4.5: Model-2 element with maximum wind pressure in undeformed state

Further, the deformation plot of the point A in figure 4.4 with respect to each loop is plotted in figure 4.6. Further, the changing wind pressure at the maximum wind pressure element on the hemispherical structure with respect to each iteration is plotted in figure 4.7. The effect of deformation on the maximum membrane stress occurring in the structure is plotted in figure 4.8 with respect to each iteration of analysis.

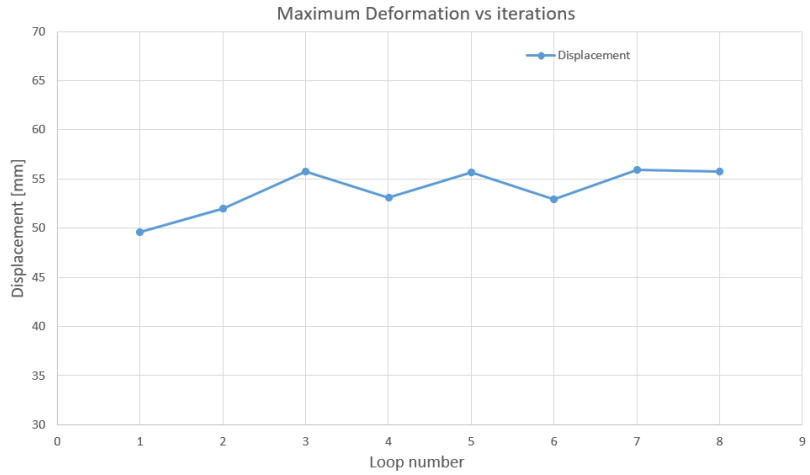

Figure 4.6: Displacement plot of point in figure 4.4 with respect to iterations

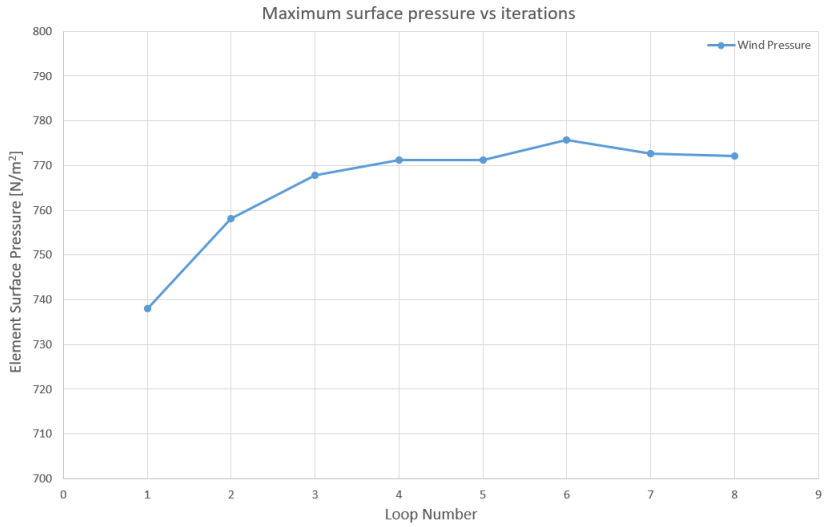

Figure 4.7: Wind pressure plot of element in figure 4.5 with respect to iterations

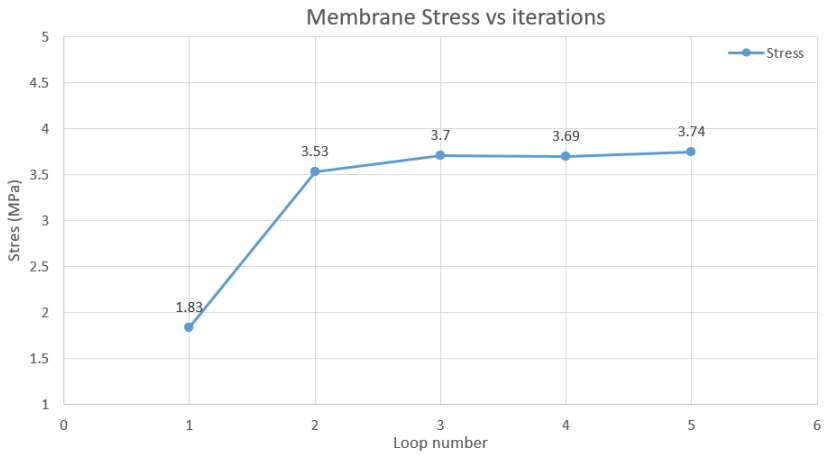

Figure 4.8: Membrane stress plot with respect to iterations

As mentioned in section 3.2, according to Eurocode the wind pressure on the structure is calculated by finding the wind pressure coefficient distribution on the surface of the structure. But the deformation in structure due to geometric non-linearity will result in changing wind pressure coefficient as well. To visualize this, the changing pressure coefficient with each analysis loop is plotted in figure 4.9 along the centre line shown in figure 3.23b.

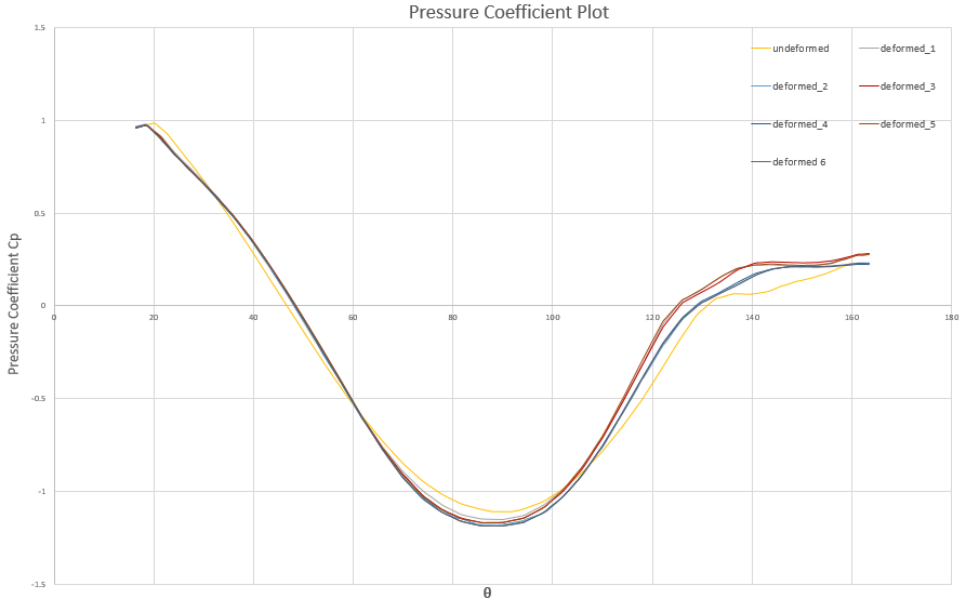

Figure 4.9: Pressure coefficient C_p plot along mid-section in figure 3.23b with respect to iterations

In the figures 4.6 and 4.7 , we can see the change in deformation and pressure due to the interaction between the membrane surface and wind. Due to the deformation of the structure after first iteration, the angle of incidence with the wind changes and consequently the wind pressure. To visualize the changing pressure on the membrane structures clearly, a wind pressure contour on the membrane surface is plotted in figures 4.10 and 4.11.

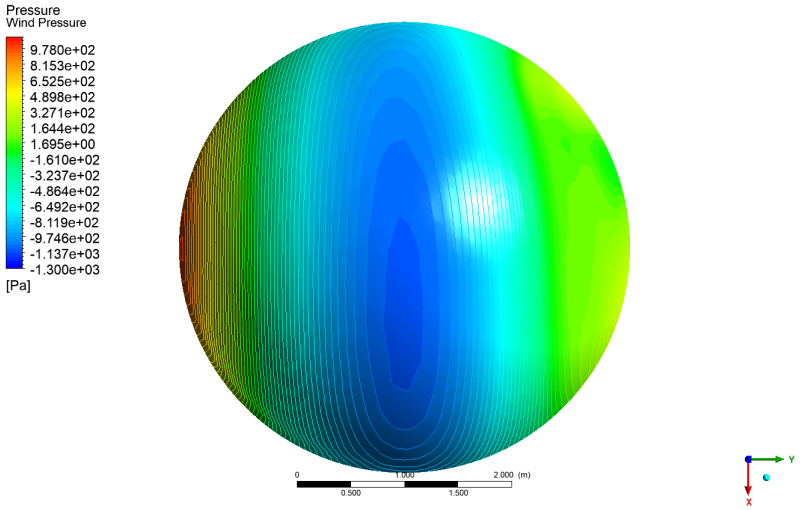

Figure 4.10: Model-2: undeformed state wind surface pressure contour

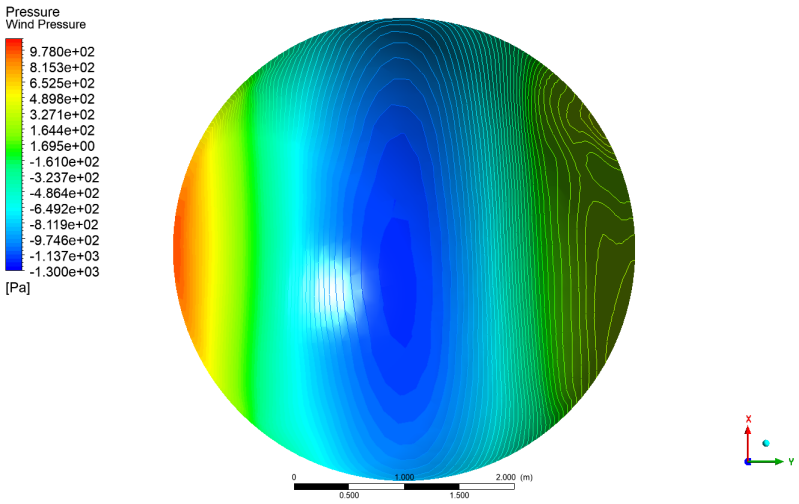

Figure 4.11: Model 2: deformed 6^{th} state wind pressure contour

To further justify the analysis performed, the natural frequency analysis of the structure is done after each iteration. As the structure deforms from its undeformed state, the stress in the membrane structure increases and consequently the stiffness of the structure. As we know that the frequency of a structure is directly proportional to the stiffness of the structure, the natural frequency should increase. A plot of natural frequency with respect to the iterations of the hemispherical model subject to the wind of 40 m/sec velocity is plotted in figure 4.12.

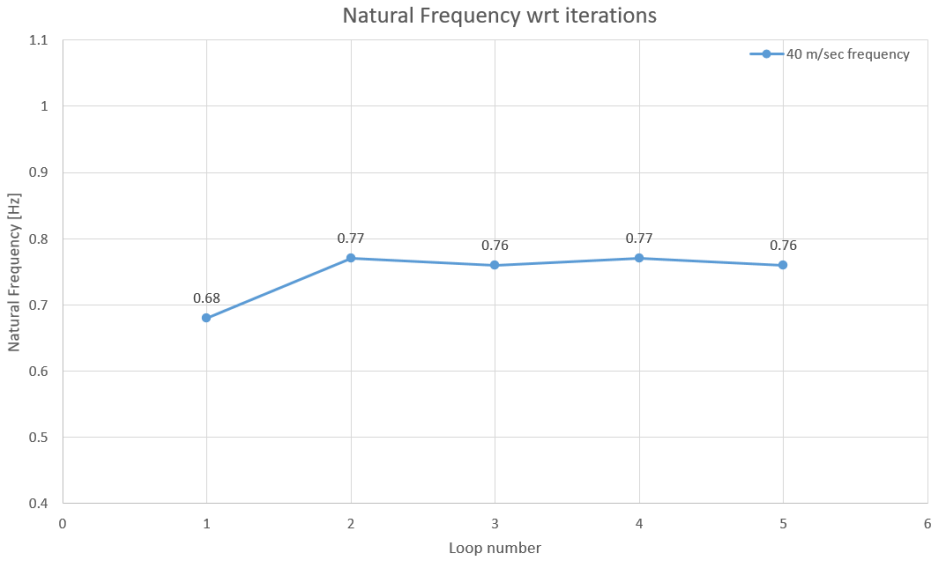

Figure 4.12: Natural Frequency plot of Model-2 with respect to iterations

The interaction between the membrane structure and wind is non-linear. The results presented before are for the hemispherical membrane structure subjected to 40 m/sec wind velocity. The deviation of maximum deformation and surface pressure from the normal practice as shown in figures 4.6 and 4.7 is highly dependent on the wind velocity on the structure. The rate of change of deviation is going to be dependent on the wind velocity as well. To investigate this dependence on the wind velocity, 3 sets of different analysis are done. In these analyses, the structure is subjected to the wind velocity of 20 m/sec, 60 m/sec and 80 m/sec. Moreover, an addition study is done to investigate the dependence of structural behaviour on the size of the structure considered. For this size variation study, the same structural and CFD setup will be used to analyse the behaviour of Hemispherical air dome with a base radius of 10 meter and 20 meter.

Structural behaviour dependence on Wind Velocity

In this section, we will investigate the dependence of fluid structure interaction on wind velocity. As mentioned before, the structure will be subjected to 3 different velocities. The base geometry is taken same as before for all 3 wind velocities. During the iterations of analysis loops, when the structure is subjected to wind pressure in first loop, the structure deforms to a different extent depending on wind velocity. With the increasing wind velocity, the structure will deform more after 1st iteration. Consequently the angle of incidence of membrane structure to wind will change. Therefore, the dependence of deviation from normal practice results is velocity dependent.
To investigate the change happening at the maximum deformation and pressure point, the node and element shown in figures 4.4, 4.5 is observed again. The plot showing the % deformation change of the maximum displacement point in comparison to the deformation when not considering the geometric non-linearity is shown in figure 4.13. Moreover, the plot shows the dependence of this % deformation change on the wind velocity.

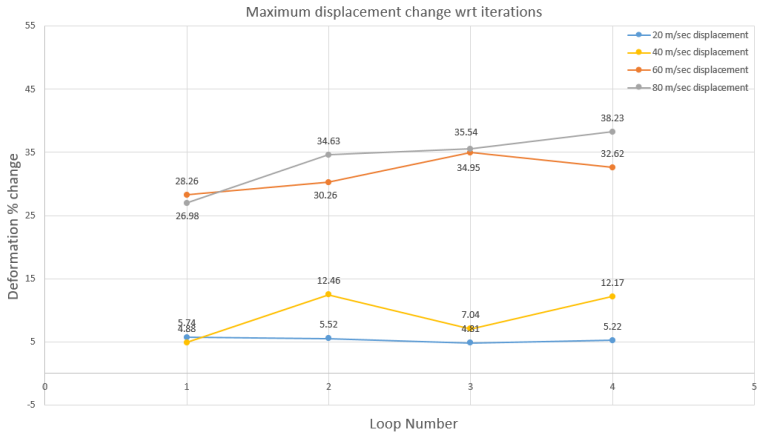

Figure 4.13: Model-2: % displacement change of point in figure 4.4 with respect to original displacement with changing wind velocity

The % change in the wind pressure at the maximum pressure point at different deformed state in comparison to the wind pressure at this point in the undeformed state is shown in figure 4.14. The plot shows the % change in wind pressure from undeformed state for the different wind velocities with respect to each iteration.

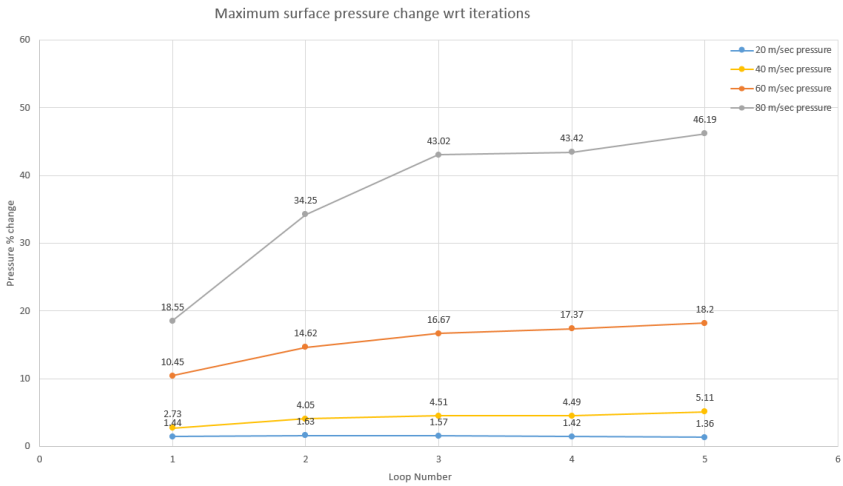

Figure 4.14: Model-2: % wind pressure change of element in figure 4.5 with respect to undeformed state with changing wind velocity

With more deformation due to increase in wind velocity, the stress in the membrane structure increases as well. In figure 4.15, the dependence of membrane stress with increasing wind velocity with respect to each iteration is plotted. As mentioned before, the stiffness of the membrane structure is directly proportional to the tensile stress in the membrane. So, with the increase in stiffness, the natural frequency should increase as well. The plot of natural frequency of the hemispherical membrane structure subjected to different wind speeds is plotted in figure 4.16.

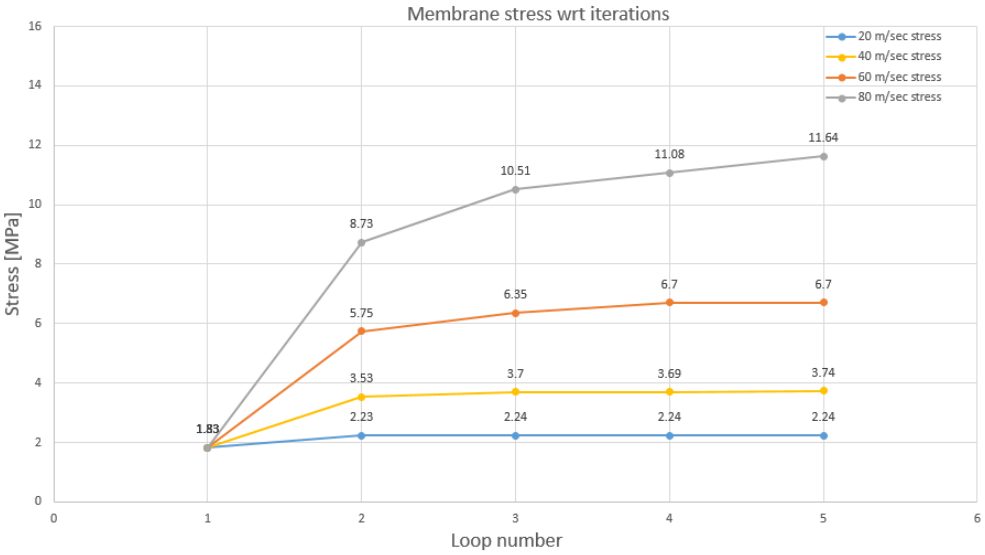

Figure 4.15: Model-2: Maximum membrane stress in the structure with respect to iterations with changing wind velocity

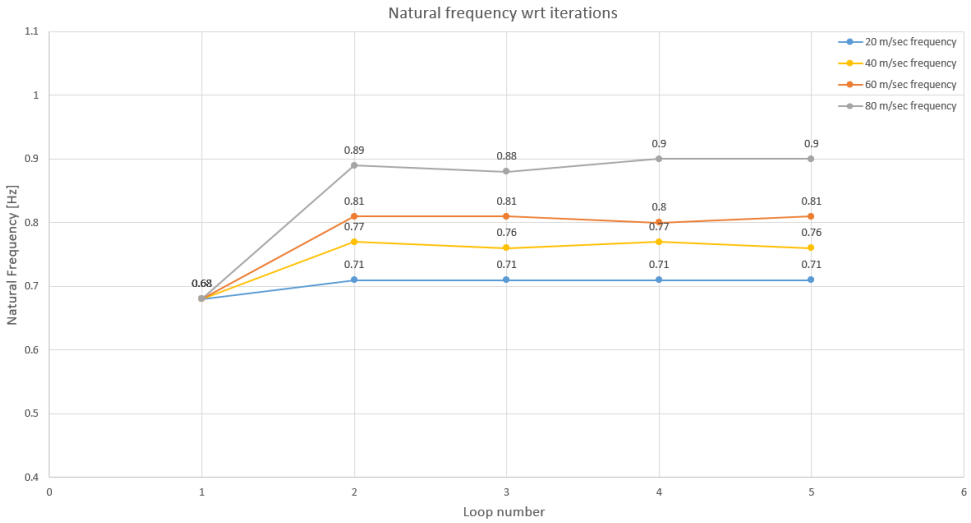

Figure 4.16: Model-2: Natural Frequency of the structure with respect to iterations with changing wind velocity

Structural behaviour dependence on Structure size

The results of the Hemispherical Air dome is shown in the previous section. The considered structure is of 2.1 metre base radius. The related results show the difference in the deformation and surface wind pressure from the normal practice of Eurocode. But one thing to note there is that the results show a discrepancy of around 5-12 %. These results definitely show the effects of structural non-linearity on structure's response, but to further justify the necessary use of the developed method while constructing a Air inflated membrane structure a consideration of structure with base radius and wind

velocity towards more realistic case is necessary. So in this section, results are shown with the wind velocity consideration of 33 m/sec and Hemispherical air dome with base radius of 10 metres and 20 metres. A detailed description regarding this study can be found in section A.1. Figure 4.17 shows the plot of percentage difference in the deformation of the membrane structure from the structure's deformation when we are not considering the geometric non-linearity. And figure 4.18 shows the plot of percentage change in maximum wind pressure occurring on the membrane structure with respect to the pressure on the structure when not considering the geometric non-linearity. These results show that the with the increase in size of the structure, the geometric non-linear behaviour influence on the structure's response increases as well.

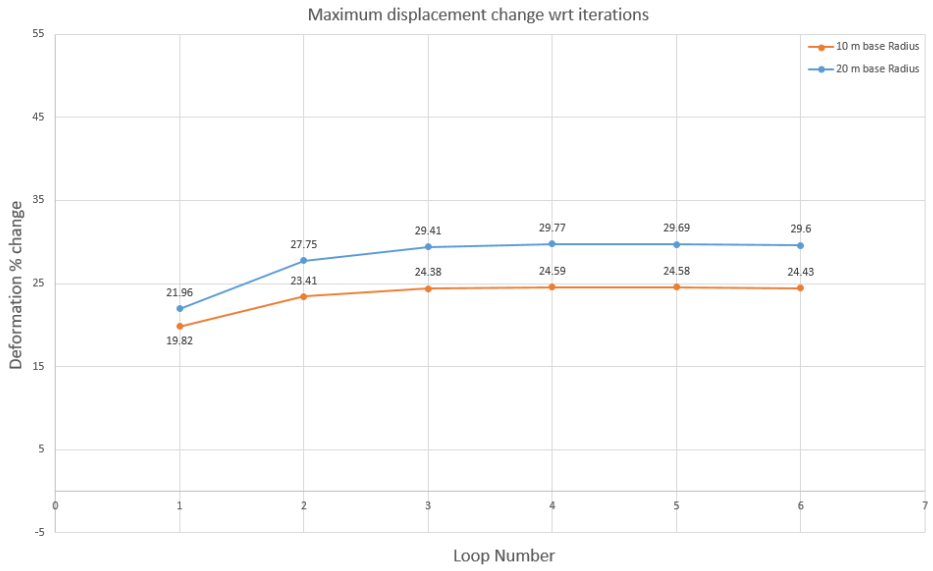

Figure 4.17: % displacement change of maximum deforming point with respect to original displacement considering size variation

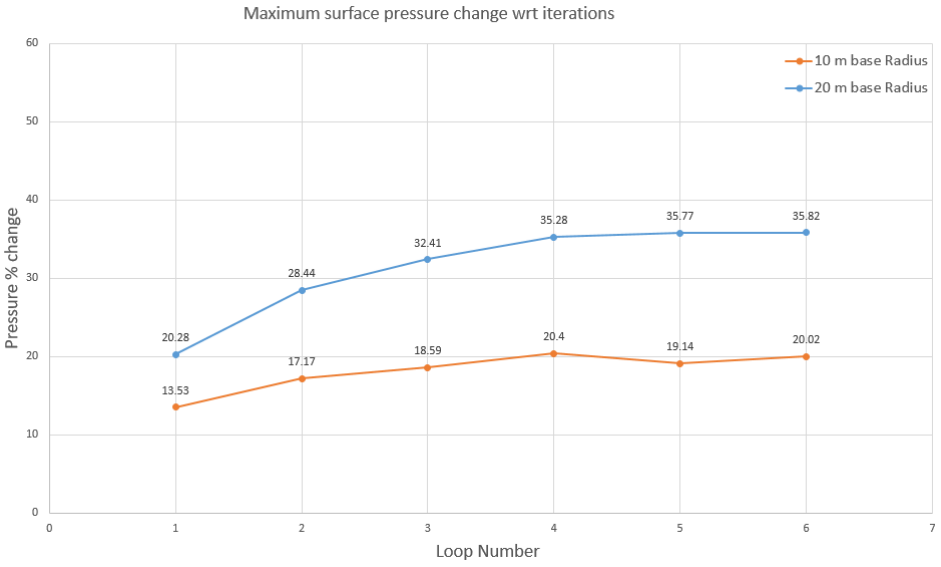

Figure 4.18: % wind pressure change of maximum pressure element with respect to undeformed geometry considering size variation

As we know that with the deformation of the structure, stress in the membrane of the structure is going to change as well. In figure 4.19, the maximum stress occurring in the membrane with respect to each iteration is plotted for both 10 m base radius model and 20 m base radius model.

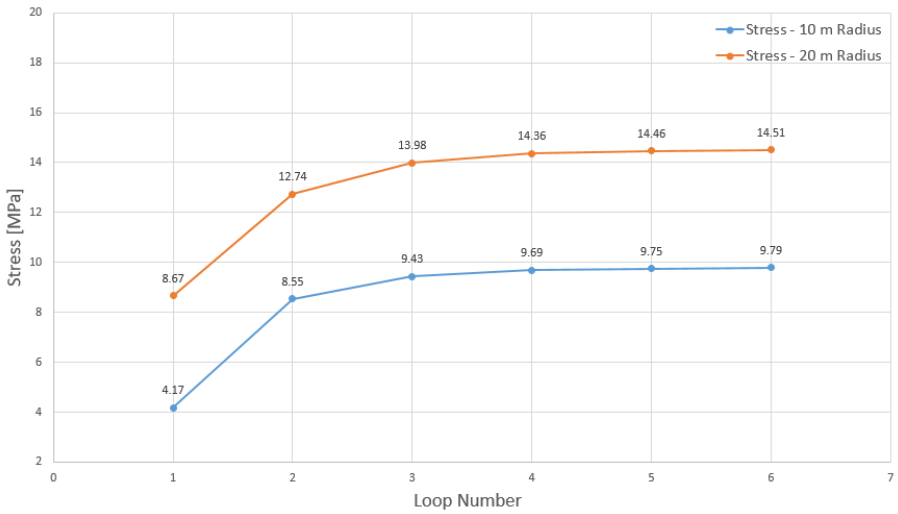

Figure 4.19: Maximum membrane stress in the structure with respect to iterations for different structure size

Square Pneumatic Structure - 3rd Model

To show the use case of the developed method, a square geometry was generated in section 2.6.2. The phenomena of fluid structure interaction will happen here as well. To investigate the effect of geometric non-linearity on the deformation of the structure and the pressure distribution on the structure, the point with maximum deformation and pressure is considered. In figure 4.20 the point (C), which has the maximum deformation after first iteration (normal practice) is shown and in figure 4.21 the element (D), which has maximum element pressure on the undeformed geometry is shown. As mentioned before, this will help us to see the error we are making in estimating the maximum deformation and maximum wind pressure on the structure.

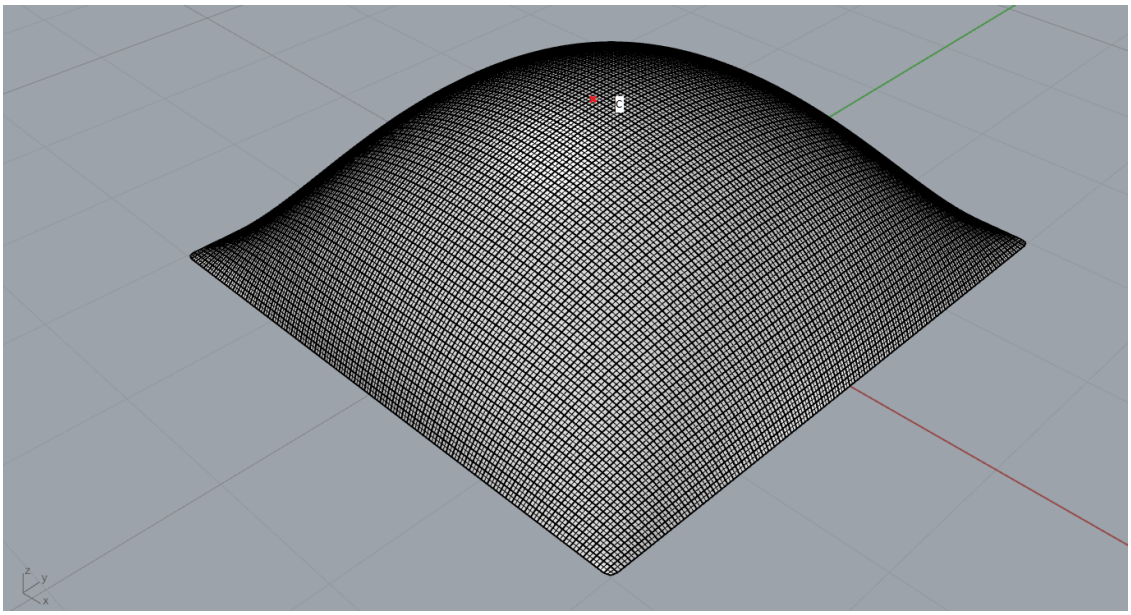

Figure 4.20: Model-3 maximum deformation point when subjected to undeformed loading case

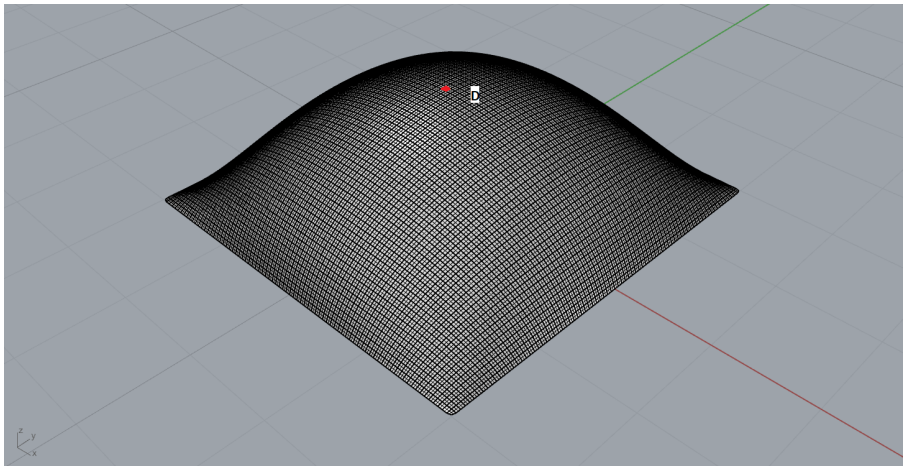

Figure 4.21: Model-3 element with maximum wind pressure in undeformed state

The deformation plot with respect to each iteration of point C is shown in figure 4.22 and the maximum wind pressure element plot with respect to each iteration is shown in figure 4.23.

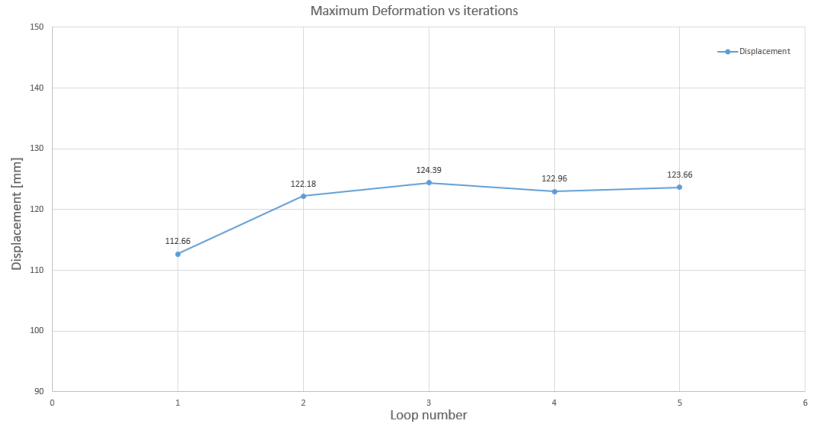

Figure 4.22: Displacement plot of point in figure 4.20 with respect to iterations

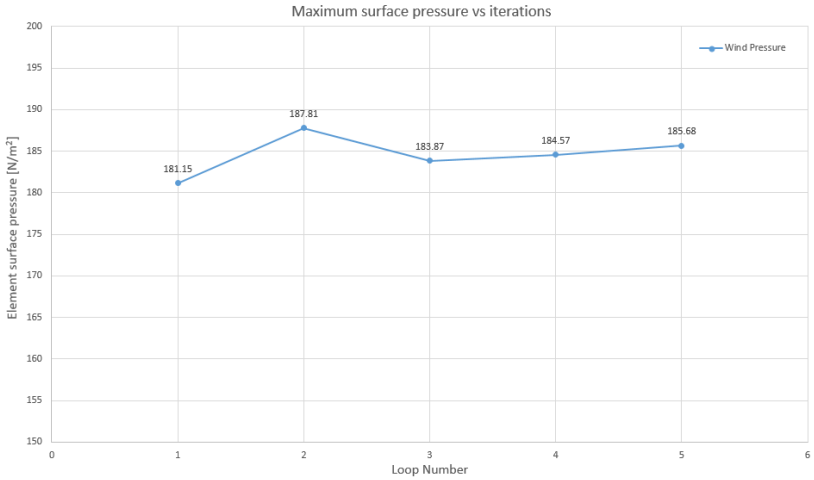

Figure 4.23: Wind pressure plot of element in figure 4.21 with respect to iterations

The change in pressure coefficient distribution on the structure along mid-section in the wind direction 3.23c is shown in figure 4.24

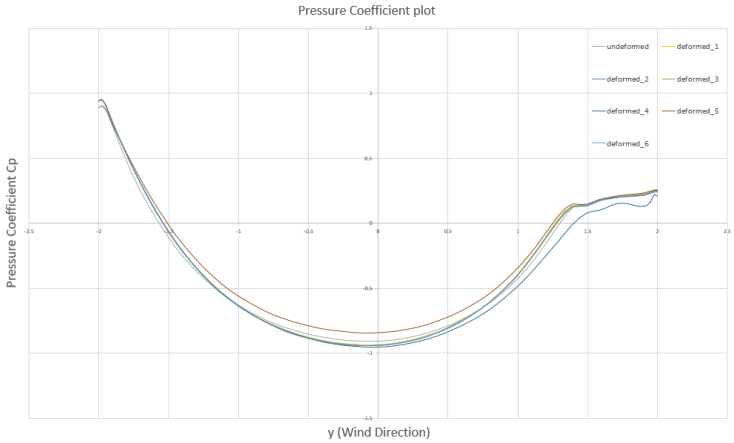

Figure 4.24: Pressure coefficient C_p plot along mid-section in figure 3.23c with respect to iterations

To visualize the changing pressure on the membrane structure with each iteration clearly, a wind pressure contour on the membrane surface is plotted in figure 4.25.

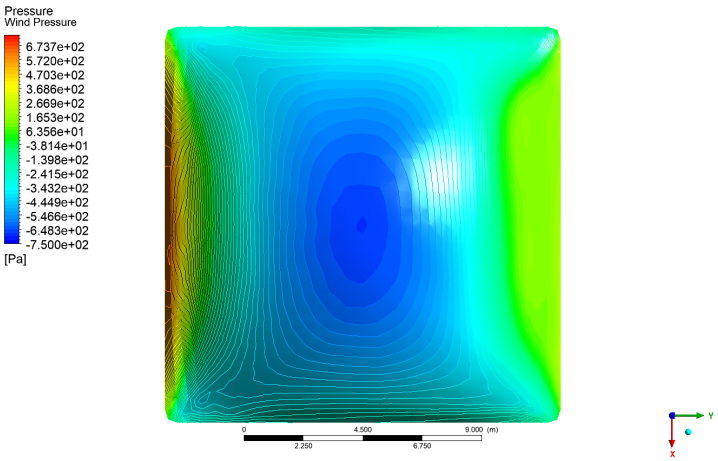

(a) Model-3: undeformed state wind surface pressure contour

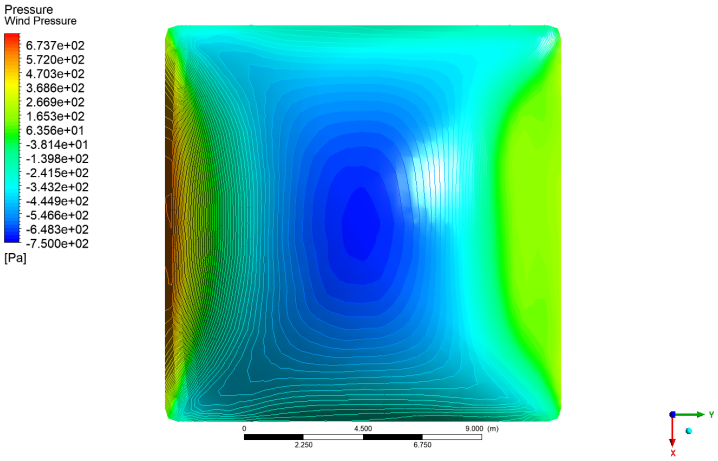

(b) Model 3: deformed 5^{th} state wind pressure contour

Figure 4.25: Model 3: Wind pressure contours

Similar to the hemispherical model, when the square geometry membrane model deforms, the stress in the membrane increases and consequently should result in increase of stiffness. As mentioned before, the stiffness is directly proportional to the frequency of the structure. In order to investigate this phenomena, the eigen frequency analysis of the structure is done after each iteration of analysis. In figure 4.26, the plot of natural frequency of the square geometry membrane structure with respect to each iteration is plotted. The structure in this case is subjected to wind velocity of 40 m/sec.

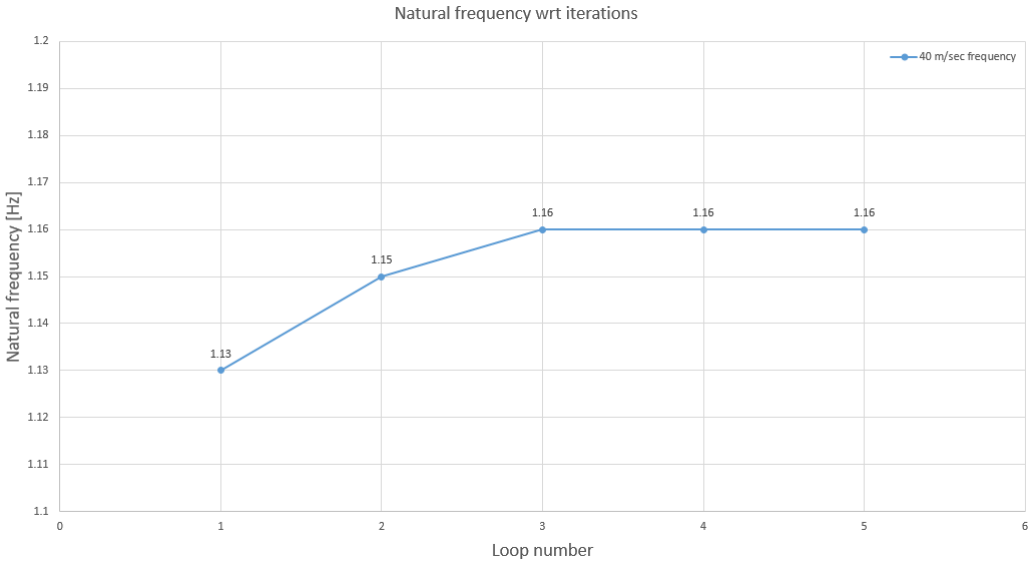

Figure 4.26: Natural Frequency plot of Model-3 with respect to iterations

Concluding from here, we can observe that the fluid structure interaction of the membrane structure subjected to wind loading provides us the first assessment of structural behaviour. Both with respect to magnitude of membrane deformation, surface wind pressure and natural frequencies involved. Moreover, the dependence of all these properties on varying wind velocities can be observed as well.

4.6. Summary

Within this chapter, we discussed the surface coupled multi-physics problem as a classification of fluid structure interaction. Different approaches were introduced to solve this problem named as Simultaneous analysis and Partitioned analysis. Partitioned analysis was chosen to perform the coupled simulation as it has the possibility to be reused. Moreover, it includes the required features to simulate the fluid-structure interaction.

Some basic requirements for the Partitioned analysis were introduced in section 4.3.1. The coupling schemes available for partitioned analysis were then introduced named as Weak partitioned coupling and Strong partitioned coupling in section 4.3.2 and 4.3.3.

In this work, the strong partitioned coupling was applied. A software environment was introduced to simulate the explained wind-membrane interaction. For the coupling of the 2 separate solvers (SOFiSTiK and ANSYS CFX), a third software (Grasshopper) is used. The method developed to couple all three softwares to transfer the coupling data is explained then in section 4.4. The key features of using the external coupling software were explained as well.

In the last section, the developed method was used to investigate the fluid-structure interaction of membrane structure. Both developed models were considered for the analysis. The results are presented with respect to the recommendations of Eurocode. Further, the deviation of the results such as maximum deformation and maximum pressure change from the normal practice is presented as well.

5

Discussion

5.1. Relevance of the Developed Methods for Wind Engineering

The two main things which this thesis focuses on are methodology and modeling aspects. The question which arises from the developed method is that to what extent it can be used in the field of wind engineering.

5.1.1. Consideration of Computational Fluid Dynamics role in Wind Engineering

For the consideration of wind loading on a structure, the designer needs the following information [6].

1. Wind environment information
2. Information regarding the forces induced on the structure due to environment
3. Structural response when subjected to these forces

In the mentioned points above, point 2 is covered by the developed software environment, though with certain limitation of CFD simulation. The main focus of the thesis lies in covering the third point. The interaction between the wind flow and structure can be modelled explicitly and moreover the effect on wind flow due to structure's behaviour can be accounted for. Though the whole process of considering the geometry at initial stage is made parametric, the software environment helps to analyse the wind flow around the structure for decided specific setups.

One question that still remains is how to proceed after simulating geometric non-linear effects to compute the design load on light weighted structures. This question has been answered in the following section which goes into the detail of how to calculate the design using the developed method in collaboration with the design code. Also, the effect geometric non-linear behaviour of the membrane is going to have on the safety factor proposed by the existing design codes for the stress limit of the membrane is discussed.

5.1.2. Possible use of the developed method considering existing design codes

Calculation of design wind loading on the structure

To find the design wind loading on a dome shaped structure, recommendations are given in the EN 1991-1-4 [1]. According to EN 1991-1-4 section 5.2, the wind pressure acting on the external surface can be obtained by the expression

$$w_e = q_p(z_e).c_{pe} \tag{5.1}$$

where: $q_p(z_e)$ is the peak velocity pressure
z_e is the reference height
c_{pe} is the pressure coefficient for external pressure

For the pressure coefficient on the curved roofs and domes, the reference height and pressure coefficient (c_{pe}) is described in the section EN 1991-1-4, 7.2.8. The pressure coefficient obtained following the graph 5.1 is along the mid-section of the structure parallel to the wind direction. Furthermore, the pressure coefficient obtained at each point in the wind direction is taken same in the direction parallel to the wind. In order to use the developed method to find the design wind loading on the structure considering the geometric non-linear behaviour of the membrane, the plot of pressure coefficient along the wind direction should be considered. The plots obtained from the Eurocode is not going to exactly match the one obtained from the developed method. The reason being that the plot in Eurocode considers the wind variation with the vertical height from the ground, while in the developed method the wind is considered constant with the height.

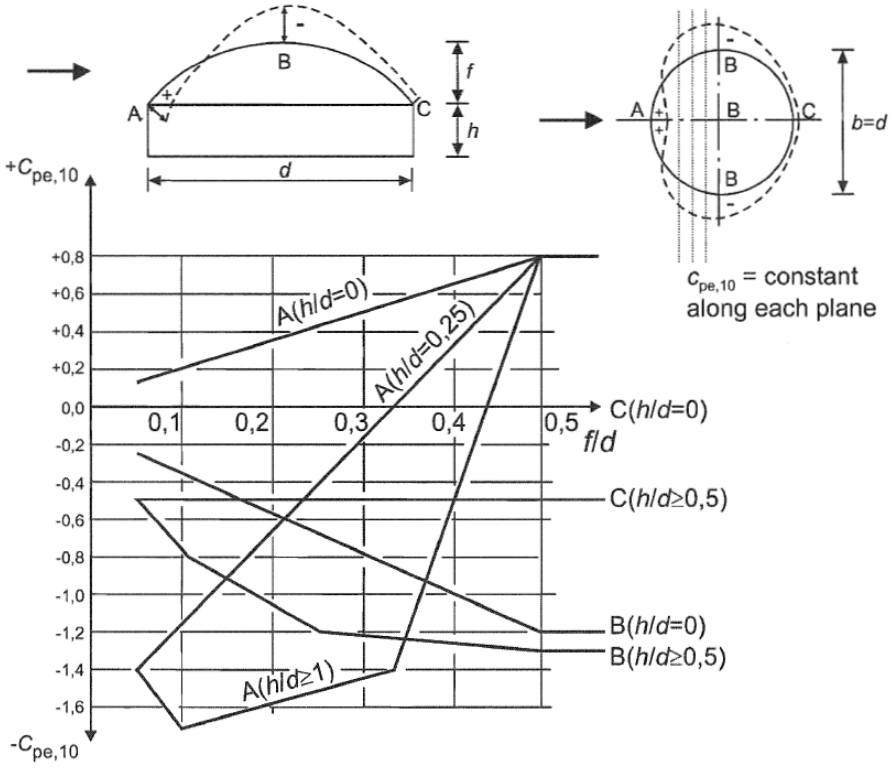

$c_{pe,10}$ is constant along arcs of circles, intersections of the sphere and of planes perpendicular to the wind; it can be determined as a first approximation by linear interpolation between the values in A, B and C along the arcs of circles parallel to the wind. In the same way the values of $c_{pe,10}$ in A if $0 < h/d < 1$ and in B or C if $0 < h/d < 0,5$ can be obtained by linear interpolation in the Figure above.

Figure 5.1: Pressure coefficient determination according to EN 1991-1-4, 7.2.8

The pressure coefficient plot from the two models developed in the section A.1 can be seen in figure 5.2 and 5.3 Both of the plots show the pressure coefficient distribution in the undeformed state and the pressure coefficient deformation after the convergence of the developed method. To take into consideration the geometric non-linear effects, the pressure coefficient plot in the deformed state using the developed method can be used.

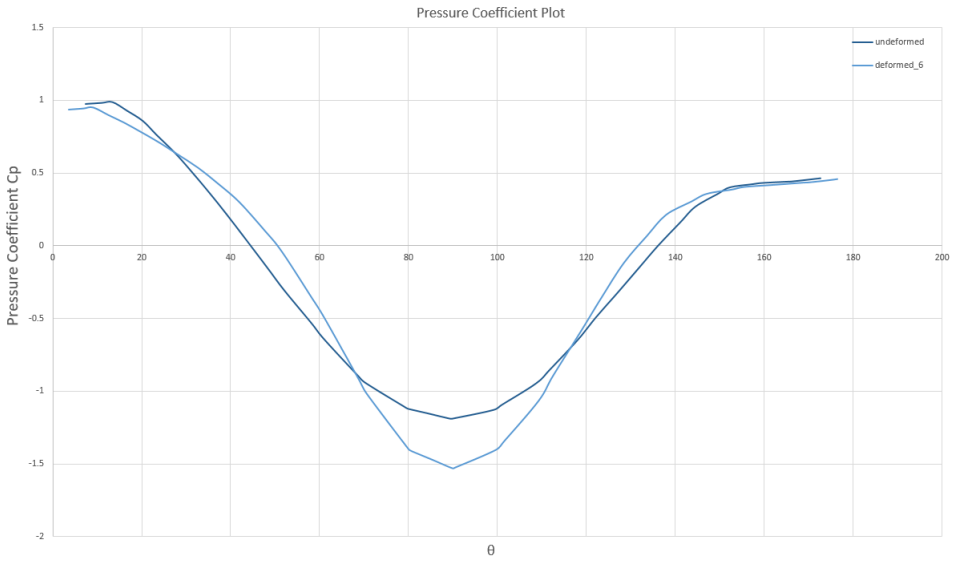

Figure 5.2: Pressure coefficient C_p plot along mid-section in figure A.6 in undeformed and deformed state after convergence

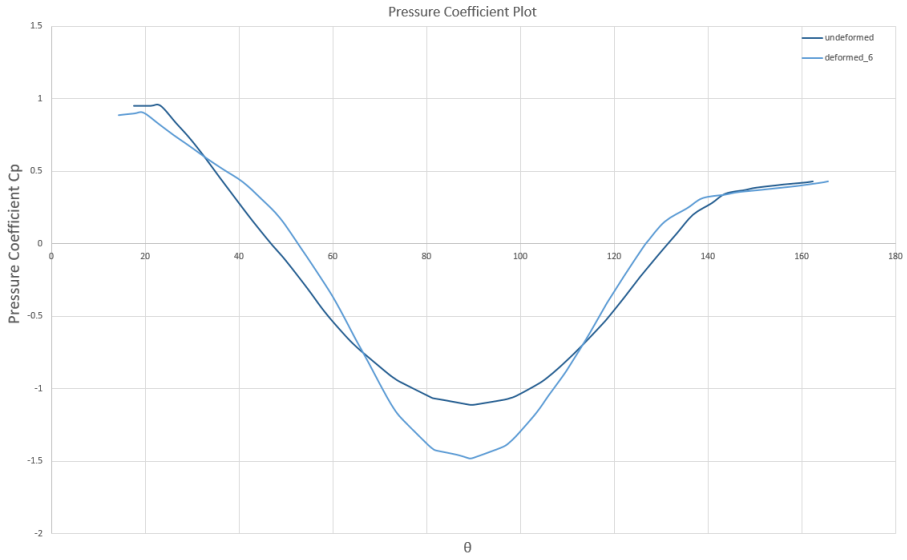

Figure 5.3: Pressure coefficient C_p plot along mid-section in figure A.13 in undeformed and deformed state after convergence

Effect on the design code regulation for membrane response

While designing the tensile membrane structures, the limit states for the membrane structures are:

1. **Deflection**
   While designing a membrane structure, the limitation of membrane deflection is project oriented and has to be agreed upon with the client.

2. **Resistance of material**
   Rather than the deflection limitation, the limitation of the membrane stress is more important for the design of membrane structures. In existing code such as Deutsches Institut für Normung German [German Institute for Standardization] [46], the A-factor concept is used. The A-factors are the stress reduction factors for the strength reduction of membrane compared to the basic value of tensile strength. For this stress reduction method, the loading is applied unfactored and thje load factor is introduced in the stress reduction factor itself. The allowable stress is defined as:

$$f_d = \frac{f_{tk}}{\gamma_f . \gamma_M . A_i} \tag{5.2}$$

where
f_d = allowable design stress
f_{tk} = tensile strength defined as 5% fractile
γ_f = load factor
γ_M = material factor coefficient (taken as 1.4 for fabric)
A_i = individual strength reduction factor

In the equation above, the A factors take into account the single material related strength reducing impacts. The values are as follows:

A_0 = 1.0 - 1.2 Strength reduction factor for biaxial loading
A_1 = 1.6 - 1.7 Strength reduction factor for long-term loads
A_2 = 1.1 - 1.2 Strength reduction factor for pollution and degradation
A_3 = 1.1 - 1.25 Strength reduction factor for high temperature load cases

As we can see in the above factors that as the membrane material is really fragile, there are several factors involved for the safety. After summarizing all the factors, the reduction factors comes in the range of 4 - 6.5. It is reasonable to say that may be the reduction factor proposed in the DIN 4134 takes into consideration the geometric non-linear behaviour of the membrane structure. But from the study done in this work, the impact of this non-linear behaviour on the safety factor can be assessed.

5.1.3. Further consideration of fsi simulation in wind engineering

When considering the aeroelastic effects in membrane structures, the assumption of considering wind load on the structures as the square of wind speed with some constant factor is not valid anymore. The deformation of the structure is dependent on the wind speed considered, which consequently changes the wind pressure distribution on the structure. In order to derive the design wind load on the structure from fluid-structure interaction computation, different wind velocities need to be considered. The number of computation iterations required depends on the wind speed in consideration. To properly understand the behaviour of the structure, different combinations of wind speed with structural properties need to be considered. In order to make this computationally less extensive, one way is to analyse the structure for worst case parameters combination for a specific geometry. This will give the design load that needs to be considered for designing the structure. This approach is more general than deriving the dimensionless pressure coefficient at each point on the membrane surface and combining them to find the worst case.

As mentioned before, the developed numerical simulation has a deterministic nature and it requires significant number of computations. It also requires the knowledge of dominant wind induced effect on the structure to properly derive the design load on the structure with fsi numerical method. To apply this developed method for the structures for which the knowledge of dynamic induced effects is limited, utmost consideration should be taken. Otherwise, due to approximations and simplifications the wind induced effects may not be revealed in the computation.

5.1.4. Dynamic aspects of Air-supported Structures

As Wind flow described in the section 3.1 , consequently the dynamics aspects of the Air-supported structures is not considered in this work. Nevertheless a detailed discussion on the dynamic behaviour is done in this section. Membrane structures are very similar to cable-net structures. In comparison to cable-net, the membrane brings some air effects which are also known as the aerodynamic effects.

The membrane decreases the natural frequency of the structure. There are mainly two effects which the surrounding air has on the membrane structure:

1. Added mass

   The extent of the added mass on the membrane structure is going to be dependent on the fact that which vibration modes of the structures are being excited by the wind flow. The vibration modes in which the movement of membrane is in-phase to each other which means moving in same direction is going to have more added mass effect. This is because when moving in one direction, the membrane is able to excite more surrounding air while in the anti-phase vibration mode, some part of the membrane will vibrate the surrounding air in one direction and other part in other direction and consequently less surrounding air will be vibrating.

2. Radiation damping

   The membrane in these structures provide a lot of damping. Similar to the concept of added mass, the in-phase vibration modes induce more damping from the surrounding air than the anti-phase vibrations modes. The extent of damping also depends on the wind velocity as well. It is observed from the experiments in [47] that with increase in the wind velocity, the damping decreases. And moreover it was found that the vibration modes with higher damping contribution are going to be effected more by the wind gust.

   In some specific cases, the negative damping was also observed but as a local phenomenon. For very short period of time, some divergent free vibration response was observed which may be attributed as negative damping. For pneumatic structures, this negative damping can induce unstable flutter like vibrations but only locally. In general, the overall stability of the structure is maintained.

6

Conclusion and Recommendation

6.1. Conclusion

The developed method in the software environment is a very useful tool for a wind engineer who has the knowledge of important wind structure interaction concepts useful for the design of these structures. With this tool, the effect of geometric non-linearity can be taken into account in the process of designing a membrane structure. This tool can act as a complement or enhancement to the already existing approaches such as analytical, semi-analytical or experimental approach. The developed method is very flexible in nature, which means that other alternate single field solvers can be used for the analysis.

From the work presented showing the use of developed method to analyse the response of membrane structures subjected to wind loading considering the geometric non-linear effect of the membrane, the problem statements formulated in section 1.1 can be answered.

First and foremost it can be concluded from the analysis of the Hemispherical model (2^{nd}- model) in section 4.5.2 that the deformation of the membrane structure has influence on the wind flow around the structure. This change is evident from the plot 4.6, 4.7. Figure 6.1 shows the modified pressure coefficient distribution considering the geometric non-linear behaviour from the use of method, which can be used to calculate the improved wind pressure on the structure.

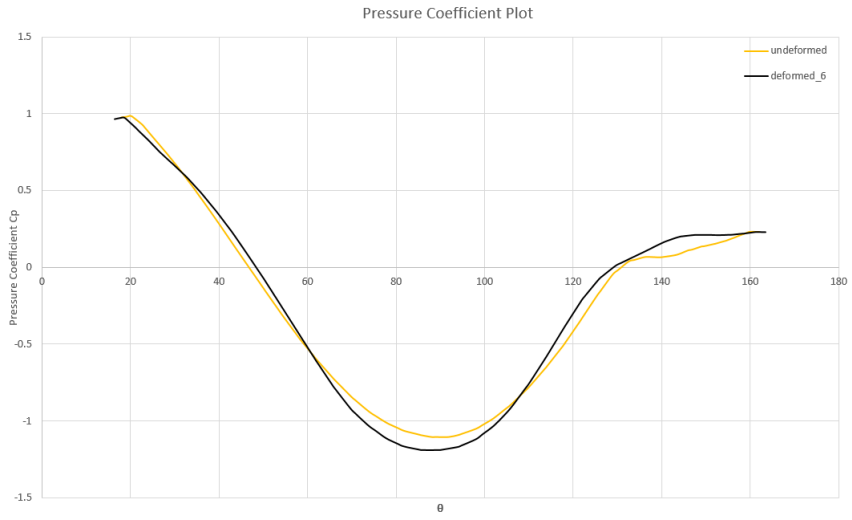

Figure 6.1: Model-2 Pressure coefficient C_p plot along mid-section in figure 3.23b in undeformed and deformed state after convergence

Furthermore, it can observed from the wind variation study of the Hemispherical air dome model in section 4.5.2 that the geometric non-linear behaviour effect on the structure's response depends on the velocity of wind being considered. From the plots 4.13 and 4.14, it can be concluded that the geometric non-linear behaviour effect on maximum deformation and maximum wind pressure increases with increase in the wind velocity being considered. From the specific setup of wind variation taken in this work, a significant change of around 38% in comparison to analysis without considering the geometric non-linear behaviour was observed, which is quite significant when designing a membrane structure.

From the size variation study with keeping the wind velocity constant, it can be concluded that geometric non-linear behaviour increases with the increase in size of the membrane structure. The effect of this non-linear behaviour can be observed in plots of maximum deformation 4.17 and maximum wind pressure 4.18. With a fairly realistic wind velocity of 33 m/sec in consideration, the percentage change from the case of analysis without considering the geometric non-linearity becomes significant. With the specific setup in this work, a significant change of around 25-30 % was observed. So, this signifies that the consideration of geometric non-linearity while designing the membrane structure is important. This change is noticeable in the plot of pressure coefficient (figure 5.2 and 5.3) of the models developed for size variation study. The pressure coefficient plot on the deformed state after the convergence can be used for design wind load calculation for the air-supported models developed.

Moreover, from the analysis of square base air dome model in section 4.5.2, it is proved that the developed method in this work to simulate the behaviour of membrane structures subjected to wind loading considering the geometric non-linear behaviour of membrane can be used for any base geometry with known internal air pressure and dimensions. The effects on the maximum wind pressure, maximum deformation, membrane stress and moreover the effect on the pressure coefficient distribution can be observed.

It is evident from the analysis of the specific cases taken in this work that from the method developed we are able to get the information of forces the wind is inducing on the air-supported structure (second point in section 5.1.1) and moreover we are able to estimate the structure's response to the loading considering the geometric non-linearity (third point in section 5.1.1). So, this method can be used to get a better knowledge of the structure's response to wind loading while design the air-supported structures. It should be noted that the method developed here does not consider the dynamic effects the membrane structure is going to have on the response of the structure. So, this developed method should be used carefully for the design.

The developed method can not only simulate the interaction between membrane and wind, but it can be used for various surface coupled multi-physics problems. The developed tool can be applied in the field of biomechanics, e.g. flexible veins with blood simulation, in the field of automotives, e.g. the wind interaction with the flexible roof of convertible cars.

6.2. Limitations

There are certain assumptions which are made in this thesis to reduce the complexity of wind-membrane interaction and also reduce the computational efforts required to simulate the behaviour of membrane structure when subjected to wind loading. These assumptions come with several advantages but disadvantages as well which impose some limitations on the capability of the developed method. These limitations are as follows:

1. The wind speed with respect to height is considered constant, which is not the realistic case.
2. Wind velocity variation with respect to time is not considered.
3. The dynamic properties of the simulation such as damping due to the surrounding air is not considered.

There are some other technical aspects which need to be considered while using the method to simulate the analysis. The discretization of the membrane surface effects the wind simulation. There

is no specific limit to the size of the element for the discretization but if discretized very fine, the curved surface of the membrane in the structure gets large number of edges from the elements. This sometimes induces vortices, which can introduce some errors in the wind simulation.

There is another technical limitation related to the CFD simulation. The wind flow in CFD model is considered as subsonic, so in general if considering the wind velocity above 160 m/sec, the wind simulation will crash as the wind flow will become supersonic. This limitation also needs to be considered in the case of decreasing flow area, as the flow velocity will increase.

6.3. Recommendations

The assumption taken in this thesis do help to simplify the simulation but also takes the simulation a bit further from the reality. We believe that the developed method can be extended and further improved. There are certain aspects of computation which are recommended as follows:

1. Wind Speed variation with height

   In this thesis work, as mentioned in section 3.4.2 the wind velocity is taken constant with respect to height. In reality, the wind velocity is dependent on height. To accurately simulate the realistic wind condition, the Neutrally Stratified Atmospheric Boundary layer (ABL) can be modelled. The wind profile in ABL simulation follows the logarithmic law.

2. Wind Variation with time

   In the presented work, the wind is considered to be constant with respect to time. To properly consider the wind flow around the structure, the wind velocity should be considered varying with time. The wind input with respect to time can be taken from recorded data. This variation will give rise to wind gust and turbulence in the wind flow, which will make the analysis complex. To analyse the structural behaviour in this case considering the wind variation as well as the geometric non-linearity, the analysis has to be done. A proposed flowchart 6.2 can be followed to take into consideration the wind speed variation with respect to time.

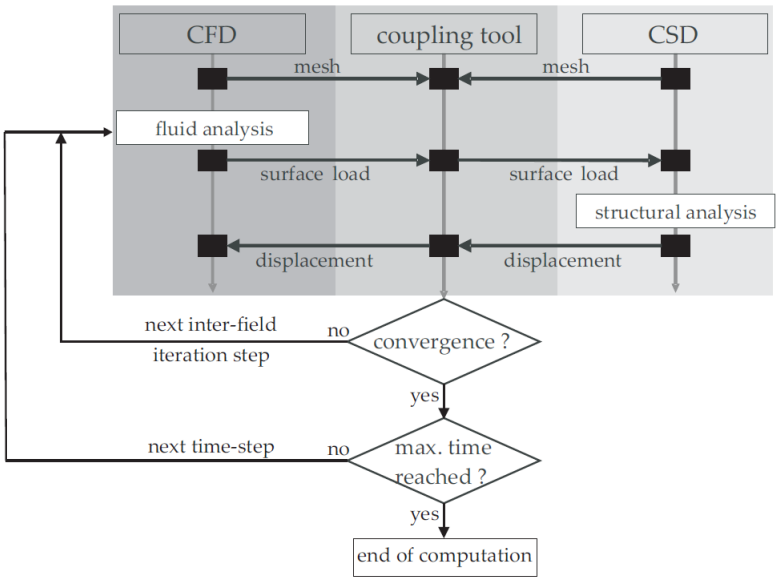

Figure 6.2: Flow chart of computations considering wind variation with time

3. Dynamic aspects of membrane structures

   The presented work considers the static analysis when subjected to wind loading. In case of membrane structures, the membrane itself doesn't have the inertia effect but the air which is surrounding the membrane has inertia effect. So, when the membrane structure is subjected to wind loading, surrounding air has a damping effect on the behaviour of the structure. The developed method in this thesis ignores this inertia effect. With the partitioned analysis method used in this thesis, this effect of inertia cannot be considered. In order to take into account this effect, simultaneous analysis has to be done.

A

Size variation study

A.1. Size variation with constant wind speed

Here in this appendix, the developed method to analyse the geometric non-linearity of membrane structures subjected to wind loading is used. This non-linear behaviour is highly dependent on the size of structure considered. In this appendix, an attempt is made to use this developed method to analyse certain realistic cases. Wind velocity is considered as 33 m/sec, which is approximately the wind speed observed in the case of hurricane. To study the dependence on size of the structure the variation in size of radius in developed model is considered. Hemispherical air dome with the radius of 10 m and 20 m will be considered. One thing to note here, with the increase in the size of the structure, the computational power required to analyse the structure will increase as well. Therefore, in this size variation study, only 2 cases are considered.

A.1.1. Model 4: Hemispherical Air Dome with 10 m Radius

As mentioned above, the extent of geometric non-linear behaviour of membrane structures highly depends on the size of the structure considered. A hemispherical air dome model is considered with a radius of 10 m. The boundary conditions in CFD model is taken the same used in section 3.4.2. The numerical model is shown in figure A.1.

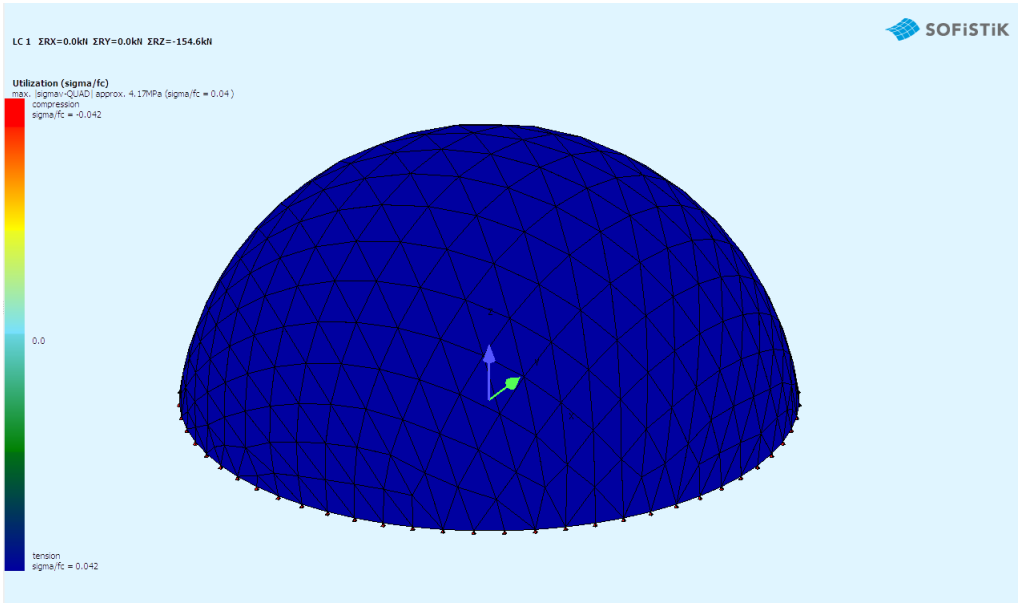

Figure A.1: Model-4: 10m Radius Hemispherical Air dome

To investigate the effect of geometric non-linearity on the deformation of the structure and the pressure distribution on the structure, the point with maximum deformation and pressure is considered. In figure A.2, the point (E) which has the maximum deformation after the first iteration (normal practice) is shown and in figure A.3, the element (F) which has maximum element wind pressure on the undeformed geometry is shown. Choosing these location for the observation will help us to calculate the maximum error we make following the general practice.

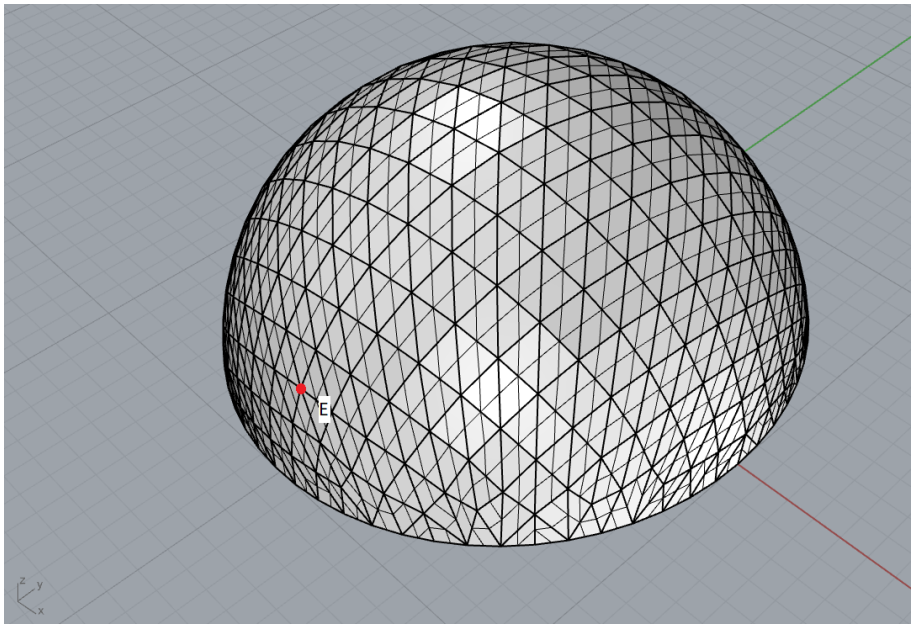

Figure A.2: Model-4: maximum deformation point when subjected to undeformed loading case

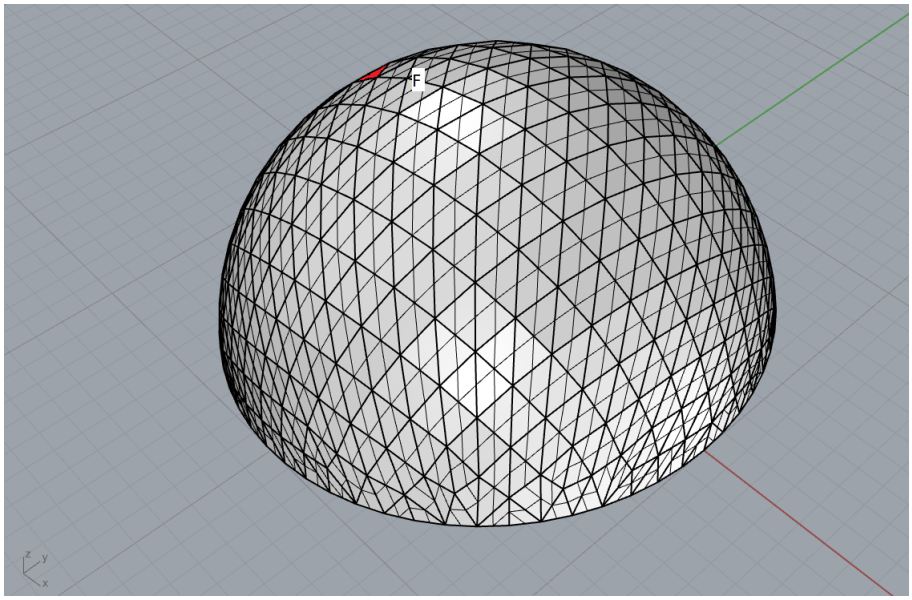

Figure A.3: Model-4 element with maximum wind pressure in undeformed state

To clearly see the effect of geometric non-linearity on the membrane structure, the plot of percentage change in deformation of point (E) A.2 with respect to iterations in comparison to the deformation when not considering the geometric non-linearity is shown in figure A.4 and the percentage change in wind pressure of element (F) A.3 with respect to wind pressure in the undeformed state is shown in figure A.5.

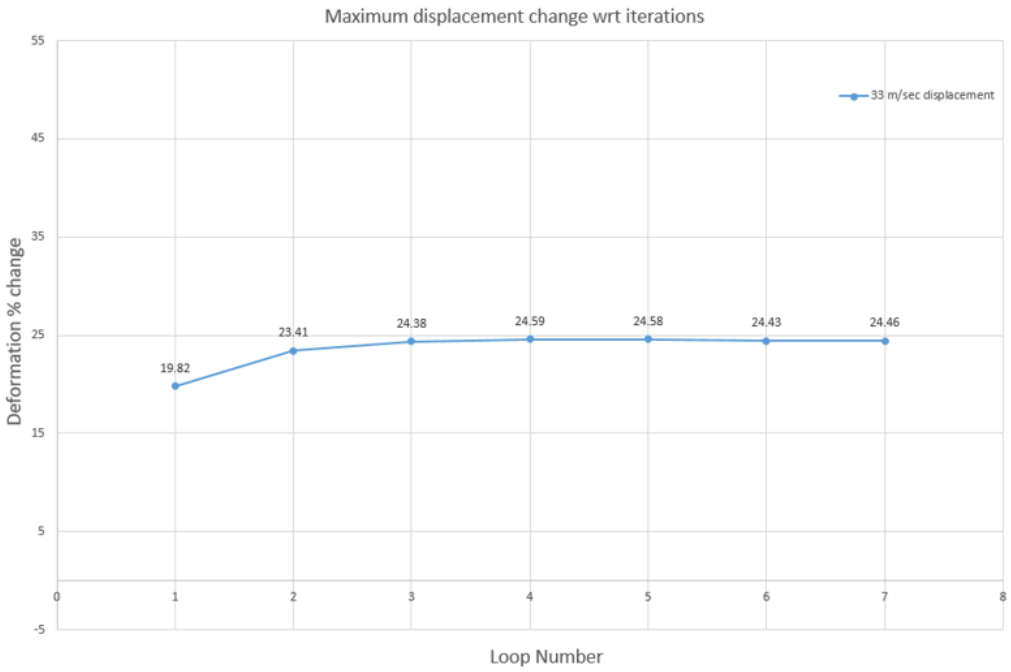

Figure A.4: % displacement change of point in figure A.2 with respect to original displacement

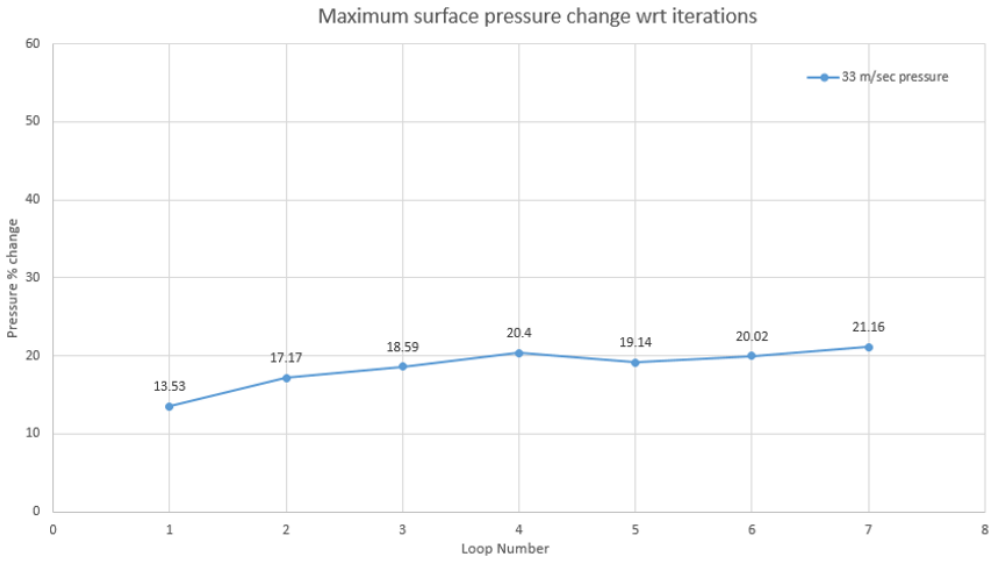

Figure A.5: % wind pressure change of element in figure A.3 with respect to undeformed state

In Eurocode, to calculate the wind pressure on the structure the pressure coefficient c_p is calculated on the mid-section of the structure in the wind direction. The mid-section for the model is shown in figure A.6. The change in pressure coefficient distribution with each iteration of analysis along the mid-section in the wind direction is shown in figure A.7.

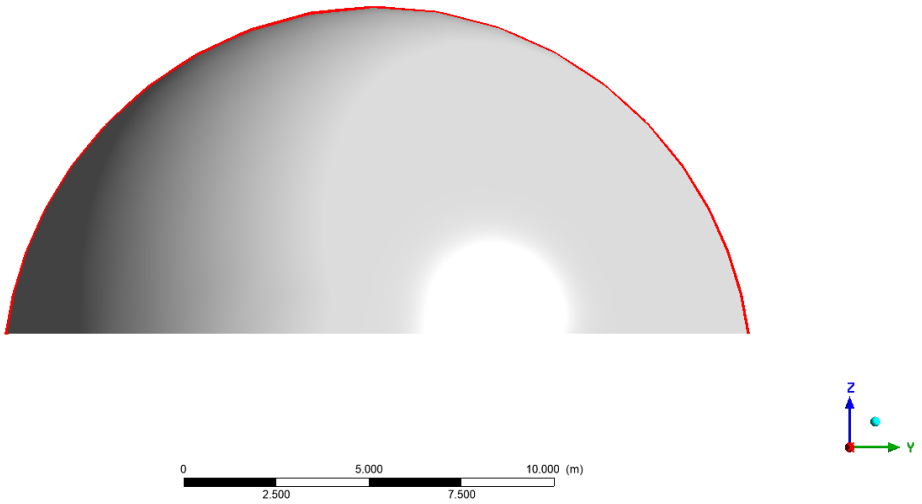

Figure A.6: Model 4: Intersection line of membrane with domain midsection

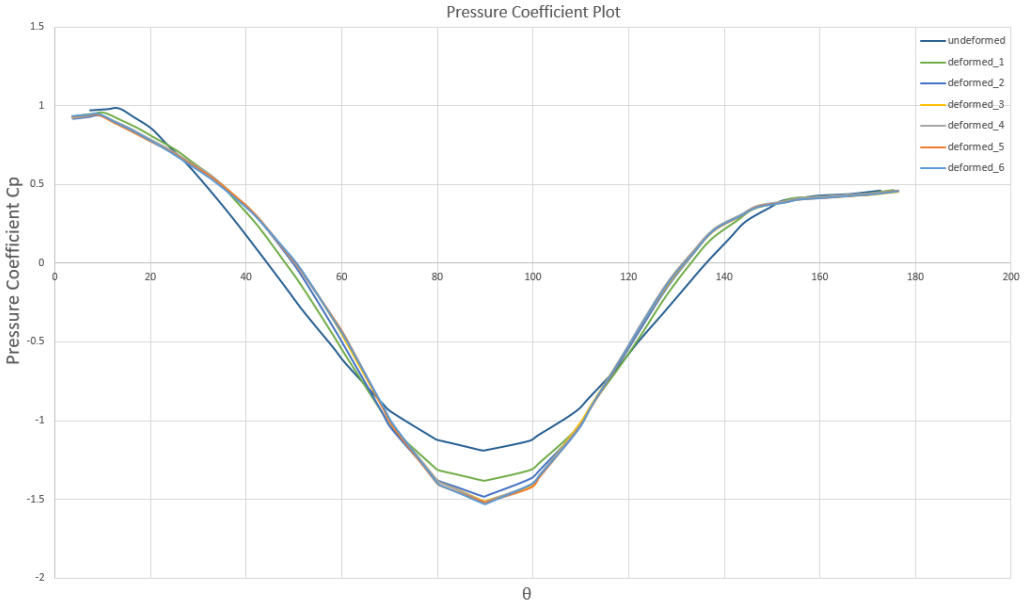

Figure A.7: Pressure coefficient c_p plot along mid-section in figure A.6 with respect to iterations

A.1.2. Model 5: Hemispherical Air Dome with 20 m Radius

To study the behaviour of geometric non-linearity with increasing size of the structure, a model similar to section A.1.1 model is taken but with a radius of 20 m. The boundary conditions of the CFD model is taken similar. The numerical model obtained after the form finding is shown in figure A.8.

Similarly, to investigate the extent of geometric non-linearity on structure's response, the point of maximum wind pressure and maximum deformation are observed. Figure A.9 shows the point (G) which has the maximum deformation when following the general practice and figure A.10 shows the element (F) which has maximum element wind pressure on the undeformed geometry.

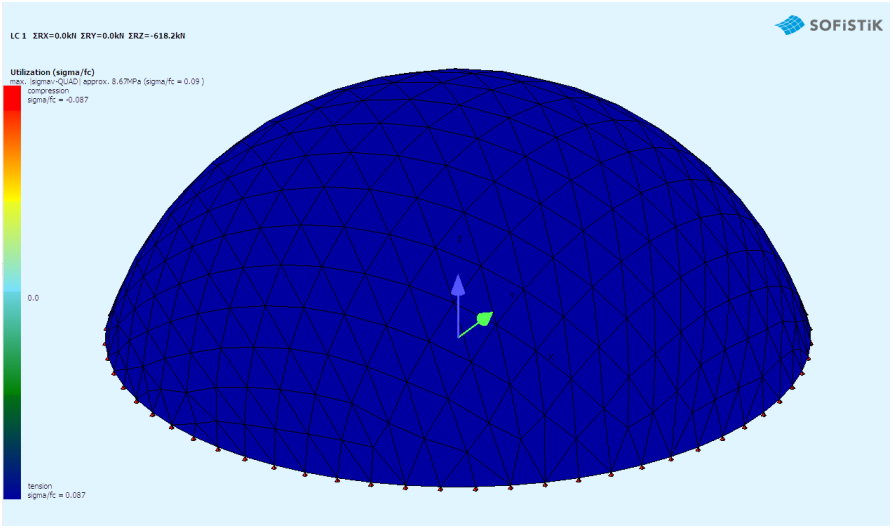

Figure A.8: Model-5: 20m Radius Hemispherical Air dome

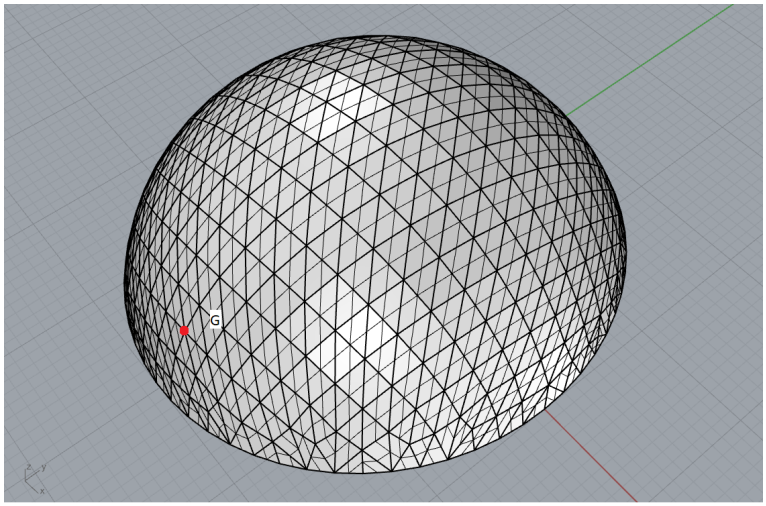

Figure A.9: Model-5: maximum deformation point when subjected to undeformed loading case

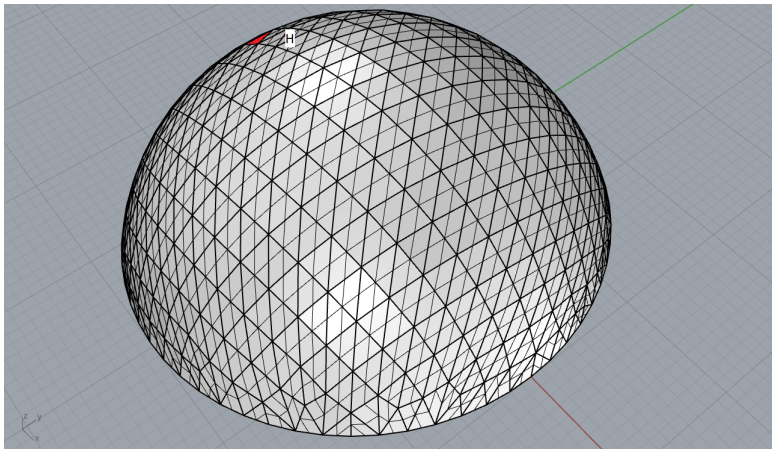

Figure A.10: Model-5 element with maximum wind pressure in undeformed state

The plot of percentage change in deformation of point G A.9 with respect to iterations in comparison to the deformation when not considering the geometric non-linearity is shown in figure A.11 and the percentage change in wind pressure of element (F) A.10 with respect to wind pressure in the undeformed state is shown in figure A.12.

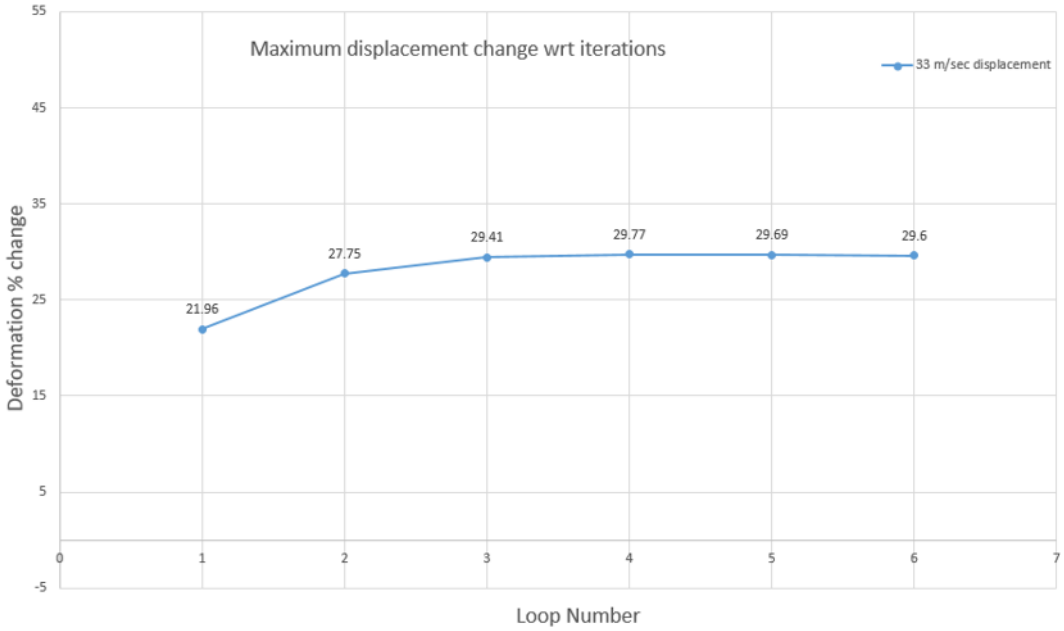

Figure A.11: % displacement change of point in figure A.9 with respect to original displacement

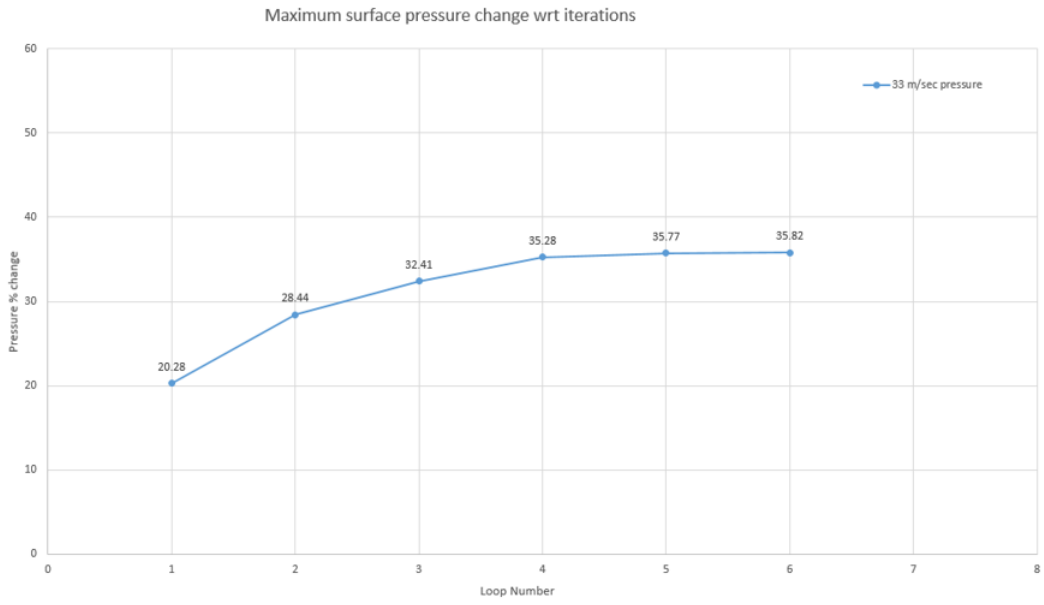

Figure A.12: % wind pressure change of element in figure A.10 with respect to undeformed state

To visualize the changing wind pressure on the structure due to deformation of the membrane, the dimensionless pressure coefficient c_p is plotted for the mid-section of the structure along the wind direction A.13. The pressure coefficient plot with each iteration is plotted in figure A.14.

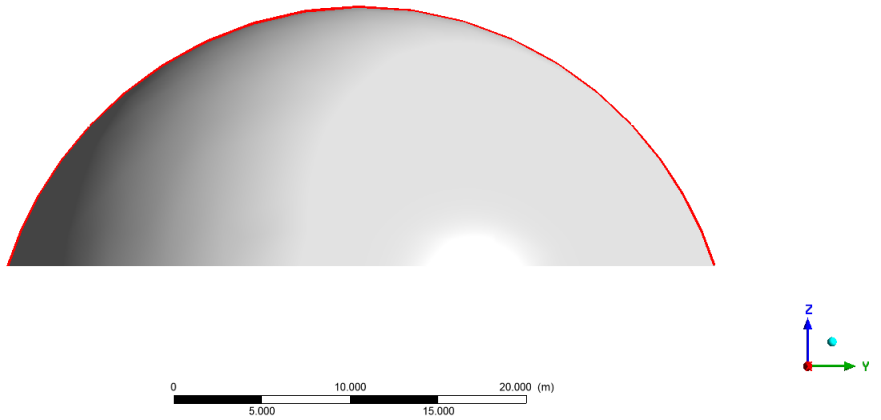

Figure A.13: Model-5: Intersection line of membrane with domain midsection

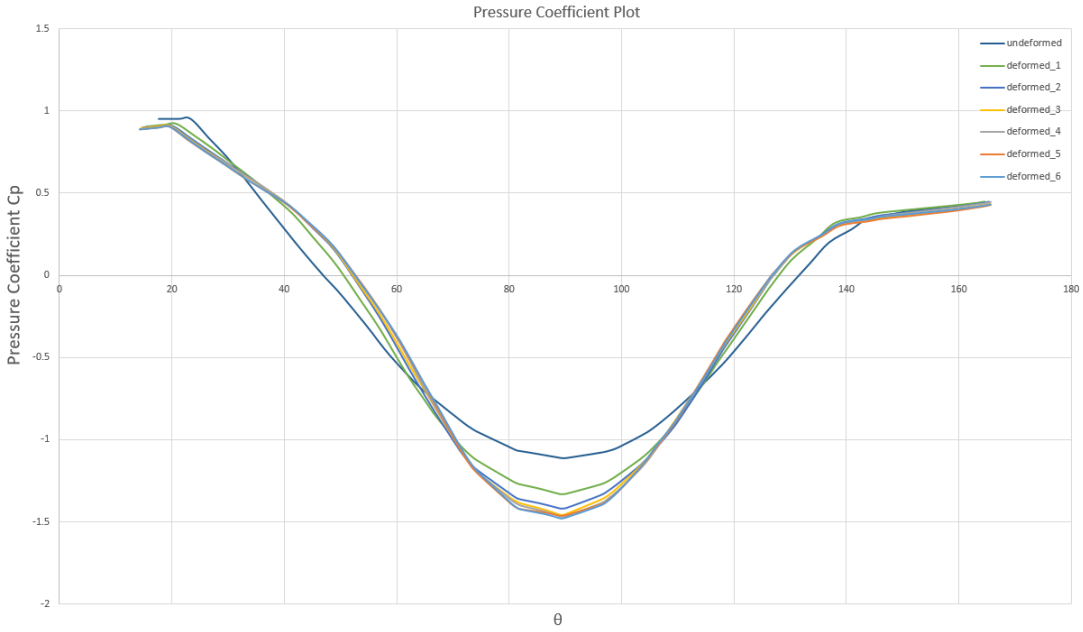

Figure A.14: Pressure coefficient c_p plot along mid-section in figure A.13 with respect to iterations

A.2. Summary

In this thesis we focus on simulating the response of the membrane structures when subjected to Wind loading considering the geometric non-linear behaviour of the membrane. With this, it becomes important to study the dependence of this non-linear behaviour on the size of the structure considered. In this appendix two sizes of Hemispherical Air Dome were considered with a wind velocity of 33 m/sec. Figures A.4, A.5, A.11 and A.12 show the deviation of maximum pressure and deformation from the normal practice. As we can see that the percentage change is more than 30 while going towards more realistic cases, it becomes important to investigate the geometric non-linear effects on the strucutre's response.

Bibliography

[1] B. En *et al.*, “Eurocode 1: Actions on structures—part 1–4: General actions—wind actions,” *NA to BS EN, Brussels, Belgium*, 1991.

[2] B. Hübner, E. Walhorn, and D. Dinkler, “A monolithic approach to fluid–structure interaction using space–time finite elements,” *Computer methods in applied mechanics and engineering*, vol. 193, no. 23-26, pp. 2087–2104, 2004.

[3] C. Michler, S. Hulshoff, E. Van Brummelen, and R. De Borst, “A monolithic approach to fluid–structure interaction,” *Computers & fluids*, vol. 33, no. 5-6, pp. 839–848, 2004.

[4] T. E. Tezduyar, “Finite elements in fluids: Stabilized formulations and moving boundaries and interfaces,” *Computers & fluids*, vol. 36, no. 2, pp. 191–206, 2007.

[5] H. G. Matthies and J. Steindorf, “Partitioned strong coupling algorithms for fluid–structure interaction,” *Computers & structures*, vol. 81, no. 8-11, pp. 805–812, 2003.

[6] E. Simiu and R. H. Scanlan, “Wind effects on structures, john wiley & sons,” *Inc., New York*, 1996.

[7] S. Topham, *Blowup: Inflatable Art, Architecture, and Design*, ser. Art and Design Series. Prestel, 2002, ISBN: 9783791326870. [Online]. Available: https://books.google.nl/books?id=dcJ1QgAACAAJ.

[8] *Tensioned membrane roofing, fabric roofing – birdair, inc*. [Online]. Available: https://www.birdair.com/.

[9] R. WHITEHEAD, “Frei otto’s pneumatic experiments for humanitarian design: The ideology and technology of lightness and adaptability.,”

[10] M. Pedretti, “Tensairity,” in *European Congress on Computational Methods in Applied Sciences and Engineering (ECCOMAS)*, 2004, pp. 1–9.

[11] A. LeCuyer, *ETFE: Technology and Design*. Birkhäuser, 2008, ISBN: 9783764386245. [Online]. Available: https://books.google.nl/books?id=%5C_Y7TAAAAQBAJ.

[12] M. Bakker and T. Peköz, “The finite element method for thin-walled members—basic principles,” *Thin-Walled Structures*, vol. 41, no. 2-3, pp. 179–189, 2003.

[13] T. Herzog, *Pneumatische Konstruktionen: Bauten aus Membranen und Luft*. Hatje, 1976.

[14] B. Forster, “Cable and membrane roofs-a historical survey,” *Structural Engineering Review*, vol. 6, no. 3-4, pp. 145–174, 1994.

[15] K. Linkwitz and H. Schek, “A few remarks on the calculation of pre-tensioned cable net structures,” *engineer archive*, vol. 40, no. 3, pp. 145–158, 1971.

[16] H.-J. Schek, “The force density method for form finding and computation of general networks,” *Computer methods in applied mechanics and engineering*, vol. 3, no. 1, pp. 115–134, 1974.

[17] S. V. Y. V. Beilin D.A. Polyakov V.I., “Using the stereophotogrammetric method to study the stress-strain state of a spherical soft shell in an air flow,” *TsAGI Scientific Notes*, vol. 13, no. 6, pp. 66–76, 1982. [Online]. Available: https://cyberleninka.ru/article/n/ispolzovanie-stereofotogrammetricheskogo-metoda-dlya-issledovaniya-napryazhenno-deformirovannogo-sostoyaniya-myagkoy-obolochki.

[18] P. van Staalduinen, “Backgrounds of the wind loads according to nen 6702: 1991,” TNO, Tech. Rep., 1992.

[19] W. Hucho, “Aerodynamics of blunt bodies. physical foundations and practical applications; aerodynamik der stumpfen koerper. physikalische grundlagen und anwendungen in der praxis,” 2002.

[20] A. G. Davenport, “The spectrum of horizontal gustiness near the ground in high winds,” *Quarterly Journal of the Royal Meteorological Society*, vol. 87, no. 372, pp. 194–211, 1961.

[21] R. Harris, *Measurements of wind structure at heights up to 598 ft above ground level*. Electrical Research Association, 1968.

[22] E. Simiu, “Wind spectra and dynamic alongwind response,” *Journal of the structural division*, vol. 100, no. 9, pp. 1897–1910, 1974.

[23] M. Balz and M. Dencher, *European design guide for tensile surface structures, chapter design loading conditions*, 2004.

[24] C. Eurocode, “1: Basis of design and actions on structures-part 2-4: Actions on structures–wind actions,” *European Committee Standardization*, 1991.

[25] N. Cook, “The designer’s guide to wind loading of building structures part 1: Background,” *Damage survey, wind data and structural classification building research establishment, Garston and Butterworths London*, 1985.

[26] J. A. Żurański, *Windbelastung von Bauwerken und Konstruktionen*. Müller, 1969.

[27] N. J. Cook, “The designer’s guide to wind loading of building structures. vol. 2: Static structures,” *Building Research Establishment Report*, 1990.

[28] J. D. Holmes and S. Bekele, *Wind loading of structures*. SPON press London, 2001, vol. 11.

[29] G. Schwarz and H. Lienhart, “Circulation of membranes and their simulation in the wind tunnel,” in *3rd International Symposium ”Wide-Spanning Fl ä chentragwerke ”, SFB*, vol. 64, 1985.

[30] M. Kazakevitch, “The aerodynamics of a hangar membrane roof,” *Journal of Wind Engineering and Industrial Aerodynamics*, vol. 77, pp. 157–169, 1998.

[31] E. Rank, A. Halfmann, M. Gluck, M. Breuer, F. Durst, U. Kaiser, D. Bergmann, and S. Wagner, “Windbelastung leichter flachentragwerke: Numerische simulation und windkanalversuch,” *Bauingenieur*, pp. 501–508, 2003.

[32] K. Saberi-Haghighi, *To determine the deformation-dependent ”a ngigen wind load at H ä nged ”a chern*. Inst. f ”u r Str ö mungs mechanics and electronic computing in construction, 1997.

[33] B. ö. r. C. H ”u bner, *Simultaneous analysis of structure-wind interactions*. Inst. f ”u r statics, 2003.

[34] J. Wendt, *Computational Fluid Dynamics: An Introduction*, ser. A von Karman Institute book. Springer Berlin Heidelberg, 2008, ISBN: 9783540850557. [Online]. Available: `https://books.google.nl/books?id=IIUkqI-HNbQC`.

[35] J. Franke, A. Hellsten, K. H. Schlunzen, and B. Carissimo, “The cost 732 best practice guideline for cfd simulation of flows in the urban environment: A summary,” *International Journal of Environment and Pollution*, vol. 44, no. 1-4, pp. 419–427, 2011.

[36] J. Franke, A. Hellsten, H. Schlunzen, and B. Carissimo, “The best practise guideline for the cfd simulation of flows in the urban environment: An outcome of cost 732,” in *The fifth international symposium on computational wind engineering*, 2010, pp. 1–10.

[37] J. Franke, “Introduction to the prediction of wind loads on buildings by computational wind engineering (cwe),” in *Wind effects on buildings and design of wind-sensitive structures*, Springer, 2007, pp. 67–103.

[38] J. Franke, C. Hirsch, A. Jensen, H. Krüs, M. Schatzmann, P. Westbury, S. Miles, J. Wisse, and N. Wright, “Recommendations on the use of cfd in predicting pedestrian wind environment,” in *Cost action C*, vol. 14, 2004.

[39] N. A. Mokin, A. A. Kustov, and S. I. Trushin, “Numerical simulation of an air-supported structure in the air flow,” in *Textiles composites and inflatable structures VIII: proceedings of the VIII International Conference on Textile Composites and Inflatable Structures, Barcelona, Spain. 9-11 October, 2017*, CIMNE, 2017, pp. 383–393.

[40] M. Heil, “An efficient solver for the fully coupled solution of large-displacement fluid–structure interaction problems,” *Computer Methods in Applied Mechanics and Engineering*, vol. 193, no. 1-2, pp. 1–23, 2004.

[41] C. Farhat and M. Lesoinne, “Two efficient staggered algorithms for the serial and parallel solution of three-dimensional nonlinear transient aeroelastic problems,” *Computer methods in applied mechanics and engineering*, vol. 182, no. 3-4, pp. 499–515, 2000.

[42] W. A. Wall, “Fluid-struktur-interaktion mit stabilisierten finiten elementen,” 1999.

[43] D. P. Mok and W. Wall, “Partitioned analysis schemes for the transient interaction of incompressible flows and nonlinear flexible structures,” *Trends in computational structural mechanics, Barcelona*, vol. 128, 2001.

[44] K.-C. Park, C. A. Felippa, and R. Ohayon, “Partitioned formulation of internal fluid–structure interaction problems by localized lagrange multipliers,” *Computer Methods in Applied Mechanics and Engineering*, vol. 190, no. 24-25, pp. 2989–3007, 2001.

[45] S. Deparis, EPFL, Tech. Rep., 2004.

[46] T. n. Bodor, “Air-supported structures: Creation of a verification concept based on the current eurocodes and din 4134,” Ph.D. dissertation, Vienna, 2020.

[47] Q. Yang, Y. Wu, and W. Zhu, “Experimental study on interaction between membrane structures and wind environment,” *Earthquake Engineering and Engineering Vibration*, vol. 9, no. 4, pp. 523–532, 2010.